

ALMA MATER STUDIORUM · UNIVERSITÀ DI BOLOGNA

SCUOLA DI SCIENZE
Corso di Laurea Magistrale in Fisica

ENTANGLEMENT ENTROPY
IN RESTRICTED INTEGRABLE
SPIN CHAINS

Relatore:
Chiar.mo Prof.
Francesco Ravanini

Presentata da:
Davide Bianchini

Correlatore:
Chiar.ma Prof.ssa
Elisa Ercolessi

Sessione I
Anno Accademico 2012/2013

ABSTRACT

In questa tesi abbiamo presentato il calcolo dell'Entropia di Entanglement di un sistema quantistico unidimensionale integrabile la cui rappresentazione statistica é data dal modello RSOS, il cui punto critico é una realizzazione su reticolo di tutti i modelli conformi minimali. Sfruttando l'integrabilitá di questi modelli, abbiamo svolto il calcolo utilizzando la tecnica delle Corner Transfer Matrices (CTM). Il risultato ottenuto si discosta leggermente dalla previsione di J. Cardy e P. Calabrese ricavata utilizzando la teoria dei campi conformi descriventi il punto critico. Questa differenza é stata imputata alla non-unitarietá del modello studiato, in quanto la tecnica CTM studia il ground state, mentre la previsione di Cardy e Calabrese si focalizza sul vuoto conforme del modello: nel caso dei sistemi non-unitari questi due stati non coincidono, ma possono essere visti come eccitazioni l'uno dell'altro. Dato che l'Entanglement é un fenomeno genuinamente quantistico e il modello RSOS descrive un sistema statistico classico bidimensionale, abbiamo proposto una Hamiltoniana quantistica unidimensionale integrabile la cui rappresentazione statistica é data dal modello RSOS.

Contents

1	Entanglement Entropy	11
1.1	The Two Qubit Archetypal	11
1.1.1	Pure and Mixed States	12
1.2	Subsystems, Reduced Density Matrix and Schmidt Decomposition	13
1.2.1	Expectation values	13
1.2.2	Schmidt Decomposition	15
1.3	Shannon, Von Neumann and Rényi Entropy	16
1.3.1	The Von-Neumann Entropy	18
1.3.2	The Rényi Entropy	20
1.4	The Von-Neumann Entropy as a measure of Entanglement	20
1.4.1	Von-Neumann Entropy - Properties	21
1.4.2	Entanglement - Properties	21
2	Corner Transfer Matrix and Reduced Density Matrix	23
2.1	Corner Transfer Matrix	23
2.1.1	Representation of expression as Product of Operators	26
2.1.2	Star-Triangle Relation (Yang-Baxter Equation)	28
2.1.3	Parametrization with elliptic functions	31
2.1.4	The thermodynamic limit	37
2.1.5	Eigenvalues of CTM	38
2.1.6	Magnetization for the eight-vertex model	42
2.2	The reduced density matrix	47
2.2.1	Equivalence between 2 dimensional classical and 1+1 dimensional quantum systems	47
2.2.2	Reduced density matrix	47
3	Entanglement Entropy in Conformal Field Theory	51
3.1	Branch-Point Twist Fields	51
3.1.1	Twist fields in Quantum Field Theory	51
3.1.2	Twist Fields in Conformal Field Theory	54
3.2	Entanglement Entropy	56

3.2.1	Von-Neumann and Rényi Entropy	56
3.2.2	Evaluation via path integrals	57
3.2.3	Entropy of a critical system	59
3.3	Off-critical models	61
4	The RSOS model	65
4.1	The model	65
4.2	The Andrews-Baxter-Forrester Model (ABF)	68
4.3	The Baxter-Forrester Model (BF)	69
4.3.1	Symmetry of the Model	70
4.4	ABF and BF Models in a Finite Lattice	71
4.4.1	Corner Transfer Matrix structure	71
4.4.2	Ground state structure	73
4.4.3	The partition function	74
4.5	Hamiltonian Limit for Critical RSOS Models	75
5	The q-deformed Quantum XXZ Spin-Chain	79
5.1	The Y-B Equation - 1: Periodic Boundary Conditions	79
5.2	The Temperley-Lieb Algebra	80
5.2.1	The Braid Group Algebra B_N	80
5.2.2	The Hecke Algebra $H_N(q)$	82
5.2.3	The Temperley-Lieb Algebra $T_N(q)$	82
5.3	The Y-B Equation - 2: Open Boundary Conditions	83
5.4	The Quantum Group	86
5.4.1	Spin- $\frac{1}{2}$ Representation	87
5.4.2	Casimir Operator and Classification of Representation	89
5.4.3	Case When q is Not a Root of Unity	90
5.5	Case When q is a Root of Unity	91
5.5.1	Example: Representations of \mathfrak{su}_2 and $U_q(\mathfrak{su}_2)$ in the ($p = 3, N = 3$) case	91
5.5.2	Generalisation to a larger number of sites	93
5.5.3	Type-II representations and Bratteli diagrams	94
5.6	Unitarity When q is a Root of Unity	95
5.7	The $U_q(\mathfrak{su}_2)$ -invariant Hamiltonian and its Conformal Structure	96
5.7.1	Spectrum of H	96
5.7.2	Thermodynamic Limit and Conformal Behaviour	97
5.8	Non-Hermitian Hamiltonians	99
5.8.1	\mathcal{PT} -symmetric Hamiltonians	99
5.8.2	Case When q is a Root of Unity	100

6	Entanglement Entropy in RSOS Models	103
6.1	Evaluation of the Rényi Entropy in ABF models	104
6.2	Evaluation of the Rényi Entropy in BF models	104
6.2.1	Interpretation of Results - Central Charge	105
6.2.2	Interpretation of results - negativity of the entropy	106
6.3	Which Hamiltonian?	108
A	Entanglement Entropy in the BF-RSOS Model: regime III	113
A.1	Computation of Z_α/Z_1^α in terms of Jacobi's θ functions	116
A.1.1	Computation of $E(x^a, y)$	117
A.1.2	Computation of $F(\dots)$	117
A.1.3	Computation of $E^\alpha F(x^{2\alpha})$	120
A.1.4	Computation of $(x^{2\alpha})_\infty$	120
A.1.5	Computation of Z_α	120
A.2	Entanglement Entropy	122
A.2.1	Computation of $\log \left(\sum_{a=1}^{*r-a} \dots (\alpha) \right)$	122
A.2.2	Computation of $\log \theta_4(\alpha)$	126
A.2.3	Full Entropy	126
B	Co-algebras and Hopf algebras	129
B.1	Co-algebras	129
B.2	Hopf co-algebras	130
B.2.1	Quasi-triangular Hopf algebras and quantum groups	131
C	From 8-vertex Boltzmann weights to the quantum XYZ Hamiltonian	133
D	QFT Appendix	137
D.1	The Effective Central Charge	137
D.2	Renormalisation group - Callan Symanzik equation	138
E	Minimal Conformal Models	143
E.1	The Verma modulus	143
E.1.1	The \mathfrak{su}_2 algebra	143
E.1.2	The Virasoro Algebra	144
E.1.3	The dimension of Verma moduli	144
E.2	Minimal models	145
E.2.1	Existence of Minimal Models	146
E.3	Unitary and non-unitary minimal models	147
E.3.1	Non-unitary minimal models	147

Introduction

Entanglement is a genuine quantum phenomenon which occurs between two interacting systems when thermal fluctuations are small enough to make the quantum behaviour arise. From a classical point of view, at finite temperature correlations between two interacting systems always exist: thanks only to thermal excitations the two systems are informationally connected in some way. When the temperature tends to zero, one expects that these connections vanish, but what happens is that a different kind of correlations leads over classical ones: Entanglement.

Entanglement plays a central role in the study and in the understanding of a lot of physical phenomena. From the arising of quantum mechanics entanglement has always attracted the attention of physicists, since it shows in a plain way the quantum behaviour of Nature.

In recent years this phenomenon has attracted also the attention of computer scientists and engineers; thanks to the discovery that quantum phenomena can be used for a sharp improvement of computation and telecommunication techniques, entanglement has started to be analysed and used in a wide class of situations.

Quantifying entanglement is a vital step in a complete theoretical description of the phenomenon. In literature it was proposed to adopt the Von Neumann and Rényi Entropy of a subsystem as a measure of the entanglement, especially for pure states. For mixed states, many indicators of Entanglement have been proposed and they are used to study system which does not belong to the ground state, e.g. systems at finite temperature.

Furthermore a measure of Entanglement is an important indicator of Quantum Phase Transitions, since in the thermodynamic limit it diverges approaching a critical point.

From a theoretical point of view, progresses in the evaluation of the Entanglement Entropy were made using conformal field theory, connecting the leading term of the entropy with the central charge of the conformal theory which described the critical point of the system.

In this thesis we will focus on one-dimensional Quantum Spin Chains, since they are described by a $1 + 1$ -dimensional quantum field theory, or, alternatively, by a 2-dimensional classical statistical theory on a lattice. These two representations allow us to use both statistical mechanics and quantum field theory in the study of these systems. Using the QFT picture we can study the system at its critical point, since the underlying theory becomes conformal; on the other hand, the statistical picture allows us to evaluate correlation functions using Corner Transfer Matrix, which is a powerful method developed by R. Baxter for the evaluation of thermodynamic quantities in statistical models.

In recent years Entanglement Entropy has been evaluated for a wide class of spin chains, in particular for the infinite bipartite XYZ spin chain, which is one of the most general systems. The XYZ model tends to the XXZ model at its critical point, which is described by a $c = 1$ conformal field theory. In the 2-dimensional statistical picture, the XYZ chain is described by the eight-vertex model, and Entanglement can be evaluated using the Corner Transfer Matrix and the results obtained near its critical point satisfy the Conformal Field Theory prediction.

Thanks to a recently proposed protocol [1, 2] which would allow experimental measures of Rényi Entropy for gapped systems, the evaluation of this quantity attracts new interests.

We are interested in a particular class of spin chains whose critical point is described by a minimal conformal model, which describes also a critical point of the classical Restricted Solid on Solid (RSOS) model. This system describes a wide variety of models, both unitary and non-unitary. In recent years, F. Franchini and A. De Luca evaluated the Entanglement Entropy for unitary RSOS models near their critical points, finding a result which agrees with the CFT prediction.

In this thesis, we extended the evaluation of Entropy to non-unitary gapped models. The results obtained can not be completely predicted by CFT, since CFT and CTM evaluate the Entropy of two different states of the system: while CTM technique probes the physical ground state of the system (i.e. the state with the minimal energy), the CFT approach analyses the *conformal vacuum*, which coincides with the physical ground state in unitary theories, but it is an excited state in non-unitary models.

Moreover, since Entanglement is a genuine quantum phenomenon, and RSOS is a classical statistical system, we searched for a suitable one-dimensional quantum system related to RSOS models.

The analysis of these non-unitary theories suggests new horizons of study, since it emphasises unexpected non-trivial properties of these models. Moreover some properties of Entanglement Entropy suggests interesting connections between particular quantum states of the spin chain and classical configurations of the statistical models.

The thesis is structured as follows:

- In the first Chapter we will introduce Entanglement in quantum systems and we will discuss Von-Neumann Entropy as a measure of it.
- In Chapter 2 and 3 we will introduce respectively Corner Transfer Matrix and the Replica's trick in Conformal Field Theory. These two techniques can be used for the evaluation of Entanglement Entropy near the critical point of a system: the first method refers to the statistical picture of the model, while the second one focuses on the quantum fields theory underlying the critical point.
- In Chapter 4 we will describe RSOS models and we will give an expression for their Corner Transfer Matrices. We will conclude this Chapter with the Hamiltonian limit of these models near its critical point. This is a procedure used to find the one-dimensional quantum system related to a statistical bi-dimensional one.
- In Chapter 5 we will analyse this one-dimensional quantum system and we will discuss its symmetry group. Moreover we will discuss some integrable Spin-Chains.
- In Chapter 6, we will conclude this thesis with the evaluation of the Entanglement Entropy and with the interpretation of results obtained. Moreover we will propose a Spin-Chain related to the RSOS model.

Chapter 1

Entanglement Entropy

In this chapter we will start with an introduction to Entanglement from a qualitative point of view. Moreover we will present some physical quantities which have been proposed in literature to quantify Entanglement, in particular we will refer to Von Neumann and Rényi Entropy as a measure of Entanglement.

1.1 The Two Qubit Archetypal

Let us consider a single qubit system, which represents one spin- $\frac{1}{2}$ particle. The state of the system is defined as

$$|\psi\rangle = \alpha|\uparrow\rangle + \beta|\downarrow\rangle \quad (1.1)$$

with $\alpha, \beta \in \mathbb{C}$ and $|\alpha|^2 + |\beta|^2 = 1$. In the previous expression the state $|\uparrow\rangle$ ($|\downarrow\rangle$) is the state with spin pointing up (down).

Of course, since this system is composed by only one particle, we can not define any kind of correlation.

Now, consider two spin- $\frac{1}{2}$ particles in the singlet state; the quantum state is given by

$$|s_0\rangle = \frac{|\uparrow\rangle_1 \otimes |\downarrow\rangle_2 - |\downarrow\rangle_1 \otimes |\uparrow\rangle_2}{\sqrt{2}} \quad (1.2)$$

where pedices 1, 2 refer to the first or the second particle.

If an observer measures the spin of the first particle and obtains a particular value, say $\langle\sigma_1^z\rangle = +\frac{1}{2}$, the value of the spin of the second particle is automatically fixed to $\langle\sigma_2^z\rangle = -\frac{1}{2}$. This kind of phenomenon implies a sort of *correlation* between the two particles.

This correlation is not always guaranteed in all two-spin systems, for example in

the triplet with total spin equal to one:

$$|t_1\rangle = |\uparrow\rangle_1 \otimes |\uparrow\rangle_2 \quad (1.3)$$

the measure of the spin of the first particle does not give **additional** informations about the state of the system.

States like the singlet for which non-local correlations arise are called *entangled*, while states which do not have this behaviour are called *separable*.

At this point, our definition about entanglement is purely qualitative: it defines when a quantum state is entangled or separable, and it does not give any information about intermediate states.

1.1.1 Pure and Mixed States

It is known that if a quantum system can be represented with a state (like previous examples) its density matrix ρ is simply given by

$$\rho = |\psi\rangle\langle\psi| \quad (1.4)$$

and the state is called *pure*. On the other hand if a system can not be simply represented by a state, the density matrix is written as

$$\rho = \sum_k p_k \rho_k \quad (1.5)$$

where ρ_k are density matrices in the form (1.4) and p_k are some real positive constants summing up to one (indeed they are genuine classical probabilistic weights); these states are called *mixed* and the archetypal example is a thermal superpositions of states:

$$\rho = \sum_k e^{-\beta E_k} |\psi_k\rangle\langle\psi_k| \quad (1.6)$$

where E_k is the energy of the state $|\psi_k\rangle$ and β is the inverse of the temperature. It is important to stress on the difference between pure/mixed states and separable/mixed states, since these concepts will be connected when one analyses only a part of the total system.

1.2 Subsystems, Reduced Density Matrix and Schmidt Decomposition

From the two-spins examples, we know that the entanglement is a phenomenon which can occur between two subsystems of the same system; for instance, in this example, the two subsystems are given by the two particles.

Notice that the quality of a state to be entangled or not can depend on the chosen partition: for instance, the three-spin state

$$|\psi\rangle = |\uparrow\rangle_1 \otimes \frac{|\uparrow\rangle_2 \otimes |\downarrow\rangle_3 - |\downarrow\rangle_2 \otimes |\uparrow\rangle_3}{\sqrt{2}} \quad (1.7)$$

is entangled if we choose $1 \cup 2$ and 3 as subsystems, while it is separable if we choose 1 and $2 \cup 3$ as subsystems.

In following sections we will consider a system $A \cup B$ which is divided into two subsystems A and B . The Hilbert space \mathcal{H} of the system, supposed to be described by a pure state, is given by

$$\mathcal{H} = \mathcal{H}_A \otimes \mathcal{H}_B \quad (1.8)$$

Thanks to this factorisation a state of the system is given by

$$|\psi\rangle = \sum_{i,j} C_{ij} |\phi_i\rangle_A \otimes |\chi_j\rangle_B \quad (1.9)$$

where $\{|\phi_i\rangle_A\}_i$ and $\{|\chi_j\rangle_B\}_j$ are complete orthonormal basis respectively of \mathcal{H}_A and \mathcal{H}_B and $C_{i,j}$ are complex constants normalised such that $\sum_{i,j} |C_{i,j}|^2 = 1$

1.2.1 Expectation values

In order to analyse correlations between subsystems it is useful to introduce the *reduced density matrix*, which is an operator similar to the density matrix but which focuses only on a subsystem.

If we are interested in the expectation value of an operator \mathcal{O} whose non-trivial part acts only on the subsystem A , (i.e. it can be written as $\mathcal{O} = \mathcal{O}_A \otimes \mathbb{1}_B$) we

have¹

$$\begin{aligned}
 \langle \psi | \mathcal{O}_A \otimes \mathbb{1}_B | \psi \rangle &= \text{Tr}_{\mathcal{H}} [\rho \mathcal{O}] = \sum_{i_1, i_2, j_1, j_2} C_{i_1, j_1} C_{i_2, j_2}^* \langle \phi_{i_2} | \mathcal{O}_A | \phi_{i_1} \rangle \langle \chi_{j_2} | \mathbb{1}_B | \chi_{j_1} \rangle \\
 &= \sum_{i_1, i_2} \left(\sum_j C_{i_1, j} C_{i_2, j}^* \right) \langle \phi_{i_2} | \mathcal{O}_A | \phi_{i_1} \rangle \\
 &= \sum_i \langle \phi_i | \rho_A \mathcal{O}_A | \phi_i \rangle = \text{Tr}_{\mathcal{H}_A} [\rho_A \mathcal{O}_A] \quad (1.10)
 \end{aligned}$$

where we have defined the *reduced density matrix* as

$$\langle \phi_{i_1} | \rho_A | \phi_{i_2} \rangle = \sum_j C_{i_1, j} C_{i_2, j}^* \quad (1.11)$$

The reduced density matrix allows us to focus on one subsystem taking automatically into account the other subsystem with which the first one interacts. In this picture one subsystem, say A , can be considered as a system embedded in a thermal bath given by the subsystem B and vice-versa.

The reduced density matrix respects all properties of density matrices of mixed states²:

- It is self-adjoint $\rho_A^\dagger = \rho_A$
- Its trace is unitary $\text{Tr}_{\mathcal{H}_A} \rho_A = 1$
- It is non-negative ${}_A \langle x | \rho_A | x \rangle_A \geq 0 \quad \forall |x\rangle_A \in \mathcal{H}_A$

Moreover the reduced density matrix of a subsystem can be obtained tracing the density matrix of the total system over all degrees of freedom of the other subsystem:

$$\rho_A = \text{Tr}_{\mathcal{H}_B} \rho \quad (1.12)$$

since

$$\begin{aligned}
 \text{Tr}_{\mathcal{H}_B} \rho &= \sum_j \langle \chi_j | \rho | \chi_j \rangle = \sum_{j, i_1, i_2, j_1, j_2} C_{i_1, j_1} C_{i_2, j_2}^* \langle \chi_j | \chi_{j_1} \rangle \langle \chi_{j_1} | \chi_j \rangle | \phi_{i_1} \rangle \langle \phi_{i_2} | \\
 &= \sum_{i_1, i_2} \left(\sum_j C_{i_1, j} C_{i_2, j}^* \right) | \phi_{i_1} \rangle \langle \phi_{i_2} | \quad (1.13)
 \end{aligned}$$

¹In following expressions $\text{Tr}_V \mathcal{O}$ means the trace of \mathcal{O} over all states belonging to the vector space V

²Recall that density matrices of pure states are also idempotent

1.2. Subsystems, Reduced Density Matrix and Schmidt Decomposition

and

$$\langle \phi_{i_1} | \text{Tr}_{\mathcal{H}_B} \rho | \phi_{i_2} \rangle = \sum_j C_{i_1,j} C_{i_2,j}^* = \langle \phi_{i_1} | \rho_A | \phi_{i_2} \rangle \quad (1.14)$$

1.2.2 Schmidt Decomposition

In order to deepen better the role of the reduced density matrix we can introduce the *Schmidt Decomposition*. As before, a given pure state $|\psi\rangle$ can be written as

$$|\psi\rangle = \sum_{i,j} C_{i,j} |\phi_i\rangle_A \otimes |\chi_j\rangle_B = \sum_i |\phi_i\rangle_A \otimes |\tilde{\chi}_i\rangle_B \quad (1.15)$$

where $|\tilde{\chi}_i\rangle_B = \sum_j C_{i,j} |\chi_j\rangle_B$. Supposing that $\{|\phi_i\rangle_A\}_i$ is an eigenbasis of ρ_A ³ with eigenvalues $\{p_i\}_i$, then the reduced density matrix is given by

$$\rho_A = \sum_i p_i |\phi_i\rangle_A \langle \phi_i| \quad (1.16)$$

Comparing (1.14) and (1.16) we have

$$\langle \tilde{\chi}_i | \tilde{\chi}'_{i'} \rangle = p_i \delta_{i,i'} \quad (1.17)$$

and then the state $|\psi\rangle$ can be expressed as

$$|\psi\rangle = \sum_i \sqrt{p_i} |\phi_i\rangle_A \otimes |\chi'_i\rangle_B \quad (1.18)$$

where $|\chi'_i\rangle_B = \frac{1}{\sqrt{p_i}} |\tilde{\chi}_i\rangle_B$ is the normalised version of $|\tilde{\chi}_i\rangle_B$.

It is important to notice how weights p_i of the reduced density matrix of the subsystem are related to quantum coefficients of the state of the total system; in particular is fundamental to emphasise that if the state of the **whole system** is **entangled**, the reduced density matrix referred to a **subsystem** is **mixed**. This remark must be taken into account in order to understand deeply these phenomena. It can be shown that the reduced density matrix ρ_B related to the second subsystem has the same form of ρ_A

$$\rho_B = \sum_j p_j |\chi_j\rangle_B \langle \chi_j| \quad (1.19)$$

where p_j are the same of (1.16). It is vital to stress the fact that even if ρ_A and ρ_B have different dimensions and a different number of eigenvalues, **they have**

³A complete eigenbasis of ρ_A can always be found, since ρ_A is a self-adjoint operator. Moreover, since it is definite positive, also its eigenvalues are non-negative.

the same non-zero eigenvalues, whose number is called *Schmidt number*. If the Schmidt number is equal to one the state is separable, if it becomes greater than one Entanglement is *turned on*, growing up to its maximal value, which is reached when the Schmidt number is equal to $\frac{d^N}{2}$, where in the spin-chain picture d and N are respectively the dimension of the Hilbert space of each site and the number of sites.

Example: Two-spin system

We present a two-spin example of the relation between mixed/pure states and entangled/separable states. In this example, if we consider the singlet state, which is entangled, the density matrix is given by

$$\rho = |s_0\rangle\langle s_0| = \frac{1}{2} (|\uparrow\downarrow\rangle\langle\uparrow\downarrow| - |\uparrow\downarrow\rangle\langle\downarrow\uparrow| - |\downarrow\uparrow\rangle\langle\uparrow\downarrow| + |\downarrow\uparrow\rangle\langle\downarrow\uparrow|) \quad (1.20)$$

and the reduced density matrix of the subsystem 1 is given by

$$\begin{aligned} \rho_1 &= \text{Tr}_2 \rho = {}_1\langle\uparrow|\rho|\uparrow\rangle_1 + {}_1\langle\downarrow|\rho|\downarrow\rangle_1 \\ &= \frac{1}{2} (|\downarrow\rangle_2 {}_2\langle\downarrow| + |\uparrow\rangle_2 {}_2\langle\uparrow|) \end{aligned} \quad (1.21)$$

which represents a mixed state.

On the other hand the density matrix of the first triplet is given by

$$\rho = |t_1\rangle\langle t_1| = |\uparrow\uparrow\rangle\langle\uparrow\uparrow| \quad (1.22)$$

and the reduced on the first subsystem is given by

$$\begin{aligned} \rho_1 &= \text{Tr}_2 \rho = {}_1\langle\uparrow|\rho|\uparrow\rangle_1 + {}_1\langle\downarrow|\rho|\downarrow\rangle_1 \\ &= |\uparrow\rangle_2 {}_2\langle\uparrow| \end{aligned} \quad (1.23)$$

which is a pure state.

1.3 Shannon, Von Neumann and Rényi Entropy

As we said before, an entangled state is related to mixed subsystems, whose density matrices can be written as **classical** superpositions of density matrices of pure states with real, non-negative probabilistic weights. As probabilistic weights, their sum has to be normalised to one and they form a *convex* combination (they are

1.3. Shannon, Von Neumann and Rényi Entropy

non-negative, less than one and their sum is equal to one):

$$\begin{aligned}\rho &= \sum_k p_k \rho_k \\ \sum_k p_k &= 1 \\ 0 &\leq p_k \leq 1\end{aligned}\tag{1.24}$$

These classical weights define a classical probability distribution, which associate to each state ρ_k its classical probability p_k .

This ‘classical nature’ can be shown noticing that the expectation value of an operator \mathcal{O} is given by

$$\langle \mathcal{O} \rangle = \sum_k p_k \langle \mathcal{O} \rangle_k\tag{1.25}$$

where $\langle \mathcal{O} \rangle_k = \text{Tr}[\rho_k \mathcal{O}]$ is the expectation value of \mathcal{O} in the k -th state; in this way the p_k s play the role of classical weights, since they quantify the weight of each state k .

To each classical probability distribution we can always associate a function, called *Shannon Entropy* which measures how much a distribution is not deterministic: for example a constant distribution maximises Shannon Entropy since each value is equally probable, while a delta distribution minimises Entropy, since there is only one possible issue for a measure.

Shannon Entropy is defined as

$$S = - \sum_k p_k \log p_k\tag{1.26}$$

which vanishes for $p_k = \delta_{k,k_0}$ and it is maximised for $p_k = \text{const}$.

The Shannon Entropy gives the lack of *information* contained in a probabilistic distribution, i.e. how much a *a priori* prediction of a measure is reliable. For this reason, a distribution with higher Shannon Entropy than another one is less deterministic than the second one.

Example: the Shannon Entropy of a passage

One of the most common examples of the Shannon Entropy is the evaluation of predictability of a passage, i.e. quantification of how much the distribution of letters and words of a paragraph is deterministic.

Let us consider, for example, the poem *Divina Commedia* and this thesis. Both of them are composed by a long sequence of words; from each passage one can

extract the probabilistic distribution of words and evaluate the Shannon Entropy for each distribution. As we said before, the passage with the highest entropy is the most complex one, since it contains less repetition and uses a wide vocabulary. Indeed the Shannon Entropy of the Divina Commedia is equal to 0.6 while this thesis's one is equal to 0.39.⁴

1.3.1 The Von-Neumann Entropy

At the quantum level, a function similar to the Shannon Entropy can be defined in order to quantify the lack of information about a system. The quantum analogous is the *Von Neumann Entropy* and it is defined as

$$S = -\text{Tr}[\rho \log \rho] \tag{1.27}$$

which coincides with the Shannon Entropy in the probabilistic picture.

According to the literature, the Von-Neumann Entropy of a **subsystem** can quantify well the amount of Entanglement of the **total system** in some models. It is vital to emphasise the object whose Entropy is evaluated: we are not interested in the Entropy of the total system (which is always zero for pure states) but in the Entropy of a subsystem in interaction with the other one, since the Entanglement is strictly related to the correlation between these two subsystems. As we showed in previous paragraphs, an **entangled** (pure) state is composed by two **mixed** sub-states, which can be seen as a system and a fictitious thermal bath, whose Entropy is non-zero, since the fictitious temperature makes the probabilistic distribution less predictable.

Example: The Von-Neumann Entropy vs. Entanglement

Consider, for instance a two-spin system. As we said before, the singlet is an entangled state, while the first triplet is a separable one. Using the expressions (1.21,1.23) of the reduced density matrices of these two states the Von-Neuman Entropy is given by

$$S_{s_0} = \log 2 \tag{1.28}$$

$$S_{t_1} = 0 \tag{1.29}$$

The entangled state is more entropic than the separable one; this fact shows that the Von-Neumann Entropy evaluates well the amount of Entanglement for this system.

⁴In order to compare two passages in the same language, I used the Longfellow's translation of the Divina Commedia.

1.3. Shannon, Von Neumann and Rényi Entropy

The Von-Neumann Entropy for the two-spin system can be evaluated not only for **completely** separable or entangled states, but allows us to investigate the Entanglement of a variety of states.

Let us consider the state

$$|\psi\rangle = \sqrt{p}|\uparrow\rangle \otimes |\downarrow\rangle + \sqrt{1-p}|\downarrow\rangle \otimes |\uparrow\rangle \quad (1.30)$$

which is completely separable for $p = 0, 1$ (first-triplet-like state) or maximally entangled for $p = \frac{1}{2}$ (singlet-like state). The reduced density matrix related to the first subsystem can be easily obtained, since the Schmidt decomposition of this state is trivial:

$$\rho_A = p|\uparrow\rangle\langle\uparrow| + (1-p)|\downarrow\rangle\langle\downarrow| \quad (1.31)$$

The Von-Neumann Entropy of this state is then given by

$$S = -p \log p - (1-p) \log(1-p) \quad (1.32)$$

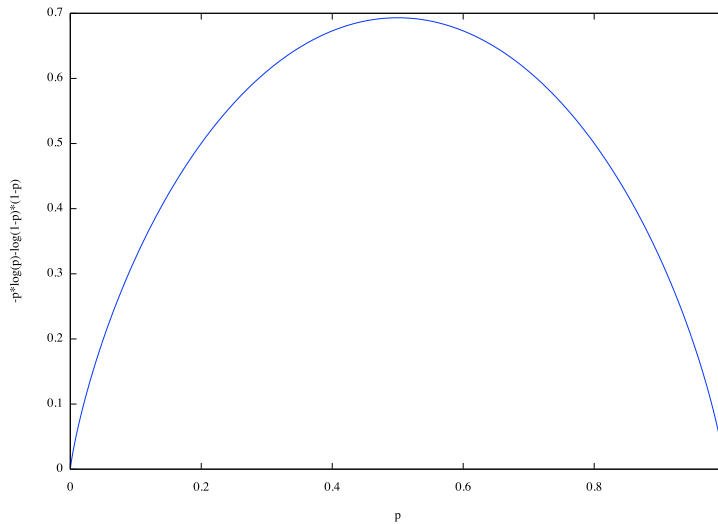


Figure 1.1: Dependence of Entropy S vs. p

whose maximum value is obtained for $p = \frac{1}{2}$ and its minimum for $p = 0, 1$. In this way the Von-Neumann Entropy measures the amount of Entanglement owned by a state.

1.3.2 The Rényi Entropy

As stated in previous paragraphs, the Von-Neumann Entropy quantifies well the amount of Entanglement in some systems. On the other hand its evaluation can be non trivial, thanks to the presence of the logarithm in the formula.

In 1960 Alfréd Rényi proposed [3] a generalisation of the Shannon Entropy for a probabilistic distribution $\mathcal{P} = (p_1, p_2, \dots)$

$$S_\alpha = \frac{1}{1-\alpha} \log \sum_k p_k^\alpha \quad \alpha \in \mathbb{R}^+ \quad (1.33)$$

which is called *Entropy of order α* or *Rényi Entropy*.

One of the most important properties [3] of the Rényi entropy is that its limit gives the Shannon Entropy when α tends to one.

$$\lim_{\alpha \rightarrow 1} S_\alpha = S \quad (1.34)$$

In the density matrix picture the Rényi Entropy is given by

$$S_\alpha = \frac{1}{1-\alpha} \log \text{Tr } \rho^\alpha \quad (1.35)$$

which recovers the Von-Neumann Entropy in the limit $\alpha \rightarrow 1$.

Since the evaluation of Rényi Entropy can be easier than the evaluation of Von-Neumann one, sometimes it is preferred to calculate the first Entropy and then to take its limit in order to reach the second one.

Notice that while the Von-Neumann Entropy is the quantum version of the Thermodynamic Entropy of a system, it is not true for the Rényi Entropy.

1.4 The Von-Neumann Entropy as a measure of Entanglement

In previous paragraphs, we have shown that Von-Neumann Entropy is a good measure of the Entanglement for a certain class of states, in particular for pure states. This relation between Entropy and Entanglement is not guaranteed for mixed states, and we will show that it is not still valid for such states.

In order to check the validity of the Von-Neumann Entropy and the Entanglement, we will compare properties of both quantities.

1.4.1 Von-Neumann Entropy - Properties

The Von-Neumann Entropy satisfies following properties [4]

1. A pure state has zero Entropy: $S(|\psi\rangle\langle\psi|) = 0$
2. Entropy is invariant under unitary transformations: $S(U^{-1}\rho U) = S(\rho)$
3. Entropy is bounded by above: $S \leq \log d$ (d dimension of the system)
4. Entropy is concave: $S(\lambda\rho_1 + (1 - \lambda)\rho_2) \geq \lambda S(\rho_1) + (1 - \lambda)S(\rho_2)$
5. The Entropy is sub-addictive: $S(\rho_{AUB}) \leq S(\rho_A) + S(\rho_B)$ ($\rho_A = \text{Tr}_{\mathcal{H}_B} \rho_{AUB}$)

We stress the fact that, in order to measure the Entanglement of a partition of a system, we are interested in the Von-Neumann Entropy of a subsystem.

1.4.2 Entanglement - Properties

Now, we list a series of properties [4, 5] which are required in order to have a ‘good’ measure $E(\rho)$ of Entanglement of a system

1. A separable state is not entangled: $E\left(\rho = \sum_k c_k \rho_A^{(k)} \otimes \rho_B^{(k)}\right) = 0$
2. A measure of Entanglement is not increasing under local operations and classical communications (LOCC): $E(U\rho U^{-1}) \leq E(\rho)$. Since a measure of Entanglement gives a measure about the amount of **quantum correlations** between two subsystems, it can not increase if we modify a subsystem (local operations) or if the two subsystems exchange classical informations (classical communications). Focusing on local operations, since they are implemented by unitary operators, they can not change the amount of Entanglement $E(U\rho U^\dagger) \leq E(\rho)$.
3. A measure of Entanglement is bounded by its value for completely entangled states.

4. A measure of Entanglement is convex: $E(\lambda\rho_1 + (1 - \lambda)\rho_2) \leq \lambda E(\rho_1) + (1 - \lambda)E(\rho_2)$

5. A measure of Entanglement is sub-addictive: $E(\rho_A \otimes \rho_B) \leq E(\rho_A) + E(\rho_B)$

The fourth property derives from the genuine quantum nature of the Entanglement: since a convex combination of density matrix is a purely classical statistical superposition of states, it can not increase the Entanglement.

Comparing properties of Entropy and Entanglement it is clear that they are compatible except only for the fourth property of each quantity, for this reason the Von-Neumann Entropy quantifies well Entanglement only for pure states, whose Schmidt decomposition is unique.

For mixed states more complex quantities have been proposed in literature [4] to measure the Entanglement, such as the *Entanglement of Formation*.

For our purposes, i.e. the evaluation of the ground state Entanglement, the Von-Neumann Entropy is a good measure, since the ground state is intrinsically a pure state.

Chapter 2

Corner Transfer Matrix and Reduced Density Matrix

In following sections we will introduce a powerful method for computation of statistical quantities: the *Corner Transfer Matrix*. Definitions and notations are the same of the Chapt. 13 of [6]. At the end of this chapter we will introduce the reduced density matrix of a quantum system and we will show a method, developed by Peschel, Kaulke, and Legeza (PKL) [7], for the evaluation of the reduced density matrix using corner transfer matrices.

2.1 Corner Transfer Matrix

In a lattice system with nearest-neighbour interaction, the total energy can be written as a summation over all links of the energy of two near sites

$$\mathcal{E} = \sum_{\langle i,j \rangle} \varepsilon(\sigma_i, \sigma_j), \quad (2.1)$$

or as a summation over all faces of the lattice

$$\mathcal{E} = \sum_{\text{faces}} \varepsilon(\sigma_i, \sigma_j, \sigma_k, \sigma_l), \quad (2.2)$$

where $\varepsilon(\sigma_i, \sigma_j, \sigma_k, \sigma_l)$ denotes the contribution to the energy given by surrounding spins of the face (i, j, k, l) .

Models whose energy can be written as a summation over all faces are usually called *Interaction Round a Face* (IRF) systems.

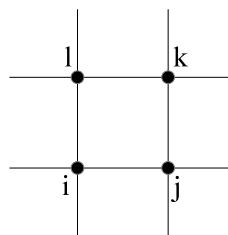


Figure 2.1: Face (i, j, k, l)

The partition function of the whole lattice is then given by:

$$Z = \sum_{\sigma} \prod_{\text{faces}} w(\sigma_i, \sigma_j, \sigma_k, \sigma_l) \quad (2.3)$$

with

$$w(a, b, c, d) = \exp \{-\beta\varepsilon(a, b, c, d)\} \quad (2.4)$$

where the above summation is over all possible spin configurations and the product over all faces.

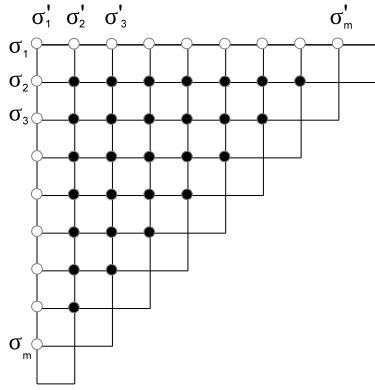


Figure 2.2: Corner of a square lattice

The system has one or more ground states, which are defined as states which minimise the total energy \mathcal{E} or, equivalently, which give the largest contribution to the partition function. For example the isotropic one-dimensional ferromagnetic Ising model has two ground states: the one with all spin pointing 'up' and the one with all spin pointing 'down'. When we refer to the ground state in following sections, we mean a particular one, since some thermodynamic quantities, such as spontaneous magnetisation, could not be invariant under the change of the ground state (in the previous example the spontaneous magnetisation has

a different sign in the two ground states).

Let us now consider a particular kind of lattice (Fig. 2.2): a square lattice with a global triangular shape. Spins on the top row are labelled by $\sigma'_1 \cdots \sigma'_m$ and ones on the left column by $\sigma_1 \cdots \sigma_m$. Since σ_1 and σ'_1 represent the same spin, they have to be chosen equal.

Denoting with $\bar{\sigma}$ the set of all values $\{\sigma_1 \cdots \sigma_m\}$ and with $\bar{\sigma}'$ the one of $\{\sigma'_1 \cdots \sigma'_m\}$, we can define the quantity $A_{\bar{\sigma}, \bar{\sigma}'}$ as

$$A_{\bar{\sigma}, \bar{\sigma}'} = \sum_{\bullet} \prod_{\square} w(\sigma_i, \sigma_j, \sigma_k, \sigma_l) \quad (2.5)$$

if $\sigma_1 = \sigma'_1$, or equal to zero if $\sigma_1 \neq \sigma'_1$. In the above expression the summation is over all 'internal' sites (solid circles in Fig. 2.2) and the product over all $\frac{1}{2}m(m+1)$ faces, where m is the number of spins in the top row (empty circles). The value

2.1. Corner Transfer Matrix

of spins on the most external diagonal edge can be chosen fixed or free.

Let us now define $B_{\bar{\sigma},\bar{\sigma}'}$ in a very similar way to $A_{\bar{\sigma},\bar{\sigma}'}$ only with an anti-clockwise rotation of the lattice through $\frac{\pi}{2}$ (see Fig. 2.3). In this case $\bar{\sigma}$ denotes the set of all spins on the bottom row and $\bar{\sigma}'$ denotes the set of all spins on the left column. Matrices $C_{\bar{\sigma},\bar{\sigma}'}$ and $D_{\bar{\sigma},\bar{\sigma}'}$ are defined as $A_{\bar{\sigma},\bar{\sigma}'}$ with a π and a $\frac{3\pi}{2}$ lattice rotation. Denoting with $\bar{\sigma}$, $\bar{\sigma}'$, $\bar{\sigma}''$ and $\bar{\sigma}'''$ the set of spins on the edge between A and D , B and A , C and B , D and C (forcing σ_1 to have the same value in all sets), we can note that the following quantity

$$A_{\bar{\sigma},\bar{\sigma}'} B_{\bar{\sigma}',\bar{\sigma}''} C_{\bar{\sigma}'',\bar{\sigma}'''} D_{\bar{\sigma}''',\bar{\sigma}} \quad (2.6)$$

is the product of all Boltzmann weights of all faces, keeping the $\bar{\sigma} \cdots \bar{\sigma}'''$ spins fixed. The partition function Z of the lattice is therefore given by the summation of the previous expression over all $\bar{\sigma} \cdots \bar{\sigma}'''$ spins:

$$Z = \sum_{\bar{\sigma} \cdots \bar{\sigma}'''} A_{\bar{\sigma},\bar{\sigma}'} B_{\bar{\sigma}',\bar{\sigma}''} C_{\bar{\sigma}'',\bar{\sigma}'''} D_{\bar{\sigma}''',\bar{\sigma}} \quad (2.7)$$

The above summation runs over all sets which satisfy the constraint $\sigma_1 = \sigma'_1 = \sigma''_1 = \sigma'''_1$, but, since $A_{\bar{\sigma},\bar{\sigma}'}$ vanishes if this constraint is not satisfied, we can neglect this constraint and obtain:

$$Z = \text{Tr} [ABCD] \quad (2.8)$$

The spontaneous magnetization $\langle \sigma_1 \rangle$ is then given by

$$\langle \sigma_1 \rangle = \frac{1}{Z} \sum_{\bullet, \circ} \sigma_1 \prod_{\square} w(\sigma_i, \sigma_j, \sigma_k, \sigma_l) \quad (2.9)$$

$$= \frac{\text{Tr} [SABCD]}{\text{Tr} [ABCD]} \quad (2.10)$$

where the summation runs over all possible spin configurations and the product runs over all faces of the lattice; the matrix S is given by:

$$S = \begin{bmatrix} \mathbb{1} & 0 \\ 0 & -\mathbb{1} \end{bmatrix} \quad (2.11)$$

if we order spins configuration so that $\sigma_1 = +1$ for the first half of configurations and $\sigma_1 = -1$ for the second half. In analogy with the fact that multiplying by a

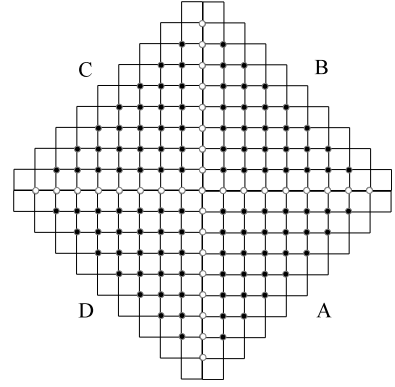


Figure 2.3: Lattice composed by four corners

row-to-row transfer matrix means add a row to the total system, we can note that multiplying by A means add the lower-right corner to the lattice.

Denoting with $\bar{s} \cdots \bar{s}'''$ the value of spin $\bar{\sigma} \cdots \bar{\sigma}'''$ of $A \cdots D$ when the system lies in the ground state, we can set

$$\alpha = A_{\bar{s}, \bar{s}'} \quad (2.12)$$

$$\beta = B_{\bar{s}, \bar{s}'} \quad (2.13)$$

$$\gamma = C_{\bar{s}, \bar{s}'} \quad (2.14)$$

$$\delta = D_{\bar{s}, \bar{s}'} \quad (2.15)$$

and define

$$A_n = \frac{1}{\alpha} A \quad (2.16)$$

$$B_n = \frac{1}{\beta} B \quad (2.17)$$

$$C_n = \frac{1}{\gamma} C \quad (2.18)$$

$$D_n = \frac{1}{\delta} D \quad (2.19)$$

which are called *normalized corner transfer matrices*. Since all thermodynamic quantities depend on the ratio of $A \cdots D$ entries, they can be evaluated using normalized matrices.

Sometimes it is useful to use a diagonalised version of corner transfer matrices A_d, B_d, C_d and D_d :

$$A_n = \alpha' P A_d Q^{-1} \quad (2.20)$$

$$B_n = \beta' Q B_d R^{-1} \quad (2.21)$$

$$C_n = \gamma' R C_d T^{-1} \quad (2.22)$$

$$D_n = \delta' T D_d P^{-1} \quad (2.23)$$

where $\alpha' \cdots \delta'$ are scalars, P is the matrix of eigenvectors of $A_n B_n C_n D_n$, Q is the one of $B_n C_n D_n A_n$, etc. Using a particular choice of $\alpha' \cdots \delta'$ we can set $A_d \cdots D_d$ so that their maxima entries are unity. Exactly as we said above for normalised matrices, thermodynamic quantities can be evaluated using diagonal corner transfer matrices too.

2.1.1 Representation of expression as Product of Operators

In order to build up the corner transfer matrix of a system, it can be useful to define some complex structure made by Boltzmann weights of faces.

2.1. Corner Transfer Matrix

Let us define first the matrix U_i as

$$(U_i)_{\bar{\sigma}, \bar{\sigma}'} = \delta(\sigma_1, \sigma'_1) \delta(\sigma_2, \sigma'_2) \cdots \delta(\sigma_{i-1}, \sigma'_{i-1}) \times \\ \times w(\sigma_i, \sigma_{i+1}, \sigma'_i, \sigma'_{i-1}) \delta(\sigma_{i+1}, \delta'_{i+1}) \cdots \delta(\sigma_m, \sigma'_m) \quad (2.24)$$

which corresponds to add a face to the lattice (Fig. 2.4). Notice that U_i and U_j commute if i and j differ by two or more. What we want to do is to find an expression to write A as a product of some U_i matrices. In order to reach our goal it is useful to introduce the two following matrices U_m^t and U_{m+1}^{stz} :

$$(U_m^t)_{\bar{\sigma}, \bar{\sigma}'} = \delta(\sigma_1, \sigma'_1) \delta(\sigma_2, \sigma'_2) \cdots \delta(\sigma_{m-1}, \sigma'_{m-1}) \times \\ \times w(\sigma_m, s, \sigma'_m, \sigma_{m-1}) \quad (2.25)$$

$$(U_{m+1}^{stz})_{\bar{\sigma}, \bar{\sigma}'} = \delta(\sigma_1, \sigma'_1) \delta(\sigma_2, \sigma'_2) \cdots \delta(\sigma_m, \sigma'_m) \times \\ \times w(s, t, z, \sigma_m) \quad (2.26)$$

The first equation is the very same of (2.24) only with $m + 1$ sites, whose last one is fixed to be equal to s ; in the second one the number of sites is extended to $m + 2$ and $\sigma_{m+1}, \sigma_{m+2}$ and σ'_{m+1} are replaced by s, t and z . In our diagrammatic representation these matrices look like:

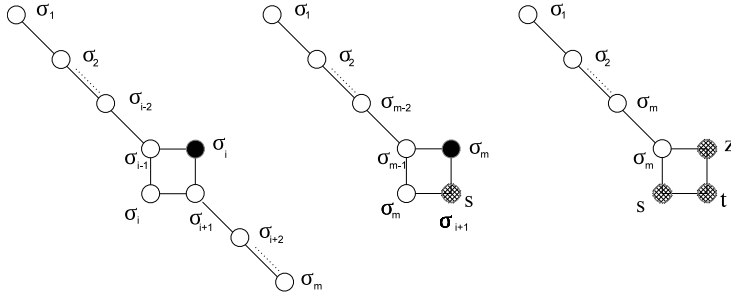


Figure 2.4: Graphical representation of U_i matrices

After setting

$$\mathcal{F}_j^{ss't} = U_{m+1}^{ss't} U_m^t U_{m-1} \cdots U_j \quad (2.27)$$

we can simply see that

$$A = \mathcal{F}_2^{ss't} \mathcal{F}_3^{tt'u} \mathcal{F}_4^{uu'v} \cdots \mathcal{F}_m^{xx'y} \mathcal{F}_{m+1}^{yy'z} \quad (2.28)$$

where $ss' \cdots z$ label fixed spins on the diagonal edge of A .

Thanks to this construction we have reached our goal to build up the whole corner transfer matrix A using singular face Boltzmann's weights.

2.1.2 Star-Triangle Relation (Yang-Baxter Equation)

In this section we will consider some important properties of face Boltzmann weights, which can be encapsulated in the Yang-Baxter equation.

Let us consider a square lattice with N columns, with cylindrical boundary conditions, i.e. the first column follows the N -th one.

The row-to-row transfer matrix is given by:

$$V_{\bar{\sigma}, \bar{\sigma}'} = \prod_{j=1}^N w(\sigma_j, \sigma_{j+1}, \sigma'_{j+1}, \sigma'_j) \quad (2.29)$$

with $\sigma_{N+1} = \sigma_1$ and $\sigma'_{N+1} = \sigma'_1$.

Defining V' in a very similar way of V , only with w' instead of w , we can evaluate the product of these two matrices:

$$\begin{aligned} (VV')_{\bar{\sigma}, \bar{\sigma}'} &= \sum_{\bar{\sigma}''} V_{\bar{\sigma}, \bar{\sigma}''} V'_{\bar{\sigma}'', \bar{\sigma}'} \\ &= \sum_{\sigma''_1} \cdots \sum_{\sigma''_N} \prod_{j=1}^N w(\sigma_j, \sigma_{j+1}, \sigma''_{j+1}, \sigma''_j) w(\sigma''_j, \sigma''_{j+1}, \sigma'_{j+1}, \sigma'_j) \\ &= \sum_{\sigma''_1} \cdots \sum_{\sigma''_N} \prod_{j=1}^N s(\sigma_j, \sigma''_j, \sigma'_j | \sigma_{j+1}, \sigma''_{j+1}, \sigma'_{j+1}) \end{aligned} \quad (2.30)$$

Notice that $s(a, a'', a' | b, b'', b') = w(a, b, b'', a'') w'(a'', b'', b', a')$ is the Boltzmann weight of two adjacent faces which share the horizontal edge.

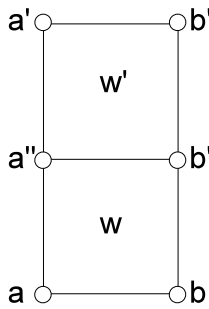


Figure 2.5: Graphical representation of the matrix $(\mathbb{S}(a, a' | b, b'))_{a'', b''}$

After defining the matrix $\mathbb{S}(a, a' | b, b')$:

$$(\mathbb{S}(a, a' | b, b'))_{a'', b''} = s(a, a'', a' | b, b'', b') \quad (2.31)$$

2.1. Corner Transfer Matrix

we can see that (2.30) can be written as:

$$(VV')_{\bar{\sigma}, \bar{\sigma}'} = \text{Tr} [\mathbb{S}(\sigma_1, \sigma'_1 | \sigma_2, \sigma'_2) \cdots \mathbb{S}(\sigma_N, \sigma'_N | \sigma_1, \sigma'_1)] \quad (2.32)$$

In order to express $V'V$ in a similar way, we define \mathbb{S}' in the same way of \mathbb{S} , only exchanging the role of w and w' . Then $V'V$ is given by:

$$(V'V)_{\bar{\sigma}, \bar{\sigma}'} = \text{Tr} [\mathbb{S}'(\sigma_1, \sigma'_1 | \sigma_2, \sigma'_2) \cdots \mathbb{S}'(\sigma_N, \sigma'_N | \sigma_1, \sigma'_1)] \quad (2.33)$$

For reason which will be clarified in following chapters, we are interested in finding condition under which V and V' commute; this request can be shifted to the existence of a matrix $\mathbb{M}(a, a')$ such that

$$\mathbb{S}(a, a' | b, b') = \mathbb{M}(a, a') \mathbb{S}'(a, a' | b, b') \mathbb{M}^{-1}(b, b') \quad (2.34)$$

Multiplying from the right the above expression by $\mathbb{M}(b, b')$ and writing down explicitly all terms we obtain:

$$\begin{aligned} & \sum_c w(a, b, c, a'') w'(a'', c, b', a') w''(c, b, b'', b') \\ &= \sum_c w''(a'', a, c, a') w'(a, b, c, a') w(c, b'', b', a') \end{aligned} \quad (2.35)$$

where

$$w''(c, a, d, a') = (\mathbb{M}(a, a'))_{c,d} \quad (2.36)$$

which is called *Star-Triangle relation* or *Yang-Baxter equation*. It can be very useful to see the above expression in a subjective graphical way:

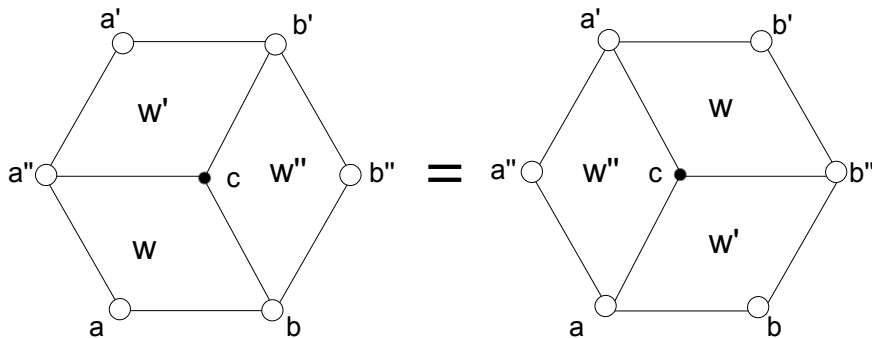


Figure 2.6: Graphical representation of the Yang-Baxter equation

Remembering the definition of matrices U_i , the star-triangle relation can be written as:

$$U_{i+1}U'_iU''_{i+1} = U''_iU'_{i+1}U_i \quad (2.37)$$

where U'_i and U''_i are defined exactly as U_i only with w replaced by w' and w'' . We are interested in non trivial solutions of the star-triangle relation, since we can solve the system with them. As shown in Chapter 9 of [6], we know that the solution of the model can be obtained by the commutability of its transfer matrices, i.e. by the solution of the Yang-Baxter equation.

The equation (2.37) can be rewritten in a more suggestive way

$$U_{i+1}(u)U_i(u')U_{i+1}(u'') = U_i(u'')U_{i+1}(u')U_i(u) \quad (2.38)$$

where we have supposed to define the Boltzmann weight w as a function of one parameter u

$$\begin{aligned} w &\equiv w(u) \\ w' &\equiv w(u') \\ w'' &\equiv w(u'') \end{aligned} \quad (2.39)$$

As we will see in (2.44), the YB equation can be satisfied if $u'' = u' - u$, allowing us to re-write (2.38) as

$$U_{i+1}(u)U_i(u')U_{i+1}(u' - u) = U_i(u' - u)U_{i+1}(u')U_i(u) \quad (2.40)$$

which is the most known form of the Yang-Baxter Equation.

Since the operator $\prod_i U_i(u)$ represents an entire row (rotated by $\frac{\pi}{4}$) its knowledge is fundamental for performing the hamiltonian limit (Section 2.2.1) of the model

$$H = \sum_i H_i = - \left. \frac{d}{du} \log \prod_i U_i(u) \right|_{u=0} = - \sum_i \left. \frac{d}{du} \log U_i(u) \right|_{u=0} \quad (2.41)$$

obtaining

$$H_i = - \left. \frac{d}{du} \log U_i(u) \right|_{u=0} = - \frac{1}{U_i(u)} \left. \frac{d}{du} U_i(u) \right|_{u=0} \quad (2.42)$$

2.1.3 Parametrization with elliptic functions

Now, let us focus our attention to non trivial solutions of the Yang-Baxter equation. Let us parametrize Boltzmann's weights using elliptic functions¹

$$\begin{aligned}
 w(a, b, a, b) &= \rho \operatorname{snh} \lambda \\
 w(a, b, -a, -b) &= \rho k \operatorname{snh} \lambda \operatorname{snh} u \operatorname{snh} (\lambda - u) \\
 w(a, b, a, -b) &= \rho \operatorname{snh} (\lambda - u) \\
 w(a, b, -a, b) &= \rho \operatorname{snh} u
 \end{aligned} \tag{2.43}$$

where $\operatorname{snh} z = i \operatorname{sn}(iz; k)$ and $\operatorname{sn}(z; k)$ denotes the elliptic sin function with argument z and modulus k . Parametrizing w' and w'' as in (2.43) but with replaced by u' and u'' respectively, the Yang-Baxter equation implies:

$$u' = u'' + u \tag{2.44}$$

The rotation of the lattice through $\frac{\pi}{2}$ implies the substitution of a, b, c, d with d, a, b, c in w ; thanks to (2.43) we can note that this rotation implies only a replacement of u by $\lambda - u$.

Supposing

$$\begin{aligned}
 \rho &> 0 \\
 0 < k &< 1 \\
 \lambda &< I(k')
 \end{aligned} \tag{2.45}$$

where $k' = \sqrt{1 - k^2}$ and $\frac{I(m)}{2}$ is the complete elliptic integral of the first kind of modulus m :

$$I(m) = 2 \int_0^{\frac{\pi}{2}} dx \frac{1}{\sqrt{1 - m \sin^2 x}} \tag{2.46}$$

we can ensure that w is non-negative for each $0 \leq u \leq \lambda$.

Using this parametrization we can say that $V = V(u)$ and $V' = V(u')$ commute $\forall u, u'$ if k, λ and ρ parameters are the same for V and V' .

Let us now consider for a while a column-inhomogeneous model, for which the anisotropy parameter u is different for each column; the above result can be generalized obtaining

$$[V(u_1, \dots, u_N), V(u'_1, \dots, u'_N)] = 0 \text{ if } u'_j - u_j \text{ do not depend on } j \tag{2.47}$$

¹For a brief review of elliptic functions, see, for example, the Chapter 15 of [6]

In $N = 2$ case, after setting $u_1 = u$ and $u_2 = v$, V and V' commute if $u - u' = v - v'$ or $u - v = u' - v'$. Since the commutativity between two operators imply that they share the same base of eigenvectors, V 's eigenvectors depend only on the difference $u - v$.

In order to understand better this method, we will list some examples of this parametrisation in some well-known models.

Example: the 8-vertex model

Let us consider the archetypal 8-vertex model. It is defined on a square lattice \mathcal{L} ; on each edge an arrow is drawn with the only constraint to have an even number of entering arrows in each edge. Thus there are eight possible vertex configurations.

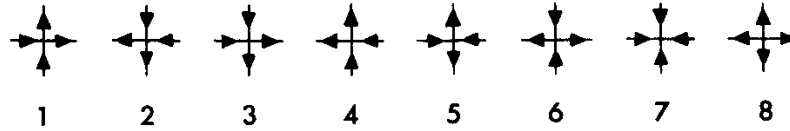


Figure 2.7: Allowed vertex configurations that define the 8-vertex model

The Boltzman weight for each vertex configuration is given by:

$$w_j = e^{-\varepsilon_j/T} \tag{2.48}$$

If one considers equally probable two vertex configurations which are related by a global flipping of all their arrows (which is equivalent to consider the configuration energy invariant under the inversion of all arrows), possible inequivalent vertex configurations are reduced to four only, whose Boltzmann weights are called here $a = w_1 = w_2, b = w_3 = w_4, c = w_5 = w_6$ and $d = w_7 = w_8$. Models which satisfy this symmetry are called zero-field 8-vertex models.

For this kind of models the Yang-Baxter equations are given by:

$$\begin{aligned} ac'a'' + da'd'' &= bc'b'' + ca'c'' \\ ab'c'' + dd'b'' &= ba'c'' + cc'b'' \\ cb'a'' + bd'd'' &= ca'b'' + bc'c'' \\ ad'b'' + db'c'' &= bd'a'' + cb'd'' \\ aa'd'' + dc'a'' &= bb'd'' + cd'a'' \\ da'a'' + ac'd'' &= db'b'' + ad'c'' \end{aligned} \tag{2.49}$$

2.1. Corner Transfer Matrix

Writing the first, the third, the fourth and the sixth equations of the above system as linear equations for double primed variables and taking the determinant of this new system one obtains:

$$\det(\cdot) = (cda'b' - abc'd') ((a^2 - b^2)(c'^2 - d'^2) + (c^2 - d^2)(a'^2 - b'^2)) \quad (2.50)$$

In order to have non trivial solutions of the YB equation, we require that the determinant (2.50) vanishes. This request is satisfied if the first term of (2.50) vanishes:

$$\frac{cd}{ab} = \frac{c'd'}{a'b'} \quad (2.51)$$

Writing down the non-trivial solution for double primed variables and substituting these in the second (or fifth) equation of (2.49) we obtain:

$$\frac{a^2 + b^2 - c^2 - d^2}{ab} = \frac{a'^2 + b'^2 - c'^2 - d'^2}{a'b'} \quad (2.52)$$

The request to have a non trivial solution of the YB equation can be written as

$$\begin{aligned} \Gamma &= \Gamma' \\ \Delta &= \Delta' \end{aligned} \quad (2.53)$$

where

$$\begin{aligned} \Gamma &= \frac{ab - cd}{ab + cd} \\ \text{and} \\ \Delta &= \frac{a^2 + b^2 - c^2 - d^2}{2(ab + cd)} \end{aligned} \quad (2.54)$$

What we want to do now is to parametrize a, b, c and d with other variables, say ρ, λ, k and v (ρ normalization factor), so that former variables are entire functions of v , but Γ and Δ are independent from v and ρ . In this way we can obtain a class of transfer matrices $V' = V(v')$ which all commute with $V = V(v)$ if their λ and k values are equal to V 's ones.

After setting

$$\gamma = \frac{1 - \Gamma}{1 + \Gamma} = \frac{cd}{ab} \quad (2.55)$$

we can eliminate d from (2.54) and obtain

$$2\Delta(1 + \gamma)\frac{ab}{cc} = \frac{a^2}{c^2} + \frac{b^2}{c^2} - 1 - \frac{a^2 b^2}{c^2 c^2} \gamma^2 \quad (2.56)$$

which can be seen as a quadratic form of $\frac{a}{c}$ for $\frac{b}{c}$ given. Its discriminant is given by

$$\text{Discr} = \Delta^2(1 + \gamma)^2 \left(\frac{b}{c}\right)^2 - \left[\left(\frac{b}{c}\right)^2 - 1\right] \left[1 - \gamma^2 \left(\frac{b}{c}\right)^2\right] \quad (2.57)$$

which is itself a quadratic form of $\frac{b}{c}$ and it can be written as:

$$\text{Discr} = \left(1 - y^2 \frac{b^2}{c^2}\right) \left(1 - k^2 y^2 \frac{b^2}{c^2}\right) \quad (2.58)$$

where new variables k and y are solution of the following equations:

$$\begin{aligned} k^2 y^4 &= \gamma^2 \\ (1 + k^2) y^2 &= 1 + \gamma^2 - \Delta^2 (1 + \gamma^2)^2 \end{aligned} \quad (2.59)$$

Using (2.57) and (2.58) the quantity $\frac{a}{c}$ can be written as:

$$\frac{a}{c} = \frac{\sqrt{\text{Discr}} \pm \frac{b}{c} \Delta}{1 + \left(\frac{b}{c}\right)^2} \quad (2.60)$$

Since Δ does not depend on v , if $\frac{b}{c}$ and the square root of (2.58) are meromorphic² function of v , $\frac{a}{c}$ will be itself meromorphic. The (2.58) structure suggests the elliptic parametrization $\frac{b}{c} = \frac{1}{y} \text{sn} iu$, since Jacobian elliptic functions satisfy the following generalized trigonometric relation (for further details on Jacobian elliptic function, we refer to chapt. 15 of [6]):

$$\begin{aligned} \text{cn}^2 u + \text{sn}^2 u &= 1 \\ \text{dn}^2 u + k^2 \text{sn}^2 u &= 1 \end{aligned} \quad (2.61)$$

Using some algebraic properties of the Jacobian functions we can write:

$$\frac{a}{c} = y \frac{\Delta(1 + \gamma) \text{sn} iu + y \text{cn} iu \text{dn} iu}{y^2 - \gamma^2 \text{sn}^2 iu} \quad (2.62)$$

recalling the meromorphic property of Jacobi's functions, we see that we have obtained our aim and parametrized the former $a \dots d$ variables in term of entire functions.

In order to eliminate the 'buffer' y variable from our expression we can write

$$k \text{sn} i\lambda = -\frac{\gamma}{y} \quad (2.63)$$

²A meromorphic function is a complex function which is not holomorphic in, at most, a numerable set of point of the complex plane.

2.1. Corner Transfer Matrix

Summarising results of this parametrisation:

$$\begin{aligned}
 y &= \operatorname{sn} i\lambda \\
 \gamma &= -k \operatorname{sn}^2 i\lambda \\
 \Gamma &= \frac{1 + k \operatorname{sn}^2 i\lambda}{1 - k^2 \operatorname{sn}^2 i\lambda} \\
 \Delta &= -\frac{\operatorname{cn} i\lambda \operatorname{dn} i\lambda}{1 - k^2 \operatorname{sn}^2 i\lambda}
 \end{aligned} \tag{2.64}$$

and

$$a : b : c : d = \operatorname{snh}(\lambda - u) : \operatorname{snh} u : \operatorname{snh} \lambda : k \operatorname{snh} \lambda : \operatorname{snh} u \operatorname{snh}(\lambda - u) \tag{2.65}$$

or

$$\begin{aligned}
 a &= \rho \operatorname{snh}(\lambda - u) \\
 b &= \rho \operatorname{snh} u \\
 c &= \rho k \operatorname{snh} \lambda \\
 d &= \rho \operatorname{snh}(\lambda - u)
 \end{aligned} \tag{2.66}$$

where

$$\operatorname{snh} u = -i \operatorname{sn} iu \tag{2.67}$$

and ρ is some positive normalization factor.

Since the behavior of the eight-vertex model depends on four physical parameters a, b, c and d , these quantities determine the thermodynamic phase in which the system lies.

If one consider $u = \frac{1}{2}(\lambda + v)$ and parametrization parameter such that

$$\begin{aligned}
 0 &< k < 1 \\
 0 &< \lambda < I(k') \\
 |v| &< \lambda \\
 \rho &> 0
 \end{aligned} \tag{2.68}$$

we have

$$0 < u < \lambda \tag{2.69}$$

With this choice all Boltzmann weights a, \dots, d are positive, then (2.68) is a physical allowable restriction. From the expression (2.64) we can see that $\Delta < -1$ in

the above (2.68) range.

From the (2.54) definitions we can recover

$$(a + b)^2 < (c - d)^2 \tag{2.70}$$

From previous considerations we can parametrize $\frac{d}{c}$ as

$$\frac{d}{c} = -k \operatorname{sn}(iu) \operatorname{sn}(i\lambda - iu) \tag{2.71}$$

which has a maximum in $u = \frac{1}{2}\lambda$, when it is considered as a function on u . Since this maximum must be less than one, we recover $d < c$. Taking the square root of (2.70) we obtain

$$c > a + b + d \tag{2.72}$$

Summarizing, the restriction (2.68) implies (2.72); conversely, there is a unique real choice of ρ, λ, v, u and k for a given a, b, c, d set which satisfy (2.72). The above (2.72) condition is therefore called *principal regime*.

Since the dominant Boltzmann weight is c , the ground state is given by the configuration in which each couple of adjacent arrows point in opposite directions (for two adjacent arrows we mean here two arrows which share a vertex).

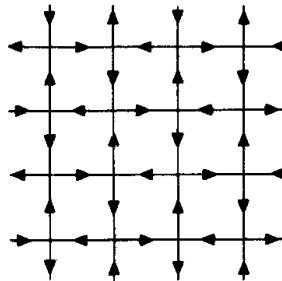


Figure 2.8: Ground State configuration in the Anti-ferroelectric regime

For this reason this regime is also called *anti-ferroelectric*. In the following considerations, we always refer to this regime, even if a, \dots, d parameters do not satisfy (2.72): in fact it any set of a, \dots, d values can be mapped into the principal regime. Considering all possible values for a, \dots, d it could be discovered that five different regimes exist:

- I. Ferroelectric: $a > b + c + d, \Delta > 1$

2.1. Corner Transfer Matrix

II. Ferroelectric: $b > a + c + d$, $\Delta > 1$

III. Disorderd: $a, b, c, d < \frac{1}{2}(a + b + c + d)$, $-1 < \Delta < 1$

IV. Anti-ferroelectric: $c < a + b + d$, $\Delta < -1$

V. Anti-ferroelectric: $d < a + b + c$, $\Delta < -1$

Thus the system is ordered if $|\Delta| > 1$ and disordered if $|\Delta| < 1$.

The eight-vertex model plays a very important role in the study of one dimensional systems, since it is the 2D classical equivalent of the quantum XYZ 1D chain.

In 1970 Sutherland demonstrated that the transfer matrix of the zero-field eight-vertex model commutes with the quantum hamiltonian H_{XYZ} ³:

$$H_{XYZ} = -\frac{1}{2} \sum_{i=1}^N J_x \sigma_i^x \sigma_{i+1}^x + J_y \sigma_i^y \sigma_{i+1}^y + J_z \sigma_i^z \sigma_{i+1}^z \quad (2.73)$$

if its parameters J_x, J_y, J_z are related to eight-vertex's ones:

$$J_x : J_y : J_z = 1 : \Gamma : \Delta \quad (2.74)$$

Recalling that our expressions have been obtained for the principal regime $\Delta < -1$, we cannot apply this correspondence for all values of J_a , but we have to re-arrange these parameters. Thanks to symmetries of the partition function, this re-arrangement can be easily shifted in the thermodynamic observables.

2.1.4 The thermodynamic limit

After having developed a solid mathematic analysis of IRF models using corner transfer matrices and elliptic parametrisation, we can now study these system in the thermodynamic limit.

Let us consider a system with N sites. Defining

$$\kappa = \lim_{N \rightarrow \infty} Z^{\frac{1}{N}} \quad (2.75)$$

we have an expression for the free-energy per site

$$f = -T \ln \kappa \quad (2.76)$$

³see, for example [6]

Recalling that the parameter α is the partition function of the system with boundary spins in the ground state we have

$$\kappa = \lim_{m \rightarrow \infty} \alpha^{\frac{2}{m(m+1)}} \quad (2.77)$$

where m is the number of sites on the horizontal edge.

What we expect from our system is that the above limit still exists if a fixed number of boundary spins are changed from their ground-state values; furthermore we expect that this change could affect the above result only for a multiplicative factor which tends to a finite-limit as $m \rightarrow \infty$. In other words we expect that the following limit exists:

$$\lim_{m \rightarrow \infty} \frac{A_{\bar{\sigma}, \bar{\sigma}'}}{A_{\bar{s}, \bar{s}'}} \quad (2.78)$$

The above convergence is provided if an integer $r > 0$ exists (independent of m) s.t.

$$\sigma_i = s_i \quad \forall i \geq r \quad (2.79)$$

and the same for primed variables.

Since the above relation (2.78) is nothing else than the normalized CTM A_n it is obvious that the limit

$$\lim_{m \rightarrow \infty} (A_n)_{\bar{\sigma}, \bar{\sigma}'} \quad (2.80)$$

exists. In a similar way we can expect the existence of the thermodynamic limit of B_n, C_n and D_n .

We will recall these formulæ in next sections.

2.1.5 Eigenvalues of CTM

In this section we will show an explicit calculation of thermodynamic observables using CTM.

Let us consider a square lattice with r rows with the bottom one equal to $\bar{\mu}$. The system is also divided in two parts by the central column; the bottom row is then divided in two parts, whose spins are denoted by $\bar{\sigma}'$ and $\bar{\sigma}$.

Boltzmann weights of the system are parametrized by w and the anisotropy parameter is equal to v for the left-side subsystem and to u for the right-side one (Fig. 2.9).

2.1. Corner Transfer Matrix

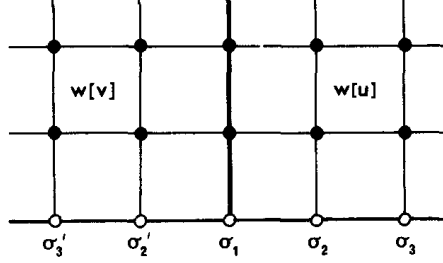


Figure 2.9: A lattice with two different anisotropy parameters

Let us denote with $\psi_{\bar{\sigma}, \bar{\sigma}'}$ the partition function of the system (keeping fixed the bottom line)

$$\psi_{\bar{\sigma}, \bar{\sigma}'} = \sum_{\bullet} \prod_{\square} w(\sigma_i, \sigma_j, \sigma_k, \sigma_l) \quad (2.81)$$

Thanks to the definition of corner transfer matrices A, \dots, D we can write the above expression as

$$\psi_{\bar{\sigma}, \bar{\sigma}'} = [B(u)C(v)]_{\bar{\sigma}, \bar{\sigma}'} \quad (2.82)$$

This partition function can also be evaluated applying r times the row-to-row transfer matrix V to $(\bar{\sigma}, \bar{\sigma}')$

$$\begin{aligned} \psi_{\bar{\sigma}, \bar{\sigma}'} &= \sum_{\bar{s}_1, \bar{s}'_1, \dots, \bar{s}_r, \bar{s}'_r} \langle \bar{\sigma}, \bar{\sigma}' | V | \bar{s}_1, \bar{s}'_1 \rangle \dots \langle \bar{s}'_{r-1}, \bar{s}_{r-1} | V | \bar{s}_r, \bar{s}'_r \rangle \\ &= \sum_{\bar{s}_r, \bar{s}'_r} \langle \bar{\sigma}, \bar{\sigma}' | V^r | \bar{s}_r, \bar{s}'_r \rangle \end{aligned} \quad (2.83)$$

expressing $|\bar{s}_r, \bar{s}'_r\rangle$ in the basis of eigenvectors of V , say $|n\rangle$, with eigenvalues λ_n , we have

$$\begin{aligned} \psi_{\bar{\sigma}, \bar{\sigma}'} &= \sum_n \langle \bar{\sigma}, \bar{\sigma}' | V^r | n \rangle \\ &= \sum_n \lambda_n^r \langle \bar{\sigma}, \bar{\sigma}' | n \rangle \end{aligned} \quad (2.84)$$

Thanks to the Perron-Frobenius theorem, since all entries of V are positive, its maximal (positive) eigenvalue λ_0 exists and is unique.

Thus, for large r , since $\lambda_0 > \lambda_{n \neq 0}$, we have $\lambda_0^r \gg \lambda_n^r$ and

$$\psi_{\bar{\sigma}, \bar{\sigma}'} \asymp \lambda_0^r \langle \bar{\sigma}, \bar{\sigma}' | 0 \rangle = \langle \bar{\sigma}, \bar{\sigma}' | V^r | 0 \rangle \quad (2.85)$$

Moreover ψ , seen as a vector with components $\psi_{\bar{\sigma}, \bar{\sigma}'}$, is the maximal eigenvector of V :

$$\begin{aligned} (V\psi)_{\sigma, \sigma'} &= \sum_{\bar{\nu}, \bar{\nu}'} V_{\bar{\sigma}, \bar{\sigma}' | \bar{\nu} \bar{\nu}'} \langle \bar{\nu}, \bar{\nu}' | V^r | 0 \rangle = \sum_{\bar{\nu}, \bar{\nu}'} \langle \bar{\sigma}, \bar{\sigma}' | V | \bar{\nu}, \bar{\nu}' \rangle \langle \bar{\nu}, \bar{\nu}' | V^r | 0 \rangle \\ &= \langle \bar{\sigma}, \bar{\sigma}' | V^{r+1} | 0 \rangle = \lambda_0^{r+1} \langle \bar{\sigma}, \bar{\sigma}' | 0 \rangle = \lambda_0 \psi_{\bar{\sigma}, \bar{\sigma}'} \end{aligned} \quad (2.86)$$

From previous considerations (2.47) about the dependance of V 's eigenvectors on anisotropy parameters, we have

$$\psi_{\bar{\sigma}, \bar{\sigma}'} = \tau'(u, v) X'(u - v)|_{\bar{\sigma}, \bar{\sigma}'} \quad (2.87)$$

from the fact that $\sigma_1 = \sigma'_1$, we can easily deduce the block-diagonal structure of X' , when it is considered as a matrix whose elements are $X'|_{\bar{\sigma}, \bar{\sigma}'}$.

Comparing the equation (2.87) with a normalised version of (2.82)⁴ we have

$$B_n(u)C_n(v) = \tau'(u, v)X'(u - v) \quad (2.88)$$

if we suppose to absorb α and β factors into τ' .

Rotating clockwise the lattice in Fig. 2.9 through $\frac{\pi}{2}$ we can make similar computation and write

$$A_n(u)B_n(v) = \tau(u, v)X(u - v) \quad (2.89)$$

Due to the infinite dimensions of A and B matrices in the thermodynamic limit, each element $(AB)_{ij}$ involves a sum of an infinite set of numbers $\sum_k A_{ik}B_{kj}$ and these sums probably do not converge. However, this divergent factor is common to all elements and then it can be absorbed into τ and plays no role in next computations.

Let us now focus on the model whose Boltzmann weights are symmetric under the exchange of opposite vertices.

$$w(a, b, c, d) = w(c, b, a, d) = w(a, d, c, b) \quad (2.90)$$

This model is not so restrictive since it describes, for instance, the ferromagnetic eight-vertex model.

⁴This normalisation can be easily obtained setting $\lambda_0 = 1$

2.1. Corner Transfer Matrix

In this case we have $D = B$ and $C = A$, moreover B can be obtained from A by an anti-clockwise rotation though $\frac{\pi}{2}$. Thanks to these arguments we have:

$$\begin{aligned} C_n(v) &= A_n(v) \\ D_n(v) &= B_n(v) = A_n(\lambda - v) \end{aligned} \quad (2.91)$$

Replacing $\lambda - v$ by v in (2.89) we have

$$A_n(u)A_n(v) = \tau(u, \lambda - v)X(u + v - \lambda) \quad (2.92)$$

and

$$A_n(v)A_n(u) = \tau(v, \lambda - u)X(u + v - \lambda) \quad (2.93)$$

where the above expression is obtained interchanging u and v in the previous one. Comparing (2.91) and (2.92), and eliminating X , we have

$$\tau(v, \lambda - u)A_n(u)A_n(v) = \tau(u, \lambda - v)A_n(v)A_n(u) \quad (2.94)$$

In the representation in which $A_n(u)$ and $A_n(v)$ are diagonal matrices, they commute and the above expression gives

$$\tau(v, \lambda - u) = \tau(u, \lambda - v) \quad (2.95)$$

In conclusion, we have found that the matrices $A_n(u)$, $A_n(v)$ and $X(u + v - \lambda)$ commute with each other and therefore they have the same basis of eigenvectors, which do not depend on u or v .

Let $a_1(u)$ be the largest eigenvalue of $A_n(u)$ and $x_1(u)$ the corresponding eigenvalue of $X(u)$ (the one related to the same eigenvector). We can now define

$$\begin{aligned} A_d(u) &= \frac{1}{a_1(u)}P^{-1}A_n(u)P \\ X_d(u) &= \frac{1}{x_1(u)}P^{-1}X(u)P \end{aligned} \quad (2.96)$$

then $A_d(u)$ and $X_d(u)$ are diagonal matrices with the top-left element equal to one.

From the equation (2.94) we can obtain the following matrix multiplication equality:

$$(P^{-1}A_n(u)P)(P^{-1}A_n(v)P) = \tau(u, \lambda - v)(P^{-1}X(u + v - \lambda)P) \quad (2.97)$$

whose top left element reads

$$\tau(u, \lambda - v)x_1(u + v - \lambda) = a_1(u)a_1(v) \quad (2.98)$$

and (2.94) becomes an equality between diagonal matrices:

$$A_d(u)A_d(v) = X_d(u + v - \lambda) \quad (2.99)$$

Thanks to the validity of the above expression for all $u, v \in]0, \lambda[$ it is easy to show that

$$A_d(u)|_{r,r} = m_r e^{-\alpha_r u} \quad (2.100)$$

where m_r and α_r are parameters which do not depend on u .
Recalling relations between CTMs:

$$\begin{aligned} C_d(u) &= A_d(u) \\ D_d(u) &= B_d(u) \\ B_d(u) &= A_d(\lambda - u) \end{aligned} \quad (2.101)$$

we can evaluate the spontaneous magnetisation using the diagonalised version of (2.9)

$$\langle \sigma_1 \rangle = \frac{\sum_{r=1}^{\infty} S_r m_r^4 \exp(2\alpha_r \lambda)}{\sum_{r=1}^{\infty} m_r^4 \exp(2\alpha_r \lambda)} \quad (2.102)$$

where S_r is the eigenvalue of the spin operator S relative to the r -th eigenvector of A_n .

2.1.6 Magnetization for the eight-vertex model

What we want to do now is to use the above explained methods in a very important specific case: the eight-vertex model.

At first, let us consider the case $u = 0$: from the Jacobi's elliptic functions parametrisation we have:

$$w(a, b, c, d) = \rho \operatorname{snh} \lambda \delta(a, c) \quad (2.103)$$

If we suppose to have fixed boundary conditions such that $s = t = \dots = z$ and $s' = t' = \dots = z'$, the (2.24) reads

$$U_i = \rho \sinh \lambda \mathbb{1} \quad (2.104)$$

2.1. Corner Transfer Matrix

using the (2.28) expression we can build up the whole corner transfer matrix A

$$A(0) = (\rho \sinh \lambda)^{\frac{m(m+1)}{2}} \mathbb{1} \quad (2.105)$$

whose normalised version is given by

$$A_n(0) = \mathbb{1} \quad (2.106)$$

The maximal eigenvalue $a_1(0)$ of $A_n(0)$ is equal to one and then

$$A_d(0) = PA_n(0)P^{-1} = \mathbb{1} \quad (2.107)$$

Comparing the above expression with (2.100) one finds $m_1 = 1$ and $\alpha_1 = 0$. From this comparison it follows that $m_r = 1$ for each r and then

$$A_d(u)|_{r,r} = \exp(-\alpha_r u) \quad (2.108)$$

Since all Boltzmann weights are periodic in the variable u with period $4iI(k)$, the matrix $A_n(u)$ is itself periodic with the same period. Thanks to these considerations we have

$$\exp(-\alpha_r u) = \exp(-\alpha_r(u + 4iI(k))) \quad (2.109)$$

which gives

$$\alpha_r = \frac{\pi}{2I} n_r \quad (2.110)$$

with n_r integer.

Now we want to evaluate the spontaneous magnetisation at zero temperature, which corresponds to $k \rightarrow 0$ while $\frac{\lambda}{I(\sqrt{1-k^2})}$ and u remain fixed. Recalling that

$$\lim_{m \rightarrow 1} I(m) = +\infty \quad (2.111)$$

and that

$$\lim_{k \rightarrow 0} \sinh u = \sinh u \quad (2.112)$$

we have

$$\begin{aligned} w(a, b, a, b) &\sim \frac{1}{2} \rho x^{-1} \\ w(a, b, -a, -b) &\sim 0 \\ w(a, b, a, -b) &\sim \frac{1}{2} \rho x^{-1} \exp\left(-\frac{\pi u}{2I(k)}\right) \\ w(a, b, -a, b) &\sim 0 \end{aligned} \quad (2.113)$$

with

$$x = \exp\left(-\frac{\pi\lambda}{2I(k)}\right) \quad (2.114)$$

The above asymptotic behaviour for small k is given by the fact that $I(k) = \frac{\pi}{2} + O(k^2)$.

Recalling the (2.24) expression for U_i , we have

$$(U_i)_{\bar{\sigma}, \bar{\sigma}'} = \frac{1}{2} \rho x^{-1} \exp\left[-\frac{\pi u(1 - \sigma_{i-1}\sigma_{i+1})}{4I(k)}\right] \delta_{\bar{\sigma}, \bar{\sigma}'} \quad (2.115)$$

using (2.28)⁵ one can see that also A is diagonal and its A_d form is obtained by a normalising to one its maximal eigenvalue

$$A_d(u)|_{\bar{\sigma}, \bar{\sigma}} = \exp\left[-\frac{\pi u}{4I(k)} \sum_{i=2}^{m+1} (i-1)(1 - \sigma_{i-1}\sigma_{i+1})\right] \quad (2.116)$$

Substituting the single index r with a multi-valued one σ and comparing (2.109) with (2.116) we obtain

$$n_{\bar{\sigma}} = \frac{1}{2} \sum_{i=2}^{m+1} (i-1)(1 - \sigma_{i-1}\sigma_{i+1}) \quad (2.117)$$

Thanks to this equality, we have an expression for $A_d(u)$ in the ferromagnetic ordered phase.

For a better developing of following formulae, it is useful to introduce a new set of spin variables μ_1, \dots, μ_m :

$$\mu_i = \sigma_i \sigma_{i+2} \quad (2.118)$$

as before we consider $\sigma_{m+1} = \sigma_{m+2} = +1$. Thus $A_d(u)$ is a diagonal matrix with a new set of multivalued indices $\bar{\mu} = \{\mu_1, \dots, \mu_m\}$:

$$A_d(u)|_{\bar{\mu}, \bar{\mu}} = \exp\left[-\frac{\pi u}{4I(k)} \sum_{i=1}^m i(1 - \mu_i)\right] \quad (2.119)$$

Using the definition (2.118) of μ_i we can see that

$$\sigma_1 = \mu_1 \mu_3 \mu_5 \dots \quad (2.120)$$

⁵This formula requires the knowledge of the values of most external spins; they can be chosen in the ferromagnetic ordered state $+1$ (or -1)

2.1. Corner Transfer Matrix

and the spin operator S has the following entries (in the $\bar{\mu}$ basis):

$$S_{\bar{\mu}, \bar{\mu}'} = \delta(\bar{\mu}, \bar{\mu}') \mu_1 \mu_3 \dots \quad (2.121)$$

At last we can write (2.119) using the tensor product notation for matrices (the Kronecker product):

$$A_d(u) = \begin{bmatrix} \exp\left(-\frac{\pi u}{4I(k)} \cdot 1 \cdot 0\right) & 0 \\ 0 & \exp\left(-\frac{\pi u}{4I(k)} \cdot 1 \cdot 2\right) \end{bmatrix} \otimes \begin{bmatrix} \exp\left(-\frac{\pi u}{4I(k)} \cdot 1 \cdot 0\right) & 0 \\ 0 & \exp\left(-\frac{\pi u}{4I(k)} \cdot 2 \cdot 2\right) \end{bmatrix} \otimes \begin{bmatrix} \exp\left(-\frac{\pi u}{4I(k)} \cdot 1 \cdot 0\right) & 0 \\ 0 & \exp\left(-\frac{\pi u}{4I(k)} \cdot 3 \cdot 2\right) \end{bmatrix} \otimes \dots \quad (2.122)$$

Let us explain this notation: each 2×2 diagonal matrix explores the two possibilities of one single index $\mu_i = \pm 1$. The i -th matrix is given by

$$\begin{bmatrix} \exp\left[\frac{\pi u}{4I(k)} i(1 - (\mu_i = +1))\right] & 0 \\ 0 & \exp\left[\frac{\pi u}{4I(k)} i(1 - (\mu_i = -1))\right] \end{bmatrix} \quad (2.123)$$

Denoting

$$s = \exp\left(-\frac{\pi u}{4I(k)}\right) \quad (2.124)$$

we can rewrite (2.122) in a more compact way:

$$A_d(u) = \begin{bmatrix} 1 & 0 \\ 0 & s \end{bmatrix} \otimes \begin{bmatrix} 1 & 0 \\ 0 & s^2 \end{bmatrix} \otimes \begin{bmatrix} 1 & 0 \\ 0 & s^3 \end{bmatrix} \otimes \begin{bmatrix} 1 & 0 \\ 0 & s^4 \end{bmatrix} \otimes \dots \quad (2.125)$$

Thanks to our previous considerations it is easy to find an expression for $B_d(u)$

$$B_d(u) = \begin{bmatrix} 1 & 0 \\ 0 & t \end{bmatrix} \otimes \begin{bmatrix} 1 & 0 \\ 0 & t^2 \end{bmatrix} \otimes \begin{bmatrix} 1 & 0 \\ 0 & t^3 \end{bmatrix} \otimes \begin{bmatrix} 1 & 0 \\ 0 & t^4 \end{bmatrix} \otimes \dots \quad (2.126)$$

with t defined as s only with u replaced by $\lambda - u$.

At last, it easily to build up the matrix expression for S

$$S = \begin{bmatrix} 1 & 0 \\ 0 & -1 \end{bmatrix} \otimes \begin{bmatrix} 1 & 0 \\ 0 & -1 \end{bmatrix} \otimes \begin{bmatrix} 1 & 0 \\ 0 & -1 \end{bmatrix} \otimes \begin{bmatrix} 1 & 0 \\ 0 & -1 \end{bmatrix} \dots \quad (2.127)$$

Substituting above expressions in (2.9) and using some trace's properties⁶ of the Kronecker product, we have

$$\langle \sigma_1 \rangle = \prod_{n=1}^{\infty} \frac{1 - x^{4n-2}}{1 + x^{4n-2}} \quad (2.128)$$

Evaluating the spontaneous magnetisation for the Ising case of the eight-vertex, we obtain:

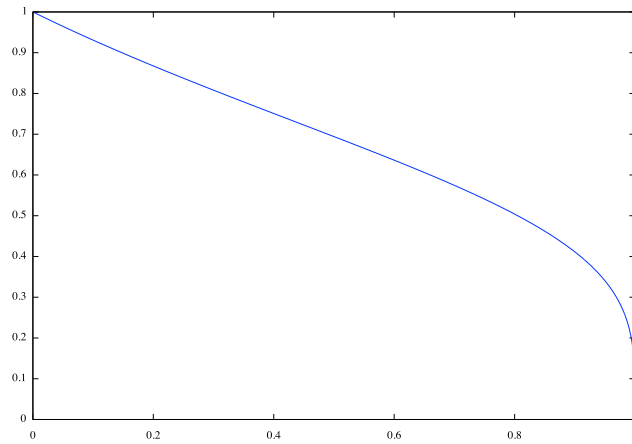


Figure 2.10: Magnetisation $\langle \sigma_1 \rangle$ vs. temperature parameter k in the Ising case

⁶ $\text{Tr } A \otimes B = \text{Tr } A \text{ Tr } B$

2.2 The reduced density matrix

The main purpose of this section is the definition of the reduced density matrix ρ_A and its representation via CTM [8, 9, 7].

2.2.1 Equivalence between 2 dimensional classical and 1+1 dimensional quantum systems

In the following paragraphs we will invoke the equivalence between 2D classical systems and 1D quantum ones.

Let \hat{H} be the hamiltonian of a 1D quantum system in continue time (the spatial dimension can be considered both continue or discrete). The time evolution operator is given by

$$\hat{O}(\tau) = e^{-\tau\hat{H}} \quad (2.129)$$

This operator transforms a quantum state $|\psi(t)\rangle$ into in its time evolved $|\psi(t + \tau)\rangle$. In the same way a row-to-row transfer matrix \hat{T} transform a row in the following one, carrying forward by the lattice spacing a .

For this reason the analogy between the time evolution and the transfer matrix arises, allowing us to consider the so called *Hamiltonian limit*, in which

$$\hat{T} = e^{-a\hat{H}} \text{ for } a \sim 0 \quad (2.130)$$

In this equivalence the largest eigenvalues of the transfer matrix (the most significative) is related to the lowest Hamiltonian's one (also the most significative), i.e. the eigenvector of \hat{T} related to the largest eigenvalue λ_M is also the ground state of \hat{H} with eigenvalue E_0 . In order to understand better this procedure, in Appendix C we will show the hamiltonian limit of the eight-vertex model, which leads to the XYZ spin chain.

2.2.2 Reduced density matrix

Let $|\phi_0\rangle$ be the ground state of the hamiltonian \hat{H} of a quantum spin chain. The density matrix ρ of the whole system is then given by:

$$\rho = |\phi_0\rangle\langle\phi_0| \quad (2.131)$$

Since we are interested in the bipartite entanglement of an infinite spin chain, the subsystem A will be the half part of our infinite chain.

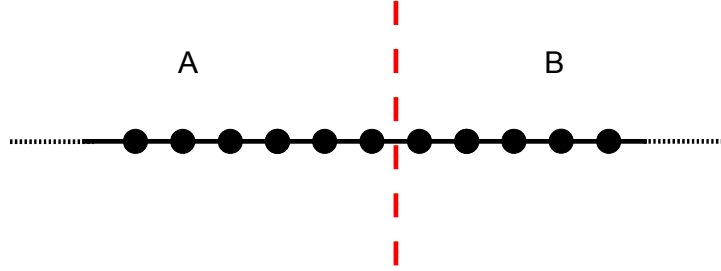


Figure 2.11: A bipartite system divided into two subsystems A and B

The Hilbert space \mathcal{H}_{AB} of the system can be factorized in the product of the Hilbert space of the two subsystems:

$$\mathcal{H}_{AB} = \mathcal{H}_A \otimes \mathcal{H}_B \quad (2.132)$$

The reduced density matrix ρ_A is given by

$$\begin{aligned} \rho_A &= \text{Tr}_B \rho \\ &= \sum_n \langle n | \rho | n \rangle_B \end{aligned} \quad (2.133)$$

where

$$\left\{ |n\rangle_B \right\}_n \quad (2.134)$$

labels a normal basis for \mathcal{H}_B .

Let $|\sigma\rangle = |\sigma_A\rangle_A \otimes |\sigma_B\rangle_B$ be a spin configuration of the whole system. Define

$$\phi_0(\sigma) = \langle \sigma | \phi_0 \rangle \quad (2.135)$$

the reduced density matrix is then given by

$$\begin{aligned} \rho_A &= \sum_{\sigma_B} \langle \sigma_B | \rho | \sigma_B \rangle_B \\ &= \sum_{\sigma_B} \langle \sigma_B | \phi_0 \rangle \langle \phi_0 | \sigma_B \rangle_B \end{aligned} \quad (2.136)$$

Thus

$$\begin{aligned} \rho_A(\sigma_A, \sigma'_A) &= \langle \sigma'_A | \rho_A | \sigma_A \rangle_B \\ &= \sum_{\sigma_B} \phi_0^*(\sigma'_A, \sigma_B) \phi_0(\sigma_A, \sigma_B) \end{aligned} \quad (2.137)$$

2.2. The reduced density matrix

Since $|\phi_0\rangle$ is the ground state of \hat{H} then

$$\hat{H}|\phi_0\rangle = E_0|\phi_0\rangle \quad (2.138)$$

Let $\hat{T} = e^{-a\hat{H}}$ be a row-to-row transfer matrix of a 2D. We have

$$[\hat{H}, \hat{T}] = 0 \quad (2.139)$$

Thanks to commutativity the two above operators share the same eigenbasis.

Let V_1 be the Hilbert space of a single site, thus $\mathcal{H} = V_1^{\otimes 2m}$, where $2m$ is the total length of the system (at the present time we consider a finite system; in further developments we will take the thermodynamic limit $m \rightarrow \infty$). Suppose that $|\psi\rangle \in \mathcal{H}$ is a vector of our Hilbert space, then it can be expressed as

$$|\psi\rangle = |\phi_0\rangle + \sum_{k \neq 0} C_k |\phi_k\rangle \quad (2.140)$$

where

$$\{|\phi_k\rangle\}_{k=0}^{(\dim_{\mathbb{C}} V_1)^{2m}} \quad (2.141)$$

is an orthonormal eigenbasis of \hat{H} and \hat{T} .

The action of the transfer matrix \hat{T} on $|\psi\rangle$ is given by

$$\hat{T}|\psi\rangle = \lambda_M|\phi_0\rangle + \sum_{k \neq 0} c_k \lambda_k |\phi_k\rangle \quad (2.142)$$

and the action of \hat{T} N times is given by

$$\hat{T}^N|\psi\rangle = \lambda_M^N \left(|\phi_0\rangle + \sum_{k \neq 0} c_k \left(\frac{\lambda_k}{\lambda_M} \right)^N |\phi_k\rangle \right) \quad (2.143)$$

which for large N tends to

$$\hat{T}^N|\psi\rangle \simeq \lambda_M^N |\phi_0\rangle \quad (2.144)$$

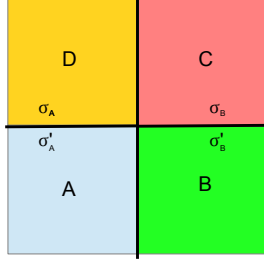
Normalising $\lambda_M = 1$ we have

$$\phi_0(\sigma) = \langle \sigma | \phi_0 \rangle \simeq \langle \sigma | \hat{T}^N | \psi \rangle \quad (2.145)$$

Notice that the RHS of the above equation is equivalent to the partition function of a system of N rows, with the top one equal to $|\psi\rangle$ and the bottom one to $|\sigma\rangle$. In the $N \rightarrow \infty$ regime the choice of $|\psi\rangle$ is completely irrelevant and then

$$\phi_0(\sigma) \quad (2.146)$$

is the partition function of an infinite half plane ($y > 0$) with the lower boundary $|\sigma\rangle$. In the same way $\phi_0^*(\sigma')$ is the partition function of the lower side of the plane with the top row equal to $|\sigma'\rangle$.



The partition function \mathcal{Z}_1 of the whole plane can be obtained taking $\phi_0(\sigma)$ and $\phi_0^*(\sigma)$ together and summing over all σ .

Since we are looking for the reduced density matrix of the bipartite system, let us explicit σ as (σ_A, σ_B) , where subscripts denote the subsystem (A for the negative semi-axis x and B for the positive one). Using the corner transfer matrix notation, the reduced density matrix is given by

Figure 2.12: The partition function \mathcal{Z} and its decompositions via CTM

$$\rho_A(\sigma_A, \sigma'_A) \propto ABCD|_{\sigma_A, \sigma'_A} \quad (2.147)$$

since $\phi_0^*(\sigma'_A, \sigma'_B) = AB$ and $\phi_0(\sigma_A, \sigma_B) = CD$.

In order to have a normalised density matrix ($\text{Tr}_A \rho_A = 1$) we can set

$$\begin{aligned} \rho_A &= \frac{ABCD}{\mathcal{Z}_1} \\ \mathcal{Z}_1 &= \text{Tr}_A ABCD \end{aligned} \quad (2.148)$$

The evaluation of the Rényi entropy $S_A^{(\alpha)}$ requires the knowledge of $\text{Tr}_A \rho_A^\alpha$, which is given by

$$\frac{\mathcal{Z}_\alpha}{\mathcal{Z}_1^\alpha} \equiv \text{Tr}_A \rho_A^\alpha = \frac{1}{\mathcal{Z}_1^\alpha} \text{Tr} \left[\overbrace{ABCD \cdots ABCD}^{\alpha \text{ times}} \right] \quad (2.149)$$

The last formula will be very useful in the evaluation of the bipartite entanglement entropy in models whose expression of CTM of an equivalent 2D classical model is known, as the Ising, the 8-vertex or the RSOS models.

Chapter 3

Entanglement Entropy in Conformal Field Theory

In this chapter we will introduce branch point twist field [10], and their application in the evaluation of Entanglement Entropy [11, 10] in Conformal Field Theory. In particular we will present a technique for the evaluation of Entanglement of a finite or infinite system at its critical point and of an infinite system near its critical point.

3.1 Branch-Point Twist Fields

In this section we will introduce *Branch-Point Twist Fields*, which are a powerful method implemented in [10] to perform the ‘replica trick’, which is a vital step [11] in the evaluation of Entanglement Entropy in Quantum Field Theory.

3.1.1 Twist fields in Quantum Field Theory

Let $\mathcal{Z}[\mathcal{L}, \mathcal{R}]$ be the partition function of a two-dimensional Quantum Field Theory (QFT) with local lagrangian density \mathcal{L} defined on a Riemann surface \mathcal{R} . Using the path integral formalism the partition function can be written as

$$\mathcal{Z}[\mathcal{L}, \mathcal{R}] = \int \mathcal{D}_{\mathcal{R}}\phi \exp \left[- \int_{\mathcal{R}} dx dy \mathcal{L}[\phi](x, y) \right] \quad (3.1)$$

Consider now a Riemann surface \mathcal{R} with zero curvature everywhere except for a discrete set A . Since the lagrangian density \mathcal{L} does not depend on the surface \mathcal{R} , the path integral can be expressed as an object evaluated on \mathbb{C} , where the structure of the Riemann surface is implemented through appropriate conditions around boundary points of A [10].

These boundary conditions can be implemented creating ‘artificial’ fields around A , whose role is to ‘apply’ boundary conditions to physical fields.

Artificial fields arising from boundaries are called *twist fields*. Twist fields exist in a QFT equipped with a global internal symmetry σ , i.e. a symmetry transformation which does not depend on the position and does not affect the action:

$$\int_{\mathbb{C}} dx dy \mathcal{L}[\phi](x, y) = \int_{\mathbb{C}} dx dy \mathcal{L}[\sigma\phi](x, y) \quad (3.2)$$

During the evaluation of correlation functions in such theories using path integral, it is important to take into account the effect of the symmetry, since it modifies the Riemann surface where physical fields live¹.

These theories can be defined in \mathbb{C} with appropriate boundary conditions around a point, say the origin $(0, 0)$; thanks to boundary conditions we can evaluate correlation functions taking them into account. The presence of the boundary conditions in $(0, 0)$ is equivalent to have a branch cut in the positive real axis.

$$\langle A_1(x_1) \cdots A_n(x_n) \rangle_{\mathcal{R}, \mathcal{L}} \propto \int_{C_\sigma(0,0)} \mathcal{D}\phi A_1(x_1) \cdots A_n(x_n) \exp \left[- \int_{\mathbb{R}^2} dx dy \mathcal{L}[\phi](x, y) \right] \quad (3.3)$$

where $C_\sigma(a, b)$ defines boundary conditions

$$\phi(x, b^+) = \sigma\phi(x, b^-) \quad x \in [a, +\infty[\quad (3.4)$$

Now, we can define [10] twist field \mathcal{T}_σ as an operator which implements directly boundary conditions:

$$\mathcal{T}_\sigma\phi(x, 0^+) = \sigma\phi(x, 0^-)\mathcal{T}_\sigma \quad x \in [0, +\infty[\quad (3.5)$$

In other words, the effect of the twist field is to take into account the effect of the symmetry turning around the origin. Notice that by definition it works only around the point which breaks the plane geometry of \mathbb{C} .

Thanks to twist fields, correlation functions can be evaluated in the whole \mathbb{C} plane without taking into account boundary conditions, since they are automatically satisfied by the action of twist fields:

$$\begin{aligned} \langle A_1(x_1) \cdots A_n(x_n) \rangle_{\mathcal{R}, \mathcal{L}} &= \langle \mathcal{T}_\sigma A_1(x_1) \cdots A_n(x_n) \rangle_{\mathbb{C}, \mathcal{L}} \\ &\propto \int \mathcal{D}\phi \mathcal{T}_\sigma A_1(x_1) \cdots A_n(x_n) \exp \left[- \int_{\mathbb{C}} dx dy \mathcal{L}[\phi](x, y) \right] \end{aligned} \quad (3.6)$$

¹For example, in the evaluation of the partition function of N indistinguishable particles, they do not live on \mathbb{R}^{6N} , but in a more complex space obtained identifying two points in the phase space which differ only for a permutation of two or more particles.

3.1. Branch-Point Twist Fields

Summarising, in order to construct twist field, we look for some fields which implement the curvature of the Riemann surface. If two or more fields with this property exist, we define twist field the one with the lower scaling dimension. This selection procedure reminds the identification of primary fields in Conformal Field Theories.

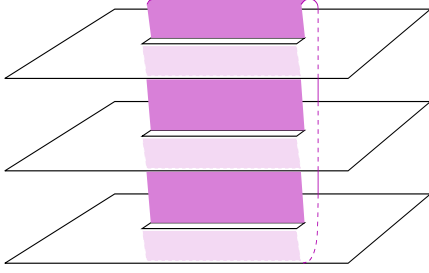


Figure 3.1: The Riemann surface $\mathcal{M}_{3,1,b}$. Picture taken from [10]

Define $\mathcal{M}_{n,a,b}$ as the Riemann surface composed by n sheets sequentially sewn to each other on the segment $(x \in [a, b], y = 0)$ with the n -th sheet sewn with the first one (see Fig. 3.1 for $n = 3$).

As we said before, the partition function on the multi-sheeted surface can be expressed as a path integral of fields belonging to the whole Riemann surface, or it can be obtained taking n -copies of a field ϕ belonging to \mathbb{C} and implementing special boundary conditions on these copies:

$$\mathcal{Z}[\mathcal{L}, \mathcal{M}_{n,a,b}] = \int_{\mathcal{C}(a,b)} \mathcal{D}\phi_1 \cdots \mathcal{D}\phi_n \exp \left[- \int_{\mathbb{C}} dx dy \mathcal{L}[\phi_1](x, y) + \cdots + \mathcal{L}[\phi_n](x, y) \right] \quad (3.7)$$

where $\mathcal{C}(a, b)$ denotes boundary conditions imposed by the geometry of the manifold:

$$\phi_i(x, 0^+) = \phi_{i+1}(x, 0^-) \quad x \in [a, b] \quad (3.8)$$

As in the previous example, boundary conditions which implement the geometry of $\mathcal{M}_{n,a,b}$ can be obtained by creating ‘artificial’ fields around $(x, y) = (a, 0)$ and $(x, y) = (b, 0)$.

Twist fields defined by (3.7) (called *branch point twist fields*) are associated to the two opposite cyclic permutation symmetries $\phi_i \mapsto \phi_{i+1}$ and $\phi_{i+1} \mapsto \phi_i$:

$$\mathcal{T} \equiv \mathcal{T}_\sigma, \quad i \xrightarrow{\sigma} i+1 \pmod n \quad (3.9)$$

$$\tilde{\mathcal{T}} \equiv \mathcal{T}_{\sigma^{-1}}, \quad i+1 \xrightarrow{\sigma^{-1}} i \pmod n \quad (3.10)$$

and their action is defined as [?]

$$\begin{aligned} \phi_i(y) \mathcal{T}(x^1, x^2) &= \theta(x^1 - y^1) \mathcal{T}(x^1, x^2) \phi_{i+1}(y) + \theta(y^1 - x^1) \mathcal{T}(x^1, x^2) \phi_i(y) \\ \phi_i(y) \tilde{\mathcal{T}}(x^1, x^2) &= \theta(x^1 - y^1) \tilde{\mathcal{T}}(x^1, x^2) \phi_{i-1}(y) + \theta(y^1 - x^1) \tilde{\mathcal{T}}(x^1, x^2) \phi_i(y) \end{aligned} \quad (3.11)$$

Thanks to this definition, (3.7) can be written as:

$$\mathcal{Z}[\mathcal{L}, \mathcal{M}_{n,a,b}] \propto \left\langle \mathcal{T}(a, 0) \tilde{\mathcal{T}}(b, 0) \right\rangle_{\mathcal{L}^{(n)}, \mathbb{C}} \quad (3.12)$$

where $\mathcal{L}^{(n)}$ is the lagrangian of the multi-copied model:

$$\mathcal{L}^{(n)}[\phi_1, \dots, \phi_n] \equiv \mathcal{L}[\phi_1] + \dots + \mathcal{L}[\phi_n] \quad (3.13)$$

The presence of a couple of twist fields in (3.12) can be justified since $\mathcal{T}(a, 0)$ connects two consecutive copies at $x > a$, but this effect vanishes for $x > b$ thanks to the simultaneous effect of both twist fields $\mathcal{T}(a, 0)$ and $\tilde{\mathcal{T}}(b, 0)$.

Thanks to twist fields, we can write the expectation value of an operator \mathcal{O} as

$$\langle \mathcal{O}(x, y) \dots \rangle_{\mathcal{L}, \mathcal{M}_{n,a,b}} = \frac{\left\langle \mathcal{T}(a, 0) \tilde{\mathcal{T}}(b, 0) \mathcal{O}_i(x, y) \dots \right\rangle_{\mathcal{L}^{(n)}, \mathbb{C}}}{\left\langle \mathcal{T}(a, 0) \tilde{\mathcal{T}}(b, 0) \right\rangle_{\mathcal{L}^{(n)}, \mathbb{C}}} \quad (3.14)$$

where \mathcal{O}_i denotes the representation of \mathcal{O} in the $\mathcal{L}^{(n)}$ model related to the i -th copy of $(\mathcal{L}, \mathbb{C})$ where (x, y) belongs.

3.1.2 Twist Fields in Conformal Field Theory

Let us consider a Conformal Field Theory (CFT) defined on $\mathcal{M}_{n,a,b}$ with local lagrangian density \mathcal{L} , stress tensor $T(z)$ and central charge c .

Taking n copies of this theory on \mathbb{C} , we define another CFT with local lagrangian density $\mathcal{L}^{(n)}$ and central charge nc .

Thanks to conformal invariance we can easily shift the evaluation of correlation functions from a manifold to another one.

The stress tensor of the multi-copied theory is given by

$$T^{(n)}(z) = \sum_{j=1}^n T_j(z) \quad (3.15)$$

where each $T_j(z)$ is a copy of the stress tensor of the original theory. Consider the stress tensor $T(w)$ of \mathcal{L} and the conformal transformation from $\mathcal{M}_{n,a,b}$ to \mathbb{C}

$$\begin{aligned} w \in \mathcal{M}_{n,a,b} &\mapsto z \in \mathbb{C} \\ z &= \left(\frac{w-a}{w-b} \right)^{\frac{1}{n}} \end{aligned} \quad (3.16)$$

3.1. Branch-Point Twist Fields

The transformation rule for the stress tensor is predicted by CFT [12]:

$$T(w) = \left(\frac{dz}{dw}\right)^2 T(z) + \frac{c}{12}\{z, w\} \quad (3.17)$$

where $\{z, w\}$ denotes the Schwarzian derivative:

$$\{z, w\} = \frac{\frac{d^3 z}{dw^3}}{\frac{dz}{dw}} - \frac{3}{2} \left(\frac{\frac{d^2 z}{dw^2}}{\frac{dz}{dw}}\right)^2 \quad (3.18)$$

Thanks to translational and rotational invariance, the expectation value of T in \mathbb{R}^2 vanishes. Taking the expectation value of (3.17), we have

$$\langle T(w) \rangle_{\mathcal{L}, \mathcal{M}_{n,a,b}} = \frac{c(n^2 - 1)}{24n^2} \frac{(a - b)^2}{(w - a)^2(w - b)^2} \quad (3.19)$$

Since $\langle T(w) \rangle_{\mathcal{L}, \mathcal{M}_{n,a,b}}$ can also be evaluated using (3.14)

$$\langle T(w) \rangle_{\mathcal{L}, \mathcal{M}_{n,a,b}} = \frac{\left\langle \mathcal{T}(a, 0) \tilde{\mathcal{T}}(b, 0) T_j(w) \right\rangle_{\mathcal{L}^{(n)}, \mathbb{R}^2}}{\left\langle \mathcal{T}(a, 0) \tilde{\mathcal{T}}(b, 0) \right\rangle_{\mathcal{L}^{(n)}, \mathbb{R}^2}} \quad (3.20)$$

we have

$$\frac{\left\langle \mathcal{T}(a, 0) \tilde{\mathcal{T}}(b, 0) T^{(n)}(w) \right\rangle_{\mathcal{L}^{(n)}, \mathbb{R}^2}}{\left\langle \mathcal{T}(a, 0) \tilde{\mathcal{T}}(b, 0) \right\rangle_{\mathcal{L}^{(n)}, \mathbb{R}^2}} = \frac{c(n^2 - 1)}{24n^2} \frac{(a - b)^2}{(w - a)^2(w - b)^2} \quad (3.21)$$

Thanks to the selection rule used to build up twist fields, they are also primary fields. The *artificial nature* of these primary fields is revealed in minimal conformal models [12], since these fields do not belong to the Kac table of the theory.

Using Ward's identities of the stress tensor [12], we obtain

$$\begin{aligned} & \left\langle \mathcal{T}(a, 0) \tilde{\mathcal{T}}(b, 0) T^{(n)}(w) \right\rangle_{\mathcal{L}^{(n)}, \mathbb{R}^2} \\ &= \left(\frac{1}{w - a} \frac{\partial}{\partial a} + \frac{1}{w - b} \frac{\partial}{\partial b} + \frac{d_n}{(w - a)^2} + \frac{\tilde{d}_n}{(w - b)^2} \right) \left\langle \mathcal{T}(a, 0) \tilde{\mathcal{T}}(b, 0) \right\rangle_{\mathcal{L}^{(n)}, \mathbb{R}^2} \end{aligned} \quad (3.22)$$

where d_n and \tilde{d}_n are the scaling dimensions respectively of \mathcal{T} and $\tilde{\mathcal{T}}$.

Comparing last two equations, we obtain

$$d_n = \tilde{d}_n = \frac{c}{12} \left(n - \frac{1}{n} \right) \quad (3.23)$$

The knowledge of scaling dimensions of the two twist fields gives the form of their correlation function.

$$\langle \mathcal{T}(a, 0) \tilde{\mathcal{T}}(b, 0) \rangle_{\mathcal{L}^{(n)}, \mathbb{R}^2} = \frac{1}{|a - b|^{2d_n}} \quad (3.24)$$

In case of some different d_n appear, we chose the lowest one, since by definition we are looking for the lowest scaling dimensional \mathcal{T} .

3.2 Entanglement Entropy

In this section we will present a technique due to J. Cardy and P. Calabrese [11] for the evaluation of Rényi and Von-Neumann Entropy in systems described by conformal fields theories.

This method can be used for the evaluation of Entanglement in critical finite and infinite systems or in infinite off-critical systems near their critical point. For critical system, we study the dependance of Entanglement on the size ℓ of the subsystem; on the other hand, for off-critical system, we are interested in the amount of Entanglement at different ‘distances’ from a critical point. Since the correlation length ξ diverges when a system is critical and decreases leaving the critical point, this physical quantity measures well how far the system is from a critical point.

3.2.1 Von-Neumann and Rényi Entropy

Following definitions of Chapt. 1, let us recall some definitions about Entanglement Entropy.

Let \mathcal{H} be the Hilbert space of a one-dimensional quantum system and \mathcal{H}_A be the space referred to a subsystem A

$$\mathcal{H} = \mathcal{H}_A \otimes \mathcal{H}_B \quad (3.25)$$

where B denotes the subsystem complementary to A .

Now, denote the ground state with $|\psi\rangle$; hence, the reduced density matrix of the subsystem A is given by

$$\rho_A = \text{Tr}_{\mathcal{H}_B} |\psi\rangle\langle\psi| \quad (3.26)$$

Rényi entropy of the subsystem A is given by

$$S_A^{(n)} = \frac{1}{1-n} \log \text{Tr}_A \rho_A^n \quad (3.27)$$

$$= \frac{1}{1-n} \log \mathcal{Z}_n(A) \quad (3.28)$$

3.2. Entanglement Entropy

and Von Neumann one can be obtained as

$$S_A = \lim_{n \rightarrow 1^+} S_A^{(n)} = -\text{Tr}_A \rho_A \log \rho_A \quad (3.29)$$

or equivalently

$$S_A = -\lim_{n \rightarrow 1^+} \frac{d}{dn} \text{Tr}_A \rho_A^n = -\lim_{n \rightarrow 1^+} \frac{d}{dn} \mathcal{Z}_n(A) \quad (3.30)$$

3.2.2 Evaluation via path integrals

Let us consider 1 + 1-dimensional QFT, which describes the time evolution of a one-dimensional discrete quantum system. Define Δ as the lattice parameter and denote with x the position of each site.

Let us denote with $\{\hat{\phi}(x)\}$ a complete set of compatible observables and with $\{\phi(x)\}$ and $\bigotimes_x |\{\phi(x)\}\rangle$ their eigenvalues and eigenvectors. In the spin-chain example, these states are spin configurations $|\sigma_1, \sigma_2 \dots\rangle$ and compatible observables are the total and the z spin operators $\mathbf{S} \cdot \mathbf{S}$ and S^z .

Now, consider a system with continuous time evolution ruled by a Hamiltonian \hat{H} . In the Wick-rotated picture, the density matrix $\hat{\rho}$ of the system is given by

$$\rho(\{\phi''(x'')\}, \{\phi'(x')\}) = \langle \{\phi''(x'')\} | \hat{\rho} | \{\phi'(x')\} \rangle \quad (3.31)$$

$$= \frac{1}{\mathcal{Z}(\beta)} \langle \{\phi''(x'')\} | e^{-\beta \hat{H}} | \{\phi'(x')\} \rangle \quad (3.32)$$

In the above expression the partition function $\mathcal{Z}(\beta)$ normalises to one the trace of the density matrix.

In the path integral formalism a matrix element of the density matrix is given by

$$\rho(\{\phi''(x'')\}, \{\phi'(x')\}) = \frac{1}{\mathcal{Z}(\beta)} \int \mathcal{D}\phi(x, \tau) \prod_x \delta(\phi(x, 0) - \phi'(x')) \prod_x \delta(\phi(x, \beta) - \phi''(x'')) e^{-S_E} \quad (3.33)$$

where S_E is the euclidean action which rules the evolution of the system

$$S_E = \int_0^\beta d\tau L_E \quad (3.34)$$

In the path integral picture, the matrix element of the density matrix $\rho(\{\phi''(x'')\}, \{\phi'(x')\})$ can be viewed as a mean over all possible evolution paths of the field $\phi(x)$ with fixed condition on the starting and the ending point.

Referring to Fig. 3.2, this path integral means an integration over all the light-blue strip.

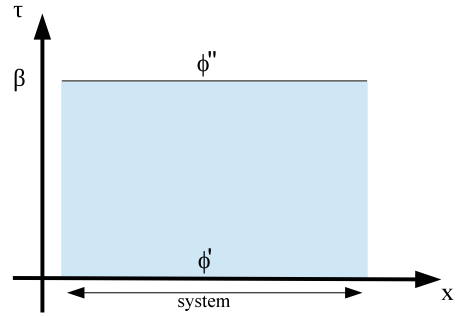


Figure 3.2: Path integral representation of the density matrix ρ

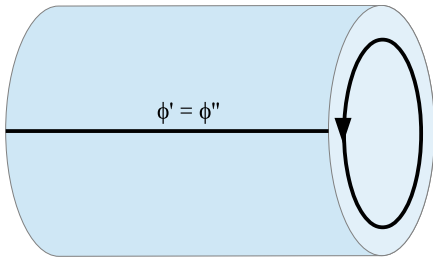


Figure 3.3: Path integral representation of the partition function $\mathcal{Z}(\beta)$

Since the partition function can be obtained tracing the density matrix over all degrees of freedom of the system, it can be got connecting the top edge of the strip with the bottom one (imposing $\phi'' = \phi'$) and tracing over ϕ' . This operation is equal to deform our strip to a cylinder and to sew the two edges (Fig. 3.3).

got as the partition function avoiding to trace over states of A .

The reduced density matrix related to the subsystem A can be obtained as the partition function, but sewing only points outside A .

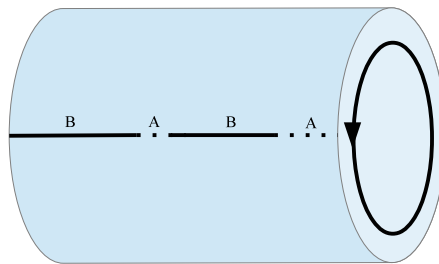


Figure 3.4: Path integral representation of the reduced density matrix ρ_A : points belonging to the dotted lines (subsystem A) are not identified and integrated, while points in the continue line (subsystem B) are identified and integrated as in the evaluation of the partition function $\mathcal{Z}(\beta)$

3.2.3 Entropy of a critical system

Now, consider an infinite system at its critical point and its subsystem $A = [a, b]$. The evaluation of n -partition function $\mathcal{Z}_n(A) = \text{Tr}_{\mathcal{H}_A} \rho_A^n$ can be obtained taking n -copies of the strip in Fig. 3.2 and sewing sequentially each copy except for points in A . Since the system is infinite, the light-blue strip in Fig. 3.2 becomes the whole \mathbb{C} plane.

In the path integral formalism the reduced density matrix reads

$$\begin{aligned}
 \langle \{\phi''_A(x''_A)\} | \rho_A | \{\phi'_A(x'_A)\} \rangle &= \int \mathcal{D}\phi'_A(x'_A) \langle \{\phi''_A(x''_A), \phi'_A(x'_A)\} | \rho_A | \{\phi'_A(x'_A), \phi'_A(x'_A)\} \rangle \\
 &= \frac{1}{\mathcal{Z}(\beta)} \int \mathcal{D}\phi'_A(x'_A) \int \mathcal{D}\phi(x, \tau) e^{-S_E[\phi]} \prod_{x \in A} \delta(\phi(x, 0) - \phi'_A(x'_A)) \delta(\phi(x, \beta) - \phi''_A(x''_A)) \times \\
 &\times \prod_{x \notin A} \delta(\phi(x, 0) - \phi'_A(x'_A)) \delta(\phi(x, \beta) - \phi'_A(x'_A)) \\
 &= \frac{1}{\mathcal{Z}(\beta)} \int \mathcal{D}\phi(x, \tau) e^{-S_E[\phi]} \prod_{x \in A} \delta(\phi(x, 0) - \phi'_A(x'_A)) \delta(\phi(x, \beta) - \phi''_A(x''_A)) \times \\
 &\times \prod_{x \notin A} \delta(\phi(x, 0) - \phi(x, \beta)) \tag{3.35}
 \end{aligned}$$

whose last product implements the sewing on points outside of A . In previous expressions, path integrals are evaluated on the \mathbb{R}^2 plane (Fig. 3.2).

If we are interested in the evaluation of $\langle \{\phi''_A\} | \rho_A^n | \{\phi'_A\} \rangle$, we can modify the previous expression performing path integral on the Riemann surface $\mathcal{M}_{n,a,b}$.

Alternatively we can insert into (3.35) n resolution of the identity

$$\frac{1}{\mathcal{Z}(\beta)} \int \mathcal{D}\phi_i(x_i) | \{\phi_i(x_i)\} \rangle \langle \{\phi_i(x_i)\} | \tag{3.36}$$

and obtain the n -sheet version of the integral over $\mathcal{M}_{n,a,b}$.

Thus the trace of $\text{Tr} \rho_A^n$ can be obtained from the partition function evaluated on the Riemann surface $\mathcal{M}_{n,a,b}$:

$$\mathcal{Z}_n(A) = \mathcal{Z}[\mathcal{L}, \mathcal{M}_{n,a,b}] \tag{3.37}$$

which can be evaluated using twist fields (3.12)

$$\mathcal{Z}[\mathcal{L}, \mathcal{M}_{n,a,b}] \propto \left\langle \mathcal{T}(a, 0) \tilde{\mathcal{T}}(b, 0) \right\rangle_{\mathcal{L}^{(n)}, \mathbb{R}^2} = \frac{1}{|a - b|^{2d_n}} \tag{3.38}$$

Since we focus on a critical point of a system described by a conformal theory with central charge c , the conformal dimension of the n -partition function can be

obtained as in (3.23). Hence, the n -partition function reads

$$\mathcal{Z}_n(A) = A_n \left(\frac{b-a}{\Delta} \right)^{-\frac{c}{6}(n-\frac{1}{n})} \quad (3.39)$$

where A_n is a normalisation parameter and the presence of Δ is due to dimensional requirements.

Rényi entropy of the subsystem A is then given by

$$S_A^{(n)} = \frac{1}{1-n} \log \mathcal{Z}_n(A) \propto \frac{c}{6} \frac{1+n}{n} \log \frac{b-a}{\Delta} = \frac{c}{6} \frac{1+n}{n} \log \ell \quad (3.40)$$

Performing derivatives and limits, we obtain

$$S_A \propto \frac{c}{3} \log \frac{b-a}{\Delta} = \frac{c}{3} \log \ell \quad (3.41)$$

where $\ell = \frac{b-a}{\Delta}$ denotes the size of the subsystem A .

Since Entanglement Entropy can be obtained from a conformal two-point correlation function, it can be simply evaluated in different geometries using conformal transformation of correlation functions.

$$\langle \phi'_1(z'_1) \phi'_2(z'_2) \rangle_{\mathcal{M}} = \left(\frac{dz'_1}{dz_1} \right)^{2h_1} \left(\frac{dz'_2}{dz_2} \right)^{2h_2} \langle \phi_1(z_1) \phi_2(z_2) \rangle_{\mathcal{N}} \quad (3.42)$$

with $z \in \mathcal{N} \mapsto z' = z'(z) \in \mathcal{M}$.

Example: Entanglement of a subsystem of a finite system

If we are interested in the Entanglement Entropy of a finite system of length L divided into two subsystems of length ℓ and $L - \ell$, we can map the whole complex plane \mathbb{C} into a cylinder with circumference $2\pi L$.

$$z \in \mathbb{C} \mapsto z' = \frac{iL}{2\pi} \log z \quad (3.43)$$

The twist-field correlation function in the new geometry is given by

$$\langle \mathcal{T}'(a', 0') \tilde{\mathcal{T}}'(b', 0') \rangle_{\mathcal{L}^{(n)}, strip} = \left(\frac{da' db'}{da db} \right)^{2d_n} \langle \mathcal{T}(a, 0) \tilde{\mathcal{T}}(b, 0) \rangle_{\mathcal{L}^{(n)}, \mathbb{C}} \quad (3.44)$$

and the Von-Neumann Entropy reads

$$S_A \propto \frac{c}{3} \log \left[\frac{L}{\pi} \sin \left(\frac{\pi \ell}{L} \right) \right] \quad (3.45)$$

which recovers the previous result for $L \gg \ell$. It is important to notice that Entropy is symmetric under the exchange $\ell \leftrightarrow L - \ell$; this symmetry reflects the fact that the two subsystems of a bi-partite system have the same Von-Neumann Entropy (see Section 1.2.2).

Moreover (3.45) has a maximum for $\ell = \frac{L}{2}$.

3.3 Off-critical models

As we said before, the Cardy-Calabrese approach [11] allows us to probe infinite off-critical systems; in particular, we are interested in a infinite one-dimensional quantum system divided into two semi-infinite subsystems.

Let us consider a massive relativistic QFT representing a 1 + 1-dimensional off-critical model in the scaling limit $\Delta \ll \xi$. We denote with ξ the correlation length, which corresponds to the inverse of the mass in theories near the conformal critical point.

Consider as a subsystem the negative real axis, whereas the complete system is represented by the whole real axis. For this reason the Riemann surface $\mathcal{M}_{n,0,\infty}$ has two branching point of order one: one at 0 and the other one at ∞ .

In QFT the stress tensor $T_{\mu\nu}$ is a Noether current, whose equations read [12]

$$\partial_{\bar{z}}T + \frac{1}{4}\partial_z\Theta = 0 \quad (3.46)$$

$$\partial_z\bar{T} + \frac{1}{4}\partial_{\bar{z}}\Theta = 0 \quad (3.47)$$

where T, \bar{T} and Θ are given by

$$T = T_{zz} \quad (3.48)$$

$$\bar{T} = T_{\bar{z}\bar{z}} \quad (3.49)$$

$$\Theta = 4T_{z\bar{z}} \quad (3.50)$$

Denote

$$\langle T(z, \bar{z}) \rangle_n = \frac{F_n(z\bar{z})}{z^2} \quad (3.51)$$

$$\langle \bar{T}(z, \bar{z}) \rangle_n = \frac{F_n(z\bar{z})}{\bar{z}^2} \quad (3.52)$$

$$\langle \Theta(z, \bar{z}) \rangle_n - \langle \Theta \rangle_1 = \frac{G_n(z\bar{z})}{z^2} \quad (3.53)$$

where

$$\langle \dots \rangle_n = \langle \dots \rangle_{\mathcal{M}_{n,0,\infty}} \quad (3.54)$$

Notice that $\langle T \rangle_1$ and $\langle \bar{T} \rangle_1$ vanish, since $\mathcal{M}_{1,\infty}$ is the usual complex plane and we expect to have a translational invariant theory. On the other hand $\langle \Theta \rangle_1$ is non-zero and constant since the theory is non critical (and then non conformal) and the curvature of the manifold is constant.

Combining (3.46) and (3.51) we obtain

$$z\bar{z}(F'_n + \frac{1}{4}G'_n) = \frac{1}{4}G_n \quad (3.55)$$

We expect that $F_n, G_n \rightarrow 0$ for $|z| \gg \xi$ at least exponentially, in order to have a well defined QFT. However, according to (3.19) we expect that

$$F_n \rightarrow \frac{c}{24} \left(1 - \frac{1}{n^2}\right) \quad (3.56)$$

$$G_n \rightarrow 0 \quad (3.57)$$

for $|z| \ll \xi$. In this limit we reach CFT expressions, since at distances $|z|$ smaller than correlation length ξ , the system ‘seems’ critical, and, in this case, conformal. After setting

$$C_n(r^2) = F_n(r^2) + \frac{1}{4}G_n(r^2) \quad (3.58)$$

we have

$$r^2 \frac{d}{d(r^2)} C_n(r^2) = \frac{1}{4}G_n(r^2) \quad (3.59)$$

and

$$\int_0^\infty d(r^2) \frac{G_n(r^2)}{r^2} = 4C_n(\infty) - 4C_n(0) \quad (3.60)$$

$$= -\frac{c}{6} \left(1 - \frac{1}{n^2}\right) \quad (3.61)$$

In the n-sheet picture we have

$$\int_{\mathcal{M}_{n,0,\infty}} d^2x \left(\langle \Theta(x) \rangle_n - \langle \Theta \rangle_1 \right) = -\frac{n\pi c}{6} \left(1 - \frac{1}{n^2}\right) \quad (3.62)$$

Let us consider

$$\begin{aligned} \frac{1}{2} \int d^2x x_\mu \partial^\mu f(x^0, x^1) &= \frac{1}{2} \int dx^1 \int dx^0 x_0 \partial^0 f(x) + \frac{1}{2} \int dx^0 \int dx^1 x_1 \partial^1 f(x) \\ &= - \int d^2x f(x) \end{aligned} \quad (3.63)$$

3.3. Off-critical models

Using the Callan-Symanzik equation (D.28) we obtain

$$\begin{aligned}
\int d^2x \langle \Theta(x) \rangle_n &= 2 \int d^2x \langle \Theta(x) \rangle_n - \int d^2x \langle \Theta(x) \rangle_n \\
&= \int d^2x \left(\hat{\gamma}(m) + \frac{1}{2} x_\mu \partial^\mu \right) \langle \Theta(x) \rangle_n \\
&= \int d^2x \beta(m) \frac{\partial}{\partial m} \langle \Theta(x) \rangle_n \\
&= -\beta(m) \frac{\partial}{\partial m} \log \mathcal{Z}_n
\end{aligned} \tag{3.64}$$

Comparing (3.62) and (3.64) we get

$$m \frac{\partial}{\partial m} \log \frac{\mathcal{Z}_n}{\mathcal{Z}_1^n} = \frac{nc}{12} \left(1 - \frac{1}{n^2} \right) \tag{3.65}$$

which leads to

$$\log \mathcal{Z}_n \propto \frac{c}{12} \left(n - \frac{1}{n} \right) \log ma \tag{3.66}$$

Recalling (3.27) and (3.29) we obtain

$$S_A^{(n)} \propto -\frac{1+n}{n} \frac{c}{12} \log ma = \frac{1+n}{n} \frac{c}{12} \log \frac{\xi}{a} \tag{3.67}$$

and

$$S_A \propto -\frac{c}{6} \log ma = \frac{c}{6} \log \frac{\xi}{a} \tag{3.68}$$

These results are very useful, since they can be compared with ones obtained exactly using CTM approach for integrable model whose Corner Transfer Matrix can be evaluated.

We stress the fact that these results are valid in the scaling limit $\xi \gg \Delta$, which allows us to describe a lattice system with a Field Theory; this scaling limit can be reached studying the system near the critical point in order to have a large correlation length ξ .

Chapter 4

The RSOS model

In this chapter we will introduce the RSOS model and its connection with conformal field theories.

Restricted Solid On Solid (RSOS) models play a central role in the study of a multitude of physical phenomena, like percolation, but they are interesting also for their integrability and their connection to conformal theories. In his seminal works [13],[14],[15] R. J. Baxter introduced the model from a purely statistical point of view, but its conformal structure has been deepened later by M. Bauer and H. Saleur [16].

We are interested in the study of particular classes of RSOS models whose critical point is described by a Minimal Conformal Model [12]; in following chapters we will study Entanglement Entropy of one dimensional quantum spin chains, whose 2d classical representation is given by these classes of RSOS. In order to perform the Peschel-Kaulke-Legeza's technique (Chapt. 2 and [7]) for the evaluation of the Entanglement, we require the knowledge of the expression of the Corner Transfer Matrix (CTM) of these models. For this reason we will include a sketch of the evaluation of corner transfer matrices for this model.

We will conclude this chapter with the Hamiltonian limit of this model at a critical conformal point, in order to show the one-dimensional quantum systems whose 2-dimensional statistical representation is given by the RSOS model.

4.1 The model

Let us define a square lattice \mathcal{L} with free boundary conditions. On each vertex i it is defined a local height $l_i = 1, 2, \dots$, with the constraint that neighbour local heights must differ by one.

$$l_i - l_j = \pm 1 \tag{4.1}$$

Thanks to this condition on local heights, there are six possible allowed configurations, modulo a global shift in all local heights.

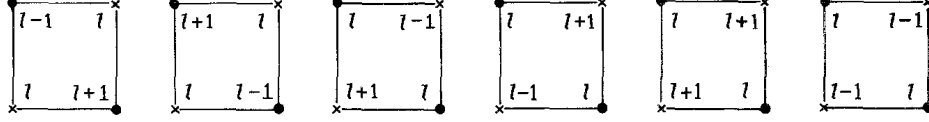


Figure 4.1: Allowed Configurations of the RSOS Model

Define $w(l, m, n, o)$ as the Boltzmann weight of a tile with local heights l, m, n, o in clockwise order (starting from the lower left corner).

In [13, 14] and [17] it is shown that Boltzmann weights can be written using Jacobi's elliptic functions:

$$\begin{aligned}
 w(l, l-1, l, l+1) &= \rho' h(v + \eta) \\
 w(l, l+1, l, l-1) &= \rho' h(v + \eta) \frac{h(w_{l+1})}{h(w_l)} \\
 w(l+1, l, l-1, l) &= \rho' h(v - \eta) \frac{h(w_{l-1})}{h(w_l)} \\
 w(l-1, l, l+1, l) &= \rho' h(v - \eta) \\
 w(l+1, l, l+1, l) &= \rho' h(2\eta) \frac{h(w_l + \eta - v)}{h(w_l)h(w_l + 1)} \\
 w(l-1, l, l-1, l) &= \rho' h(2\eta) h(w_l - \eta + v) \\
 w_l &= w_0 + 2l\eta
 \end{aligned} \tag{4.2}$$

where ρ' is a normalisation constant, v is the anisotropy parameter and η is the so-called *crossing parameter*, which depends on the *nome* p . The function h is defined as

$$\begin{aligned}
 h(u) &= \theta_1(u)\theta_4(u) \\
 &= (p^2)_\infty 2p^{\frac{1}{4}} \sin \frac{\pi u}{2K} \prod_{n=1}^{\infty} \left[1 - 2p^n \cos \frac{\pi u}{K} + p^{2n} \right]
 \end{aligned} \tag{4.3}$$

where $(q)_\infty$ is the *q-Pochhammer* symbol:

$$(q)_\infty = \prod_{n=1}^{\infty} (1 - q^n) \tag{4.4}$$

4.1. The model

and $\frac{K}{2}$ is the complete elliptic integral of the first kind with *modulus* k :

$$\frac{K}{2} = \int_0^{\frac{\pi}{2}} \frac{d\phi}{\sqrt{1 - k \sin^2 \phi}} \quad (4.5)$$

From (4.3) it can be shown that the semi-period of all the Boltzmann weights is equal to $2K$.

The nome p plays a temperature-like role, since its value depends on the phase of the system:

$$-1 < p < 1 \quad (4.6)$$

and it tends to zero when the system reaches the critical point.

The parameter K and p are related by the following relation

$$p = \exp \left[-\pi \frac{K'}{K} \right] \quad (4.7)$$

where K' is equal to K , only with k changed to $\sqrt{1 - k^2}$.

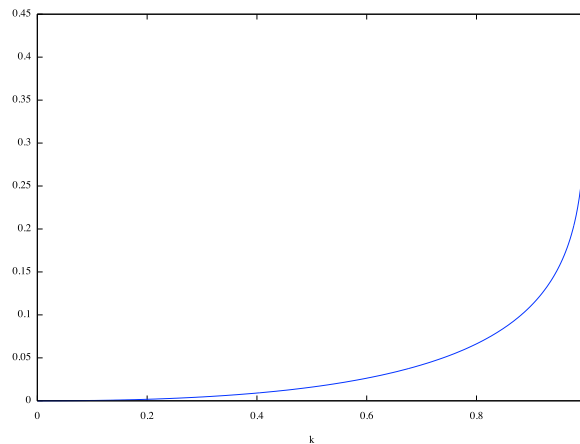


Figure 4.2: Dependence of the parameter p on the parameter k

The above model is the so-called *Solid On Solid SOS* model. If we restrict the maximal local height to $r - 1$, then this model is called *Restricted Solid On Solid RSOS*.

The archetypal statistical system described by these models is the adsorption,

i.e. the accumulation of atoms of a gas on atoms of a metallic surface. Since the number of gas atoms on each site of the metallic surface must be almost equal for neighbour sites, the condition (4.1) is requested in modelling these systems.

It is important to emphasise that the explicit expression of Boltzmann weights (4.2) derives also by the solution of the Yang-Baxter equation (2.40); for this reason the model is *integrable* and its physical quantities can be evaluated exactly.

4.2 The Andrews-Baxter-Forrester Model (ABF)

Even if the RSOS models are integrable, they have been solved in literature only with some conditions on the crossing parameter η .

It has been shown (see, for example [18]) that the Hard-Hexagon model and the zero field Ising model are equivalent to the RSOS model with crossing parameter η

$$\eta = \frac{K}{r} \quad (\eta \rightarrow \frac{\pi}{r} \text{ for } k, p \rightarrow 0) \quad (4.8)$$

and r respectively equal to 5 and 4.

As suggested by this equivalence, G. E. Andrews, R. J. Baxter and J. P. Forrester studied RSOS models with crossing parameter defined as above and with a generic integer value of r greater than two [17].

This model, called *Andrews-Baxter-Forrester* or *ABF* model, can be completely solved [17] using CTM technique.

It can be demonstrated [17] that varying parameters v and p , this model runs into four different regimes, or phases, (I, ..., IV)

I	$-1 < p < 0$	$\eta < v < 3\eta$
II	$0 < p < 1$	$\eta < v < 3\eta$
III	$0 < p < 1$	$-\eta < v < \eta$
IV	$-1 < p < 0$	$-\eta < v < \eta$

This model attracts our attention for its conformal behaviour, since it has been demonstrated [16, 19] that the critical point between the regimes III and IV is described by the unitary conformal theory with central charge

$$c = 1 - \frac{6}{r(r-1)} \quad (4.9)$$

4.3. The Baxter-Forrester Model (BF)

which corresponds to the $r - 1$ -th unitary minimal conformal model [12].

4.3 The Baxter-Forrester Model (BF)

The ABF model can be further generalised (R.J. Baxter and J.P. Forrester, [20]) allowing the crossing parameter η to be equal to

$$\eta = \frac{sK}{r} \quad (4.10)$$

where s and r are two relatively prime positive integers ($r > s \geq 3$).

Thanks to the presence of a second parameter s , the system can belong to a great number of regimes, but, as before, we are interested only in transition between regimes III and IV¹

III	$0 < p < 1$	$s = 1, 2, \dots, r - 2$	$-\eta < v < \eta$
IV	$-1 < p < 0$	$s = 1, 2, \dots, \lfloor \frac{r-2}{2} \rfloor$	$-\eta < v < \eta$

This critical point is described by a minimal conformal theory with central charge [19]

$$c = 1 - 6 \frac{s^2}{r(r-s)} \quad (4.11)$$

which represents the $\mathcal{M}(r-s, r)$ minimal conformal model.

As noticed in [20], this model is unphysical, since some Boltzmann weights are negative; this negativity gives some problems in the interpretation in terms of classical probabilistic weights.

The presence of such states can be expected since the conformal field theory underlying the system at its critical point is non-unitary and for this reason it contains some states with negative norm, also called *ghosts* [12].

In Chapt. 5 we will study one-dimensional models related to RSOS and we will show that in the $s \neq 1$ case some states with negative norm arise.

In following sections, we will focus on statistical properties of regime III, since we are interested in approaching the critical point from this regime.

¹ $[k]$ denotes the integer part of x

4.3.1 Symmetry of the Model

In this section we will introduce a more compact parametrisation [17, 20] of Boltzmann weights in order to make easier further computations and parametrisations. Let us consider a simple variation of the model: if we multiply each Boltzmann weight $w(l, m, n, 0)$ by $\frac{F(l,m)G(l,o)}{F(o,n)G(m,n)}$ (F, G arbitral functions) these contributions do not affect the partition function and then they do not modify physical properties of the model. Defining F and G as

$$F(l, l \pm 1) = G(l + 1, l) = \frac{1}{G(l - 1, l)} = \sqrt{h(w_l)} \quad (4.12)$$

we have

$$\begin{aligned} w(l, l + 1, l, l - 1) = w(l, l - 1, l, l + 1) &= \alpha_l = \rho' h(v + \eta) \\ w(l + 1, l, l - 1, l) = w(l - 1, l, l + 1, l) &= \beta_l = \rho' h(\eta - v) \frac{\sqrt{h(w_{l-1})h(w_{l+1})}}{h(w_l)} \\ w(l + 1, l, l + 1, l) &= \gamma_l = \rho' h(2\lambda) \frac{h(w_l + \eta - v)}{h(w_l)} \\ w(l - 1, l, l - 1, l) &= \delta_l = \rho' h(2\eta) \frac{h(w_l - \eta + v)}{h(w_l)} \end{aligned} \quad (4.13)$$

and thus possible configurations with different energy are reduced to four for each value of l .

Defining

$$\begin{aligned} E(z, x) &= \sum_{n \in \mathbb{Z}} (-1)^n x^{\frac{n(n-1)}{2}} z^n \\ &= \prod_{n=1}^{\infty} (1 - x^{n-1}z)(1 - x^n z^{-1})(1 - x^n) \end{aligned} \quad (4.14)$$

we can parametrize Boltzmann weights as

$$\begin{aligned} \alpha_l &= \rho \sqrt{w} E(xw^{-1}, y) \\ \beta_l &= \rho \sqrt{\frac{x}{w}} \sqrt{\frac{E(x^{l-1}, y)E(x^{l+1}, y)}{E^2(x^l, y)}} E(w, y) \\ \gamma_l &= \rho E(x, y) \frac{E(x^l w, y)}{E(x^l, y)} \\ \delta_l &= \rho E(x, y) \frac{E(x^l w^{-1}, y)}{E(x^l, y)} \end{aligned} \quad (4.15)$$

where

$$\begin{aligned} x &= \exp \left[-4\pi \frac{\eta}{K'} \right] \\ y &= \exp \left[-4\pi \frac{r\eta}{sK'} \right] \\ w &= \exp \left[-2\pi \frac{\eta - v}{K'} \right] \end{aligned} \tag{4.16}$$

This choice of x, y and w is valid in the regime III and it has to be modified a bit in other regimes; we refer always to this regime, since we are interested in approaching the critical point through this regime. Parametrisation for other regimes can be found in [20].

In following sections we will use this parametrisation for the evaluation of the partition function and other thermodynamic quantities using Corner Transfer Matrices.

4.4 ABF and BF Models in a Finite Lattice

In this section we will sketch the procedure to obtain the expression of Corner Transfer Matrices for these model in a finite lattice [17, 20], i.e. before performing the thermodynamic limit. Moreover using the CTM formulation, we will analyse the ground state structure of these models and we will find an expression for the n -partition function, which is vital in the evaluation of Entanglement Entropy.

4.4.1 Corner Transfer Matrix structure

In the following passages we will briefly review the process of building up the CTM, generalising what we have done in Chapt. 2 for IRF Ising-like models [6]. Also RSOS systems are IRF models, but while in Ising-like systems each vertex (or edge) can assume only two distinct values, each local height runs from 1 to $r - 1$, making these models more complicated than Ising-like ones.

Starting from (2.24) and following equations we know that [6, 17, 20] the Corner Transfer Matrix A of the first quadrant of the lattice (Fig. 2.2) is given by

$$A = \mathcal{F}_2^{ss't} \mathcal{F}_3^{tt'u} \dots \mathcal{F}_{m+1}^{yy'z} \tag{4.17}$$

where

$$\mathcal{F}_j^{ss't} = U_{m+1}^{ss't} U_m^t U_{m-1} \dots U_j \tag{4.18}$$

where U_{m+1}^{abc} is defined as in (2.24) but with l_{m+1}, l_{m+2} and l'_{m+1} fixed to a, b and c . Notice that, while U_i matrices in (2.24) are defined in the Ising basis ($\sigma_i = \pm 1$), in this chapter they are defined on the RSOS basis: each matrix element $U_i|_{\vec{l}, \vec{l}'}$ depends on a couple of multi-indices $\vec{l} = (l_1, l_2, \dots, l_{m+2})$ and $\vec{l}' = (l'_1, l'_2, \dots, l'_{m+2})$. In Chapt. 2, we have shown that expectation values of physical quantities can be evaluated using a diagonalised or normalised version of CTM. Using a procedure similar to (2.1.5) we can derive the following expression for the matrix product $ABCD$

$$ABCD = R_1^2 \exp \left[-2\pi\eta \frac{\mathcal{H}}{M'} \right] \quad (4.19)$$

where

$$R_1^2|_{\vec{l}, \vec{l}'} = E(x^{l_1}, y) \delta(\vec{l}, \vec{l}') \quad (4.20)$$

$$\exp \left[-2\pi\eta \frac{\mathcal{H}}{M'} \right] \Big|_{\vec{l}, \vec{l}'} = x^{\Phi(\vec{l})} \delta(\vec{l}, \vec{l}') \quad (4.21)$$

Then

$$\mathcal{Z}_1 = \sum_{l_1, \dots, l_m}^* E(x^{l_1}, y) x^{\Phi(l)} \quad (4.22)$$

with

$$x = \exp \left[-4\pi \frac{\eta}{M'} \right] \quad (4.23)$$

and

	y	M'
$0 < p < 1$	$x^{\frac{r}{s}}$	K'
$-1 < p < 0$	$-x^{\frac{r}{2s}}$	$2\Re K'$

The function Φ is given by

$$\Phi(\mathbf{l}) = c(l_1, l_2, l_3) + 2c(l_2, l_3, l_4) + \dots + mc(l_m, l_{m+1}, l_{m+2}) = \sum_{k=1}^m kc(l_k, l_{k+1}, l_{k+2}) \quad (4.24)$$

with

$$\begin{aligned} c(l, l-1, l) &= \left\lfloor \frac{l\mu}{r} \right\rfloor \\ c(l, l+1, l) &= - \left\lfloor \frac{l\mu}{r} \right\rfloor \\ c(l-1, l, l+1) = c(l+1, l, l-1) &= \frac{1}{2} \end{aligned} \quad (4.25)$$

where $\lfloor \cdot \rfloor$ denotes the integer part and μ is equal to s in the regime III and to $2s$ in the regime IV. Notice that since $\lfloor \frac{l}{r} \rfloor = 0$ for all l , taking $s = 1$ (4.24) coincides with the one founded by F. Franchini and A. De Luca for the ABF model [17, 9]:

$$\Phi_{III}^{(s=1)}(\mathbf{l}) = \sum_{k=1}^m k \frac{|l_k - l_{k+2}|}{4} \quad (4.26)$$

In the BF model, i.e. in the $s \neq 1$ case, this expression is not valid anymore, due to the arising of different terms

$$\Phi_{III}^{(s \neq 1)}(\mathbf{l}) = \sum_{k=1}^m \left\{ k \frac{|l_k - l_{k+2}|}{4} + (l_k - l_{k+1}) \left\lfloor \frac{l_s}{r} \right\rfloor \right\} \quad (4.27)$$

Since $x = \exp \left[\frac{4\pi^2 s}{r \log p} \right]$ and $\log p \leq 0$, the one-dimensional height configurations which minimise $\Phi(\mathbf{l})$ can be identified as the ground states of the system, since they give the maximum contribution to the partition function (4.22). Since $\Phi(\mathbf{l})$ defines ground states of the system, it can be identified as Hamiltonian related to the CTM [9]:

$$\mathcal{Z}_1 = \text{Tr } ABCD = \text{Tr} [R_1^2 e^{-c_0 \Phi}] \quad (4.28)$$

where c_0 is a positive parameter which depends on p .

4.4.2 Ground state structure

Since ground states play the most important role in the statistical description of a model, it is important to briefly sketch their structure.

Denoting with a, b and c respectively l_1, l_{m+1} and l_{m+2} , the ground state energy of this regime depends on these three parameters [19]

$$E_0^{(r,s)} = \frac{1}{4}(a-b)(a-c) + \frac{1}{2}[(a-c) + (c-b)m] \left\lfloor \frac{cs}{r} \right\rfloor_I \quad (4.29)$$

which, in the $s = 1$ case, gives

$$E_0^{(r,s=1)} = \frac{1}{4}(a-b)(a-c) \quad (4.30)$$

Thus boundary conditions set the ground state and its energy.

ABF model

If boundary conditions are free, the above energy has a minimum if odd and even sites have respectively the same value of the local height. The configuration associated with the ground state in regime III is given by [9]

$$\begin{aligned} l_{2k} &= X \\ l_{2k+1} &= Y \end{aligned} \quad (4.31)$$

with $X - Y = \pm 1$. This configuration is ordered and it is $2r - 4$ degenerate [9, 17]; the state depends only on l_1 and l_2 values: for each value of $l_1 = 1, \dots, r - 1$, l_2 can assume two different values $l_2 = l_1 \pm 1$, except for $l_1 = 1, r - 1$ when the choice of l_2 is forced. Thanks to this simple argument, we can demonstrate the amount of degeneration of the ground state.

BF model

In the case $s \neq 1$ the energy is minimised by a alternate-heights state if $\frac{cs}{r} < 1$; for this reason the number of degenerate ground states is different than the $s = 1$ case. It is given by [20]

$$\begin{cases} 2(r-s-1) & s \neq r-1 \\ 2r-4 & s = r-1 \end{cases} \quad (4.32)$$

Also in the BF model the ground state in the regime III is ordered.

4.4.3 The partition function

Recalling (4.22) the partition function is given by

$$\mathcal{Z}_1 = \text{Tr}[ABCD] = \sum_{a=1}^{r-1} E(x^a, y) D_m(a, b, c; x^2) \quad (4.33)$$

4.5. Hamiltonian Limit for Critical RSOS Models

where

$$D_m(a, b, c; x^2) = \sum_{l_2, l_3, \dots, l_m} x^{\Phi(l)} \quad (4.34)$$

with l_1, l_{m+1} and l_{m+2} fixed to a, b and c . Notice that in (4.33) the sum is performed only on odd or even values of a , since boundary conditions fix allowed central local heights.

In order to evaluate Rényi Entropy, we require the knowledge of the α -partition function $\mathcal{Z}_\alpha = \text{Tr } \rho_A^\alpha$, which is given by

$$\begin{aligned} \mathcal{Z}_\alpha &= \text{Tr} \left[\overbrace{ABCD \cdots ABCD}^{\alpha\text{-times}} \right] \\ &\propto \text{Tr} \left[R_1^{2\alpha} \exp \left[-2\pi\eta\alpha \frac{\mathcal{H}}{M'} \right] \right] \\ &= \sum_{a=1}^{r-1} [E(x^a, y)]^\alpha D_m(a, b, c; x^{2\alpha}) \end{aligned} \quad (4.35)$$

Since these formulæ have been obtained for finite systems, we need to perform the thermodynamic limit in order to study infinite systems. Such a limit has been performed in [20] and it will be used in Chapt. 6 and Appendix A for the evaluation of Entanglement Entropy in bi-partite infinite systems.

4.5 Hamiltonian Limit for Critical RSOS Models

As previously said, Entanglement is a genuine quantum phenomenon; for this reason it is vital to know which is the one-dimensional quantum system whose two-dimensional statistical representation is given by the RSOS model.

In order to find this model, in this section we will perform the Hamiltonian limit of the RSOS model at its critical conformal point $p \rightarrow 0$. In this limit Boltzmann weights are given by [16, 19]

$$w(u|a, b, c, d) = \frac{\sin(\eta - u)}{\sin \eta} \delta(a, c) + \frac{\sin u}{\sin \eta} \sqrt{\frac{\sin(\eta a) \sin(\eta c)}{\sin(\eta b) \sin(\eta d)}} \delta(b, d) \quad (4.36)$$

which allows us to write the matrix U_i (2.24) as

$$U_i(u) = \frac{\sin(\eta - u)}{\sin \eta} \mathbb{1} + \frac{\sin u}{\sin \eta} e_i \quad (4.37)$$

where the crossing parameter η tends² to $\frac{\pi s}{r}$ in the limit $p \rightarrow 0$. The matrix e_i is given by [21]

$$e_i|_{1,r} = \left(\prod_{j \neq i} \delta(l_j, l'_j) \right) \delta(l_{i-1}, l_{i+1}) \sqrt{\frac{\sin\left(\frac{\pi s}{r} l_i\right) \sin\left(\frac{\pi s}{r} l'_i\right)}{\sin\left(\frac{\pi s}{r} l_{i-1}\right) \sin\left(\frac{\pi s}{r} l_{i+1}\right)}} \quad (4.38)$$

It can be shown that these e_i matrices satisfy the Temperley-Lieb Algebra [19, 22]

$$e_i^2 = Q^{\frac{1}{2}} e_i \quad (4.39)$$

$$e_i e_{i \pm 1} e_i = e_i \quad (4.40)$$

$$e_i e_j = e_j e_i \text{ if } |i - j| > 1 \quad (4.41)$$

where $\sqrt{Q} = 2 \cos \eta = 2 \cos\left(\frac{\pi s}{r}\right)$. In following chapters we will define a second parameter q as

$$\sqrt{Q} = -(q + q^{-1}) \quad (4.42)$$

It is very important to notice that the solution can be also obtained [23] as a solution of the Yang-Baxter equation (2.40).

In order to perform the Hamiltonian limit, we need to construct a double row-to-row transfer matrix. Referring to Fig. 4.3 we consider two rows of tiles (the red and the blue one). The row-to-row transfer matrix of the red row is given by [21]

$$\mathbf{T}_R(u) = \prod_{i \text{ even}} U_i(u) \quad (4.43)$$

while the transfer matrix of the blue row reads

$$\mathbf{T}_B(u) = \prod_{i \text{ odd}} U_i(u) \quad (4.44)$$

where U_i are given by (4.5).

The double row transfer matrix \mathbf{T} is then given by the product of the two single row matrices

$$\mathbf{T}(u) = \mathbf{T}_B(u) \mathbf{T}_R(u) \quad (4.45)$$

²This can be obtained from $\lim_{k \rightarrow 0} \int_0^{\frac{\pi}{2}} \frac{dx}{\sqrt{1 - k \sin^2 x}} = \frac{\pi}{2}$

4.5. Hamiltonian Limit for Critical RSOS Models

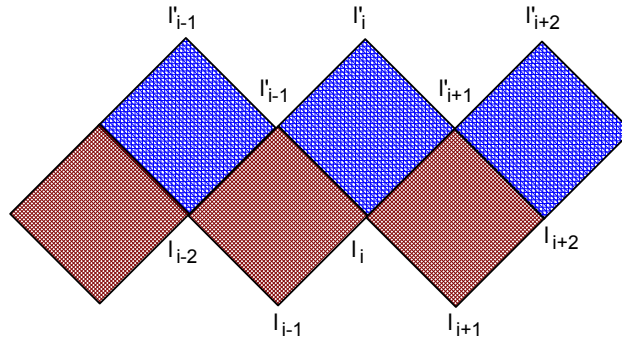


Figure 4.3: Double row-to-row transfer matrix

and the hamiltonian limit gives [21, 23]

$$H = - \sum_i e_i \quad (4.46)$$

It is very difficult to study this Hamiltonian, since it contains three-sites interaction and it is expressed as matrices in the RSOS basis. In [21] and in previous works this Hamiltonian has been related to some anyonic models.

It was noted in [24] that the Q -state Potts Hamiltonian provides another realisation of the Temperley-Lieb Algebra; moreover it has been shown that a m sites Q -states Potts model is equivalent to the q -invariant XXZ spin chain with fixed boundaries [24, 25, 22], which will be introduced and studied in the next chapter.

Chapter 5

The q -deformed Quantum XXZ Spin-Chain

In this chapter we will introduce the Temperley-Lieb Algebra and the Quantum Group [26, 22, 27] and we will show how they are connected [25] with the Virasoro Algebra [12].

Furthermore we will study the integrable XXZ quantum spin chain with open periodic boundary conditions; in particular we will focus on its connection with Minimal Conformal Models.

We will conclude this chapter discussing the the non-Hermiticity of this Hamiltonian.

5.1 The Y-B Equation - 1: Periodic Boundary Conditions

In this section we will briefly review the Yang-Baxter Equation (2.40) focusing on quantum one-dimensional models with periodic boundary conditions ([26] and references therein).

Consider a spin-chain and denote with V the Hilbert space of each site. For each couple of neighbour sites, we can define the *permutation operator* \mathcal{P} as

$$\begin{aligned}\mathcal{P} : V \otimes V &\rightarrow V \otimes V \\ a \otimes b &\mapsto b \otimes a\end{aligned}\tag{5.1}$$

In a spin- $\frac{1}{2}$ representation ($V = \mathbb{C}^2$) \mathcal{P} reads

$$\mathcal{P} = \frac{1}{2}(\sigma^x \otimes \sigma^x + \sigma^y \otimes \sigma^y + \sigma^z \otimes \sigma^z + \mathbb{1} \otimes \mathbb{1})\tag{5.2}$$

In the quantum spin-chain picture, the Yang-Baxter Equation is given by [26]

$$R_{12}(\lambda_1 - \lambda_2)R_{13}(\lambda_1 - \lambda_3)R_{23}(\lambda_2 - \lambda_3) = R_{23}(\lambda_2 - \lambda_3)R_{13}(\lambda_1 - \lambda_3)R_{12}(\lambda_1 - \lambda_2) \quad (5.3)$$

where

$$\begin{aligned} R_{12} &= R \otimes \mathbb{1} \\ R_{13} &= (\mathcal{P} \otimes \mathbb{1})(\mathbb{1} \otimes R)(\mathcal{P} \otimes \mathbb{1}) \\ R_{23} &= \mathbb{1} \otimes R \end{aligned} \quad (5.4)$$

In the quantum chain picture, the solution of the Yang-Baxter equation is related to the form of the quantum Hamiltonian \hat{H} of a periodic system with N sites ($\hat{H}_{N,N+1} = \hat{H}_{N,1}$)

$$\hat{H} = \sum_{j=1}^N \hat{H}_{j,j+1} \quad (5.5)$$

In [26] it has been shown that

$$\hat{H}_{j,j+1} \propto \check{R}_{j,j+1}^{-1}(\lambda) \left. \frac{d\check{R}_{j,j+1}(\lambda)}{d\lambda} \right|_{\lambda=0} \quad (5.6)$$

where

$$\check{R} = \mathcal{P}R \quad (5.7)$$

Different solutions of the Yang-Baxter equation lead to different Hamiltonians and then to different quantum models.

5.2 The Temperley-Lieb Algebra

Studying the Yang-Baxter equation [6, 26] for the XXX and the XXZ models, two different algebras of solutions arise. It can be shown that R matrices in the XXX model belong to the *braid group*. In the XXZ case R matrices are more complicated and related to the *Temperley-Lieb* algebra.

5.2.1 The Braid Group Algebra B_N

The braid group B_N is defined by $N - 1$ generators g_1, \dots, g_{N-1} and by their exchange relations:

$$g_i g_{i+1} g_i = g_{i+1} g_i g_{i+1} \quad (5.8)$$

$$[g_i, g_j] = 0 \quad \text{if } |i - j| > 1 \quad (5.9)$$

5.2. The Temperley-Lieb Algebra

As previously said, the braid group represents the solution of the Yang-Baxter equation for the simple XXX model.

The R matrix of this model is given by

$$R(\lambda) = \begin{pmatrix} \sin \lambda & 0 & 0 & 0 \\ 0 & \sin \lambda & 0 & 0 \\ 0 & 0 & \sin \lambda & 0 \\ 0 & 0 & 0 & \sin \lambda \end{pmatrix} \quad (5.10)$$

and the two-site Hamiltonian \hat{H}_2 obtained from (5.6) is given by

$$\hat{H}_2 \propto [\mathcal{P}R(\lambda)]^{-1} \left. \frac{d}{d\lambda} \mathcal{P}R(\lambda) \right|_{\lambda=0} = \mathcal{P} \quad (5.11)$$

which is the two-site XXX Hamiltonian with an energy shift. The matrix \check{R} for this model is given by

$$\check{R}(\lambda) = \begin{pmatrix} \sin \lambda & 0 & 0 & 0 \\ 0 & 0 & \sin \lambda & 0 \\ 0 & \sin \lambda & 0 & 0 \\ 0 & 0 & 0 & \sin \lambda \end{pmatrix} \quad (5.12)$$

and it can be written as

$$\begin{aligned} \check{R}(\lambda) &= \sin \lambda \begin{pmatrix} 1 & 0 & 0 & 0 \\ 0 & 0 & 1 & 0 \\ 0 & 1 & 0 & 0 \\ 0 & 0 & 0 & 1 \end{pmatrix} \\ &\equiv \sin \lambda g \end{aligned} \quad (5.13)$$

Setting

$$g_i = \mathbb{1} \otimes \cdots \otimes \mathbb{1} \otimes g \otimes \mathbb{1} \otimes \cdots \otimes \mathbb{1} \quad (5.14)$$

it can easily be shown that g_i 's satisfy the Braid group Algebra.

The Braid Group Algebra describes only particular systems, such as the XXX spin-chain, whose 'symmetry level' is very high. In order to describe systems with less symmetries, such as the XXZ model, we will restrict our analysis to quotients of the Braid Group Algebra.

5.2.2 The Hecke Algebra $H_N(q)$

The Hecke algebra $H_N(q)$ is obtained from B_N requiring the extra condition

$$(g_i - q)(g_i + q^{-1}) = 0 \quad (5.15)$$

It is useful to express elements of $H_N(q)$ with new generators $U_i = g_i - q$. With these new generators the algebra is defined by the following relations:

$$U_i U_{i+1} U_i - U_i = U_{i+1} U_i U_{i+1} - U_{i+1} \quad (5.16)$$

$$U_i^2 = -(q + q^{-1})U_i \quad (5.17)$$

$$[U_i, U_j] = 0 \text{ if } |i - j| > 1 \quad (5.18)$$

5.2.3 The Temperley-Lieb Algebra $T_N(q)$

The Temperley-Lieb algebra $T_N(q)$ is obtained from $H_N(q)$ by requiring the extra condition [26, 27]

$$U_i U_{i\pm 1} U_i = U_i \quad (5.19)$$

This algebra plays a vital role in the solution of the XXZ model, since it can be shown that solutions of the Yang-Baxter equation of this model can be written using elements belonging to the Temperley-Lieb algebra.

The R matrix of the XXZ model is given by

$$R(\lambda) = \begin{pmatrix} \sin(\lambda + \mu) & 0 & 0 & 0 \\ 0 & \sin \lambda & ie^{i\lambda} \sin \mu & 0 \\ 0 & ie^{-i\lambda} \sin \mu & \sin \lambda & 0 \\ 0 & 0 & 0 & \sin(\lambda + \mu) \end{pmatrix} \quad (5.20)$$

The \check{R} matrix reads

$$\check{R}(\lambda) = \begin{pmatrix} \sin(\lambda + \mu) & 0 & 0 & 0 \\ 0 & ie^{-i\lambda} \sin \mu & \sin \lambda & 0 \\ 0 & \sin \lambda & ie^{i\lambda} \sin \mu & 0 \\ 0 & 0 & 0 & \sin(\lambda + \mu) \end{pmatrix} \quad (5.21)$$

and it can be expressed as

$$\begin{aligned} \check{R}(\lambda) &= e^{i\lambda} \begin{pmatrix} \frac{1}{2}e^{i\mu} & 0 & 0 & 0 \\ 0 & 0 & \frac{1}{2} & 0 \\ 0 & \frac{1}{2} & i \sin \mu & 0 \\ 0 & 0 & 0 & \frac{1}{2}e^{i\mu} \end{pmatrix} - e^{-i\lambda} \begin{pmatrix} \frac{1}{2}e^{-i\mu} & 0 & 0 & 0 \\ 0 & -i \sin \mu & \frac{1}{2} & 0 \\ 0 & \frac{1}{2} & 0 & 0 \\ 0 & 0 & 0 & \frac{1}{2}e^{-i\mu} \end{pmatrix} \\ &= \frac{1}{2}e^{i\lambda}g - \frac{1}{2}e^{-i\lambda}g^{-1} \end{aligned} \quad (5.22)$$

5.3. The Y-B Equation - 2: Open Boundary Conditions

where

$$g = \begin{pmatrix} e^{i\mu} & 0 & 0 & 0 \\ 0 & 0 & 1 & 0 \\ 0 & 1 & 2i \sin \mu & 0 \\ 0 & 0 & 0 & e^{i\mu} \end{pmatrix} \quad (5.23)$$

which satisfies

$$(g - q)(g + q^{-1}) = 0 \quad (5.24)$$

for $q = e^{i\mu}$.

As before we can set

$$g_i = \mathbb{1} \otimes \cdots \otimes \mathbb{1} \otimes g \otimes \mathbb{1} \otimes \cdots \otimes \mathbb{1} \quad (5.25)$$

and

$$U_i = g_i - q \quad (5.26)$$

to obtain the Temperley-Lieb Algebra $T_N(e^{i\mu})$.

Using (5.6) we obtain the two-site XXZ hamiltonian

$$\hat{H}_2 = \sigma^x \otimes \sigma^x + \sigma^y \otimes \sigma^y + \cos \mu \sigma^z \otimes \sigma^z \quad (5.27)$$

5.3 The Y-B Equation - 2: Open Boundary Conditions

Up to now, we have studied solutions of the Yang-Baxter Equation for closed spin-chains with periodic boundary conditions.

It is important to notice that the Temperley-Lieb Algebra $T_N(q)$ provides solutions not only for the closed XXZ, but also for the open chain [25, 22].

$$H = \sum_{n=1}^{N-1} \sigma_n^x \sigma_{n+1}^x + \sigma_n^y \sigma_{n+1}^y + \frac{q + q^{-1}}{2} \sigma_n^z \sigma_{n+1}^z + \frac{q - q^{-1}}{2} (\sigma_1^z - \sigma_N^z) \quad (5.28)$$

The Y-B equation for systems with open boundary conditions requires a little modification of boundary terms.

The Y-B equation does not change for *bulk* sites and it is given by (5.3), like in closed chains. In order to implement the effect of boundaries, E. K. Sklyanin [28]

introduced a couple of matrices K^+ and K^- whose role is to provide boundary conditions. The Y-B equation for boundary sites is given by [26, 29]

$$R_{12}(\lambda_1 - \lambda_2)K_1^-(\lambda_1)R_{21}(\lambda_1 + \lambda_2)K_2^-(\lambda_2) = K_2^-(\lambda_2)R_{12}(\lambda_1 + \lambda_2)K_1^-(\lambda_1)R_{21}(\lambda_1 - \lambda_2) \quad (5.29)$$

and is called *reflection* or *boundary Yang-Baxter* equation. This equation implements the left-side boundary; it has to be coupled with a similar one for the right-side boundary using the matrix K^+ .

Thanks to the presence of boundary matrices K^\pm , the related quantum Hamiltonian will have boundary terms. For instance, the most general integrable XYZ spin- $\frac{1}{2}$ chain with boundaries is given by [29]

$$\begin{aligned} \hat{H} &= \sum_{n=1}^{N-1} [(1 + \Gamma)\sigma_n^x \sigma_{n+1}^x + (1 - \Gamma)\sigma_n^y \sigma_{n+1}^y + \Delta \sigma_n^z \sigma_{n+1}^z] \\ &+ \text{sn } \eta [A_- \sigma_1^z + B_- \sigma_1^+ + C_- \sigma_1^- + A_+ \sigma_N^z + B_+ \sigma_N^+ + C_+ \sigma_N^-] \end{aligned} \quad (5.30)$$

with

$$\begin{aligned} \Gamma &= k \text{sn}^2 \eta \\ \Delta &= \text{cn } \eta \text{dn } \eta \\ A_\pm &= \frac{\text{cn } \xi_\pm \text{dn } \xi_\pm}{\text{sn } \xi_\pm} \\ B_\pm &= \frac{2\mu_\pm(\lambda_\pm + 1)}{\text{sn } \xi_\pm} \\ C_\pm &= \frac{2\mu_\pm(\lambda_\pm - 1)}{\text{sn } \xi_\pm} \end{aligned} \quad (5.31)$$

where η denotes the usual crossing parameter, k denotes the distance from the critical point, while ξ_\pm, μ_\pm and λ_\pm are constants parameters which fix boundary conditions.

Notice that in (5.30) the first line is the usual XYZ hamiltonian while the second line is due to boundary matrices. The (5.28) can be obtained from (5.30) taking the limit $k \rightarrow 0$ and fixing parameters $q = e^{i\eta}$, $\mu_\pm = 0$ and $\xi_\pm \rightarrow \pm i\infty$.

In order to study solutions of the boundary Y-B equation at their critical point, previous algebras have been modified in order to take into account the effect of the boundaries. For instance, solutions of the boundary Y-B equation for the XXZ model belong to the *Blob Temperley-Lieb Algebra* $\mathcal{B}_N(q, Q)$ with generators

5.3. The Y-B Equation - 2: Open Boundary Conditions

U_0, \dots, U_{N-1} which obey to

$$\begin{aligned} U_{i\pm 1}U_iU_{i\pm 1} &= U_{i\pm 1} \\ U_i^2 &= -(q + q^{-1})U_i \\ U_1U_0U_1 &= (qQ^{-1} + q^{-1}Q)U_1 \\ U_0^2 &= -(Q + Q^{-1})U_0 \end{aligned} \quad (5.32)$$

In the special (5.28) case, even if the system has boundaries, the algebra of solution of the Y-B equation is simply given by the bulk Temperley-Lieb Algebra, since its \check{R} matrix is given by

$$\check{R}_i(\lambda) = \mathbb{1} + \lambda U_i \quad (5.33)$$

where

$$U_i = \overbrace{\mathbb{1} \otimes \dots \otimes \mathbb{1}}^{i-1 \text{ times}} \otimes U \otimes \overbrace{\mathbb{1} \otimes \dots \otimes \mathbb{1}}^{N-2-i \text{ times}} \quad (5.34)$$

and

$$U = \begin{pmatrix} 0 & 0 & 0 & 0 \\ 0 & q^{-1} & -1 & 0 \\ 0 & -1 & q & 0 \\ 0 & 0 & 0 & 0 \end{pmatrix} \quad (5.35)$$

With this parametrisation the Hamiltonian (5.28) can be written as [25]

$$\hat{H} = \sum_{i=1}^{N-1} \left(\frac{q + q^{-1}}{2} - 2U_i \right) \quad (5.36)$$

As we said before, this *bounded* Hamiltonian can be described using a bulk Temperley-Lieb Algebra; this fact is due to the telescopic form of the two-site Hamiltonian \hat{H}_{12}

$$\hat{H}_{12} = \sigma_i^x \sigma_{i+1}^x + \sigma_i^y \sigma_{i+1}^y + \Delta_+ \sigma_i^z \sigma_{i+1}^z + \Delta_- (\sigma_i^z - \sigma_{i+1}^z) \quad (5.37)$$

where

$$\Delta_{\pm} = \frac{q \pm \frac{1}{q}}{2} \quad (5.38)$$

In other words, it can be expressed as a sum of bulk terms which automatically provide boundary term, indeed Δ_- terms vanish in the bulk, thanks to a recursive annihilation.

From an algebraic point of view, the presence of the bulk Temperley-Lieb algebra is due to the triviality of the boundary matrices K^{\pm} [26].

This special Hamiltonian does not enjoy only this peculiar property, but it is very interesting for its symmetric properties. Furthermore for particular choices of the parameter q this model is described [25] by a Minimal Conformal Model [12].

5.4 The Quantum Group

As we said before, the Hamiltonian (5.28) has special symmetry properties; in particular it is invariant under the action of the *Quantum Group*, which will be briefly introduced in this section.

Despite its name, the quantum group $U_q(\mathfrak{su}_2)$ is an algebra. It is generated [25, 26, 22] by $J^+, J^-, q^{2J^z}, q^{-2J^z}$ whose commutation relations are given by

$$\begin{aligned} [J^+, J^-] &= \frac{q^{2J^z} - q^{-2J^z}}{q - q^{-1}} = [2J^z]_q \\ q^{J^z} J^\pm q^{-J^z} &= q^{\pm 1} J^\pm \end{aligned} \quad (5.39)$$

where the q -integer $[k]_q$ is defined as

$$[k]_q = \frac{q^k - q^{-k}}{q - q^{-1}} \quad (5.40)$$

The quantum group enjoys the Hopf algebra structure¹ on \mathbb{C} , with co-product $\Delta : U_q(\mathfrak{su}_2) \rightarrow U_q(\mathfrak{su}_2) \otimes U_q(\mathfrak{su}_2)$, co-unit $\epsilon : U_q(\mathfrak{su}_2) \rightarrow \mathbb{C}$ and antipode $\gamma : U_q(\mathfrak{su}_2) \rightarrow U_q(\mathfrak{su}_2)$ defined by

$$\Delta(J^\pm) = q^{J^z} \otimes J^\pm + J^\pm \otimes q^{-J^z}, \quad \Delta(q^{\pm J^z}) = q^{\pm J^z} \otimes q^{\pm J^z} \quad (5.41)$$

$$\epsilon(q^{\pm J^z}) = 1, \quad \epsilon(J^\pm) = 0 \quad (5.42)$$

$$\gamma(q^{\pm J^z}) = q^{\mp J^z}, \quad \gamma(J^\pm) = -q^{\pm 1} J^\pm \quad (5.43)$$

The Hopf structure allows us to define the action of the quantum group on an N -site system using recursive application of the co-product $\Delta_n = (\Delta \otimes \mathbb{1})\Delta_{n-1}$, ($\Delta_2 \equiv \Delta$).

This N -site structure can be easily clarified applying it on a representation of the quantum group. Let π be a representation of $U_q(\mathfrak{su}_2)$ with representation space V :

$$\begin{aligned} \pi : U_q(\mathfrak{su}_2) &\rightarrow \text{End}V \\ U_q(\mathfrak{su}_2) \ni J^\pm &\mapsto s^\pm \in \text{End}V \\ U_q(\mathfrak{su}_2) \ni J^z &\mapsto s^z \in \text{End}V \end{aligned} \quad (5.44)$$

The action of this representation on an N -site model is given by [22]

$$U_q(\mathfrak{su}_2) \ni x \mapsto \pi^{\otimes N}(\Delta_N(x)) \in \text{End}V^{\otimes N} \quad (5.45)$$

¹For further details about Hopf Algebras see Appendix B and references therein

5.4. The Quantum Group

and, at explicit level

$$\begin{aligned} q^{\pm J^z} &\mapsto q^{\pm S^z} \\ J^\pm &\mapsto S^\pm \end{aligned} \quad (5.46)$$

where

$$\begin{aligned} q^{\pm S^z} &= q^{\pm s^z} \otimes \cdots \otimes q^{\pm s^z} \\ S^\pm &= \sum_{i=1}^N \underbrace{q^{s^z} \otimes \cdots \otimes q^{s^z}}_{i-1 \text{ times}} \otimes S^\pm \otimes \overbrace{q^{-s^z} \otimes \cdots \otimes q^{-s^z}}^{N-i-1 \text{ times}} \end{aligned} \quad (5.47)$$

As we said before the Hamiltonian (5.28) is invariant under the action of the Quantum Group. Thanks to a theorem [22, 30] due to M. Jimbo, this invariance does not depend on the representation chosen, since all generators of the Quantum Group $U_q(\mathfrak{su}_2)$ in a given representation commute with all generators of the Hecke Algebra $H_N(q)$ in the same representation (and of the Temperley-Lieb Algebra $T_N(q)$).

5.4.1 Spin- $\frac{1}{2}$ Representation

Since we are interested in quantum spin-chain models, we will focus on spin- $\frac{1}{2}$ representations of the quantum group ($V = \mathbb{C}^2$).

$$\pi : U_q(\mathfrak{su}_2) \rightarrow \text{End } \mathbb{C}^2 \quad (5.48)$$

$$\begin{aligned} \pi(J^\pm) &= \frac{\sigma^\pm}{2} \\ \pi(q^{\pm J^z}) &= q^{\pm \frac{\sigma^z}{2}} \end{aligned} \quad (5.49)$$

If we consider a chain of N sites, the Hilbert space would be \mathbb{C}^{2^N} and the representation would be given by

$$\pi_U : U_q(\mathfrak{su}_2) \rightarrow \text{End } \mathbb{C}^{2^N} \quad (5.50)$$

As before, the Hopf co-product is implemented in the spin- $\frac{1}{2}$ representation defining

$$\begin{aligned} \Delta_n &\equiv (\Delta \otimes \mathbb{1}) \Delta_{n-1} \\ \Delta_2 &\equiv \Delta \end{aligned} \quad (5.51)$$

and

$$x \in U_q(\mathfrak{su}_2) \xrightarrow{\pi_U} \pi^{\otimes N}(\Delta_N(x)) \in \text{End } V^{\otimes N} \quad (5.52)$$

The images of the generators (i.e. their End \mathbb{C}^{2N} representations) are denoted by S^\pm and $q^{\pm S^z}$

$$\begin{aligned}
 J^\pm \mapsto \pi_U(J^\pm) \equiv S^\pm &= \sum_{i=1}^N \overbrace{q^{\frac{\sigma^z}{2}} \otimes \cdots \otimes q^{\frac{\sigma^z}{2}}}^{i-1 \text{ times}} \otimes \frac{\sigma^\pm}{2} \otimes \overbrace{q^{-\frac{\sigma^z}{2}} \otimes \cdots \otimes q^{-\frac{\sigma^z}{2}}}^{N-1-i \text{ times}} \\
 q^{\pm J^z} \mapsto \pi_U(q^{\pm J^z}) \equiv q^{\pm S^z} &= q^{\frac{\sigma^z}{2}} \otimes \cdots \otimes q^{\frac{\sigma^z}{2}}
 \end{aligned} \tag{5.53}$$

It is very important to notice that for $q \in S^1$ these generators are not Hermitian, indeed

$$(S^\pm)^\dagger = S_{op}^\pm = \pi^{\otimes N}(\Delta_N^{op}(J^\mp)) \neq S^\mp \tag{5.54}$$

where Δ^{op} defines the opposite co-product

$$\Delta^{op}(J^\pm) = q^{-J^z} \otimes J^\pm + J^\pm \otimes q^{J^z} \tag{5.55}$$

The associated Hopf algebra equipped with the opposite co-product Δ^{op} is denoted with $U_q^{op}(\mathfrak{su}_2)$

Higher-spin Representations

The construction of a spin- s representation of the $U_q(\mathfrak{su}_2)$ is very similar to the one used to build up a \mathfrak{su}_2 one. It can simply be obtained by considering the spin- $\frac{1}{2}$ representation for $2s$ sites and then projecting on the requested sector. For example, if we are interested in the spin-1 representation, we can combine two spin- $\frac{1}{2}$ representations and then project on the spin-1 sector. Explicitly

$$\begin{aligned}
 S^+ &= \frac{\sigma^+}{2} \otimes q^{-\frac{\sigma^z}{2}} + q^{\frac{\sigma^z}{2}} \otimes \frac{\sigma^+}{2} \\
 &= \begin{pmatrix} 0 & \sqrt{q} & \frac{1}{\sqrt{q}} & 0 \\ 0 & 0 & 0 & \sqrt{q} \\ 0 & 0 & 0 & \frac{1}{\sqrt{q}} \\ 0 & 0 & 0 & 0 \end{pmatrix}
 \end{aligned} \tag{5.56}$$

where we have used

$$\begin{aligned}
 q^{\pm \frac{\sigma^z}{2}} &= e^{\sigma^z \log q^{\pm \frac{1}{2}}} = \sum_{n=0}^{\infty} \frac{(\log q^{\pm \frac{1}{2}})^n}{n!} (\sigma^z)^n \\
 &= \mathbb{1} \sum_{n=0}^{\infty} \frac{(\log q^{\pm \frac{1}{2}})^{2n}}{2n!} + \sigma^z \sum_{n=0}^{\infty} \frac{(\log q^{\pm \frac{1}{2}})^{2n+1}}{(2n+1)!} \\
 &= \mathbb{1} \cosh(\log \sqrt{q}) + \sigma^z \sinh(\pm \log \sqrt{q}) \\
 &= \frac{\sqrt{q} + \frac{1}{\sqrt{q}}}{2} \mathbb{1} \pm \frac{\sqrt{q} - \frac{1}{\sqrt{q}}}{2} \sigma^z
 \end{aligned} \tag{5.57}$$

5.4. The Quantum Group

If we are interested in the spin-1 case, we have to evaluate the three eigenvectors of the total spin operator with the same eigenvalue (i.e. the three eigenvector of the triplet) and use them to project S^+ :

$$P = \begin{pmatrix} 1 & 0 & 0 & 0 \\ 0 & 1 & 1 & 0 \\ 0 & 0 & 0 & 1 \end{pmatrix}$$

$$S^+|_{s=1} = PS^+P^T = \begin{pmatrix} 0 & \sqrt{q} + \frac{1}{\sqrt{q}} & 0 \\ 0 & 0 & \sqrt{q} + \frac{1}{\sqrt{q}} \\ 0 & 0 & 0 \end{pmatrix} \quad (5.58)$$

5.4.2 Casimir Operator and Classification of Representation

The Casimir operator C of $U_q(\mathfrak{su}_2)$ is given by [25]

$$C = q^{2J^z+1} + q^{-2J^z-1} + (q - q^{-1})^2 J^- J^+ \quad (5.59)$$

Since

$$\left(q^{J^z+\frac{1}{2}} - q^{-J^z-\frac{1}{2}}\right)^2 = q^{2J^z+1} + q^{-2J^z-1} - 2 \quad (5.60)$$

the Casimir operator C is equivalent to

$$C \sim \mathbf{S}^2 \equiv J^- J^+ + \left(\frac{q^{J^z+\frac{1}{2}} - q^{-J^z-\frac{1}{2}}}{q - q^{-1}}\right)^2 - \left(\frac{q^{\frac{1}{2}} - q^{-\frac{1}{2}}}{q - q^{-1}}\right)^2 = J^- J^+ + \left[J^z + \frac{1}{2}\right]_q^2 - \left[\frac{1}{2}\right]_q^2 \quad (5.61)$$

whose eigenvalues are labelled by

$$S^2 = \left[j + \frac{1}{2}\right]_q^2 - \left[\frac{1}{2}\right]_q^2 \quad (5.62)$$

where

$$[k]_q = \frac{q^k - q^{-k}}{q - q^{-1}} \quad (5.63)$$

Eigenvalues of the Casimir operator are vital for the study of representations of $U_q(\mathfrak{su}_2)$, since the associate eigenspaces label representations.

Notice that in the $q = 1$ case the above expressions is equal to $j(j+1)$, recovering the \mathfrak{su}_2 case.

In following sections, we will study how representations of $U_q(\mathfrak{su}_2)$ differ from \mathfrak{su}_2 ones for particular choices of the parameter q .

5.4.3 Case When q is Not a Root of Unity

When q is not a root of unity, representations ρ_j of $U_q(\mathfrak{su}_2)$ are in one-to-one correspondence with usual \mathfrak{su}_2 ones. For example in the case $s = \frac{1}{2}$ and $N = 2$ we have

$$\rho_0 \cap \rho_1 = \emptyset \quad (5.64)$$

$$\mathbb{C}^4 = \rho_0 \oplus \rho_1 \quad (5.65)$$

where ρ_j contains the highest weight state $|j, j\rangle$ and its descendants. An highest weight state $|j, j\rangle$ is defined by

$$S^+|j, j\rangle = 0 \quad (5.66)$$

Descendants of a given state are obtained applying recursively S^- on it. In this example the highest weight state $|a\rangle$ of ρ_1 is given by

$$|a\rangle = |\uparrow\uparrow\rangle \quad (5.67)$$

and its descendants are given by

$$S^-|a\rangle = \sqrt{q}|\uparrow\downarrow\rangle + \frac{1}{\sqrt{q}}|\downarrow\uparrow\rangle \quad (5.68)$$

and

$$(S^-)^2|a\rangle = |\downarrow\downarrow\rangle \quad (5.69)$$

On the other hand the representation ρ_0 contains only the state $|b\rangle$

$$|b\rangle = \sqrt{q}|\uparrow\downarrow\rangle - \frac{1}{\sqrt{q}}|\downarrow\uparrow\rangle \quad (5.70)$$

which has not any descendant.

Notice that in this case eigenvalues of the Casimir operator are given by an injective function, i.e. two different representations ρ_j with the same value of the Casimir operator do not exist.

The case when q is a root of unity is more complicated, since a simple decomposition of the Hilbert space does not exist anymore and its study requires a deep analysis.

5.5 Case When q is a Root of Unity

When q is a root of unity, say $q^p = \pm 1$, representations of $U_q(\mathfrak{su}_2)$ do not have the usual \mathfrak{su}_2 form, since a simple decomposition is not possible anymore [25].

As consequence of the cyclicity of q , eigenvalues of the Casimir operator are not still injective, since

$$\left[j' + \frac{1}{2} \right]_q^2 = \left[j'' + \frac{1}{2} \right]_q^2 = \left[j + \frac{1}{2} \right]_q^2 \quad (5.71)$$

for

$$j' = j + np \quad (5.72)$$

$$j'' = p - 1 - j + np \quad (5.73)$$

$$n \in \mathbb{Z}$$

As before, each representation ρ_j is defined from one of the highest weigh states, but thanks to the cyclicity of the Casimir operator, there is an ambiguity in the choice of the highest weight state. Moreover two representations ρ_j and $\rho_{j'}$ with j and j' related by (5.72) are mixed by the action of S^\pm operators.

Being a root of unity implies that S^\pm vanishes when it is applied p times

$$(S^\pm)^p = 0 \quad (5.74)$$

For example in the $p = 3$ case the highest weight state of the $\rho_{\frac{3}{2}}$ representation is given by $\left| \frac{3}{2}, \frac{3}{2} \right\rangle$, which satisfies

$$J^+ \left| \frac{3}{2}, \frac{3}{2} \right\rangle = 0 \quad (5.75)$$

but also the state $J^- \left| \frac{3}{2}, \frac{3}{2} \right\rangle$ is a highest weight state, since

$$\begin{aligned} J^+ J^- \left| \frac{3}{2}, \frac{3}{2} \right\rangle &= (J^- J^+ + [J^+, J^-]) \left| \frac{3}{2}, \frac{3}{2} \right\rangle \\ &= [2J^z]_q \left| \frac{3}{2}, \frac{3}{2} \right\rangle = [3]_q \left| \frac{3}{2}, \frac{3}{2} \right\rangle = 0 \end{aligned} \quad (5.76)$$

This *mixing* effect can be clarified considering the simple three-site case.

5.5.1 Example: Representations of \mathfrak{su}_2 and $U_q(\mathfrak{su}_2)$ in the $(p = 3, N = 3)$ case

Representations of \mathfrak{su}_2

The Hilbert space of this system is given by \mathbb{C}^6 and it splits into

$$\mathbb{C}^6 = \rho_{\frac{1}{2}} \oplus \rho_{\frac{1}{2}} \oplus \rho_{\frac{3}{2}} \quad (5.77)$$

We can make the following choice for highest weight states:

$$|a\rangle = |\uparrow\uparrow\uparrow\rangle \quad (5.78)$$

$$|b\rangle = \frac{|\uparrow\uparrow\downarrow\rangle - |\downarrow\uparrow\uparrow\rangle}{\sqrt{2}} \quad (5.79)$$

$$|c\rangle = \frac{|\uparrow\uparrow\downarrow\rangle - 2|\uparrow\downarrow\uparrow\rangle + |\downarrow\uparrow\uparrow\rangle}{\sqrt{6}} \quad (5.80)$$

These states are not only orthogonal, but also generate orthogonal descendant states, i.e. descendant states generated from different highest weight states are orthogonal.

The orthogonality of ρ_j representations allows us to write (5.77) using direct sum, since all terms are orthogonal.

Representations of $U_q(\mathfrak{su}_2)$

As before the Hilbert space is given by \mathbb{C}^6 , but it can not be represented by a direct sum

$$\mathbb{C}^6 = \rho_{\frac{1}{2}} + \rho_{\frac{1}{2}} + \rho_{\frac{3}{2}} \quad (5.81)$$

since ρ_j are not orthogonal between them.

Let $|a\rangle = |\uparrow\uparrow\uparrow\rangle$ be the highest weight state of $\rho_{\frac{3}{2}}$. Thanks to (5.76) also $J^-|a\rangle$ is a highest weight state, i.e. $S^-|a\rangle = 0$ and $S^z|a\rangle = \frac{3}{2}|a\rangle$

$$S^+S^-|a\rangle = [3]_q|a\rangle = 0 \quad (5.82)$$

and it has zero norm:

$$\|S^-|a\rangle\|^2 = \langle a|S^-|S^+a\rangle = 0 \quad (5.83)$$

For each representation ρ_j one state in the $S^z = \frac{1}{2}$ sector exists; thus orthogonal space of $S^-|a\rangle$ is two-dimensional and it contains $S^-|a\rangle$ itself. For this reason a state $|b\rangle \in \rho_{\frac{1}{2}}$ non-orthogonal to $S^-|a\rangle$ exists, i.e.

$$\langle S^-a|b\rangle = \langle a|S^+b\rangle \neq 0 \quad (5.84)$$

Thanks to this fact the splitting of the Hilbert space is not given by a direct sum of representations, since we have shown the arising of a mixture between $\rho_{\frac{3}{2}}$ and one of the two $\rho_{\frac{1}{2}}$ representations.

The Hilbert space \mathbb{C}^6 is then decomposed irreducibly into one big representation, given by a mixture of $\rho_{\frac{3}{2}}$ and $\rho_{\frac{1}{2}}$, and into a smaller simple $\rho_{\frac{1}{2}}$. The big representation $\rho_{\frac{3}{2}} + \rho_{\frac{1}{2}}$ is indecomposable but not irreducible (it contains $\rho_{\frac{3}{2}}$) and it

5.5. Case When q is a Root of Unity

is called a *type-I* representation. On the other hand we can define the small $\rho_{\frac{1}{2}}$ representation as a *type-II* representation.

Type-I representation presents another peculiar property, due to (5.74): starting from the highest weight state $|a\rangle = |\uparrow\uparrow\uparrow\rangle$ and applying S^- once, we can not come back to $|a\rangle$ and we can not reach $|\downarrow\downarrow\downarrow\rangle$, since $S^+S^-|a\rangle = 0 = (S^-)^3|a\rangle$.

5.5.2 Generalisation to a larger number of sites

The decomposition of the Hilbert space \mathcal{H} can also be done for an arbitrary number of sites N ($\mathcal{H} = \mathbb{C}^{2^N}$) and it provides a splitting into some type-I big representations and some other type-II. In order to classify these representations it can be useful to introduce the q -dimension of a representation ρ_j

$$\dim_q \rho_j = [2j + 1]_q \quad (5.85)$$

which is invariant under (5.72) up to a global sign.

Thanks to its properties, the q -dimension gives information about the type of the considered representation: type-I representations have zero q -dimension, while type-II ones have the q -dimension different from zero. A zero q -dimension representation can be obtained taking a couple of representations ρ_j and $\rho_{j'}$, with different sign; this couple can be easily identified, since their indices are connected by (5.72).

States belonging to type-I representations are not considered in the analysis of physical properties of these systems. For this reason, the Hilbert space describing these models is **restricted**. The presence of zero-norm states and their dismissing reminds the procedure to obtain Minimal Conformal Models [12], in which these null states are not considered in the building up of the Hilbert space of the system. Indeed the Hilbert space $\mathcal{M}(p', p)$ of a minimal model is smaller than the entire Verma module.

type-II representations

As we said before, physical states belong to type-II representations.

Let $|a_j\rangle$ be the highest weight state of a type-II representation ρ_j , then

$$|a_j\rangle \in \ker S^+ \quad (5.86)$$

This definition is not sufficient to identify the correct state $|a_j\rangle$, since we require that it does not belong to any other representation. For this reason we ‘remove’ from $\ker S^+$ all states which can be obtained from recursive applications of S^+ :

$$|a_j\rangle \in \frac{\ker S^+}{\text{Im}(S^+)^{p-1}} \quad (5.87)$$

or, alternatively

$$|a_j\rangle \in \frac{\ker(S^-)^{2j+1}}{\text{Im}(S^-)^{p-1-2j}} \quad (5.88)$$

The number of highest weight states in a given $S^z = j$ sector of a N -site system is denoted by $\Omega_j^{(N)}$, and it takes the form

$$\Omega_j^{(N)} = \Gamma_j^{(N)} - \Gamma_{p-1-j}^{(N)} + \Gamma_{j+p}^{(N)} - \Gamma_{p-1-j+p}^{(N)} + \dots \quad (5.89)$$

where $\Gamma_j^{(N)}$ denotes the number of the \mathfrak{su}_2 representations in the sector $S^z = j$. For the spin- $\frac{1}{2}$ representation of \mathfrak{su}_2 we have

$$\Gamma_j^{(N)} = \binom{N}{\frac{N}{2} - j} - \binom{N}{\frac{N}{2} + j + 1} \quad (5.90)$$

5.5.3 Type-II representations and Bratteli diagrams

Bratteli diagrams ([25] and references therein) are a useful graphical method to analyse possible spin sectors of a model.

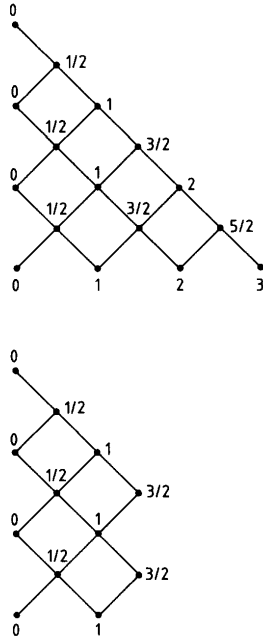


Figure 5.1: Bratteli Diagram for \mathfrak{su}_2 and $U_q(\mathfrak{su}_2)$. Picture taken from [25]

For instance, the first picture represents the Bratteli diagram for \mathfrak{su}_2 and the vertical scale denotes the number N of spin- $\frac{1}{2}$ sites, starting from $N = 0$ at the top dot. In a one-site model, the only possible spin sector is the $S^z = \frac{1}{2}$ one, while a two-site system can belong to a $S^z = 0$ or to a $S^z = 1$ sector. Since the ‘height’ of a spin sector is bounded only by the number of sites ($S_{max}^z = \frac{N}{2}$), the width of this diagram grows as its height.

As we said before, in a $U_q(\mathfrak{su}_2)$ model with $q^p = \pm 1$ possible values of the spin are bounded, since $(J^+)^p = 0$ and then $S^z \leq \frac{p}{2}$. This restriction is implemented in the Bratteli diagram removing all sectors with a forbidden value of the spin. The second diagram represents possible spin sectors for a $U_q(\mathfrak{su}_2)$ system with $q = e^{\frac{i\pi}{4}}$. Referring to the

5.6. Unitarity When q is a Root of Unity

first diagram, the number of paths in a N -site \mathfrak{su}_2 system starting in the top left corner and ending in the sector j in the bottom line is given by $\Gamma_j^{(N)}$ [25, 22]: since a state in the j sector in a N -site model is built up adding sequentially spin- $\frac{1}{2}$ sites, the number of such states $S^z = j$ sector is given by the number of possible combinations of these spin- $\frac{1}{2}$ states. A similar argument can be developed for the $U_q(\mathfrak{su}_2)$ diagram with N sites: in this case the number of paths to reach a given j sector is given by $\Omega_j^{(N)}$. As in the \mathfrak{su}_2 case, a state in a given sector is made adding sequentially N spin- $\frac{1}{2}$ sites. The main difference from the \mathfrak{su}_2 case is that some sectors are forbidden and for this reason the number of allowed paths is reduced.

5.6 Unitarity When q is a Root of Unity

Let us focus on unitarity of type-II states. Parametrize q as

$$q = \exp \left[\frac{i\pi p'}{p} \right] \quad (5.91)$$

with p and p' relatively prime integers ($1 \leq p' < p$).

Let us consider a highest weight state $|a_j\rangle$ of an irreducible type-II representation and its descendants. Setting $\langle a_j|a_j\rangle = 1$, the norm of its descendant states is given by [25]

$$\langle a_j|(S^+)^n(S^-)^m|a_j\rangle = \delta_{m,n}[n]_q! \prod_{k=1}^n [2j - n + k]_q \quad (5.92)$$

which is always non-negative for $j < \frac{p}{2p'}$.

The presence of such negative normed states is not a surprise, since it is foreseen in Minimal Conformal Models $\mathcal{M}(p', p)$ with $p' \neq 1$ [12]. Moreover in Chapt. 4 we noticed that in Forrester-Baxter RSOS models [20], some Boltzmann weights are negative; this negativity is reflected in negative-norm states in the spin-chain via the Hamiltonian limit which links these two models.

Furthermore the negativity of states will be required in Chapt. 6: the negativity of the Entanglement Entropy (obtained from the statistical model) has to be reflected at the quantum level (spin-chain); otherwise there would be a discrepancy in the connection between the FB-RSOS model and the $U_q(\mathfrak{su}_2)$ -invariant Hamiltonian (5.28).

5.7 The $U_q(\mathfrak{su}_2)$ -invariant Hamiltonian and its Conformal Structure

Let us recall the expression of the $U_q(\mathfrak{su}_2)$ -invariant Hamiltonian (5.28)

$$H = \sum_{i=1}^{N-1} \left[\sigma_i^x \sigma_{i+1}^x + \sigma_i^y \sigma_{i+1}^y + \frac{q + q^{-1}}{2} \sigma_i^z \sigma_{i+1}^z \right] + \frac{q - q^{-1}}{2} (\sigma_1^z - \sigma_N^z) \quad (5.93)$$

As we said before, its symmetry group is implemented by the Quantum Group, since

$$[H, S^\pm] = 0 = [H, S^z] \quad (5.94)$$

Thanks to its symmetry, the spectrum of this Hamiltonian can be classified using representations of $U_q(\mathfrak{su}_2)$.

The presence of the boundary terms in the Hamiltonian makes it invariant under the action of the quantum group, but makes the Hamiltonian non-hermitian if $q \notin \mathbb{R}$. This non-hermiticity may look unphysical, since a complete eigenbasis of the Hilbert space is not guaranteed anymore.

If we take $q \in S^1$, i.e. a complex number with modulus one, the Hamiltonian is still non-hermitian but its eigenvalues are real, since the Hamiltonian obtained re-labelling all sites from N to 1 is similar to $H(q^{-1}) = H^\dagger(q)$; this transformation does not affect eigenvalues, and so that they are real.

The existence of a complete eigenbasis of the Hilbert space will be discussed at the end of this Chapter.

5.7.1 Spectrum of H

The spectrum of the Hamiltonian can be obtained via Bethe Ansatz [25, 24]. Since S^z is conserved, it is a good quantum number for the parametrisation Bethe states. Let $|n\rangle$ be defined as the state with n states pointing down

$$|n\rangle = \sum_{1 \leq x_1 < x_2 < \dots < x_n \leq N} f(x_1, \dots, x_n) |x_1, \dots, x_n\rangle \quad (5.95)$$

where x_i s denote the positions of pointing down spins.

Bethe equation for energy is given by

$$E = (N - 1) \left(\frac{q + q^{-1}}{2} \right) + 4 \sum_{j=1}^n \left[\cos k_j - \left(\frac{q + q^{-1}}{2} \right) \right] \quad (5.96)$$

5.7. The $U_q(\mathfrak{su}_2)$ -invariant Hamiltonian and its Conformal Structure

while Bethe momenta are defined by

$$Nk_j = \pi I_j + \frac{1}{2} \sum_{l=1, l \neq j}^n [\Psi(k_j, k_l) + \Psi(k_j, -k_l)] \quad (5.97)$$

where $I_j \in [1, N]$ are distinct integers and the function Ψ reads

$$\Psi(k_1, k_2) = -i \log \left[\frac{1 - (q + q^{-1})e^{ik_1} + e^{i(k_1+k_2)}}{1 - (q + q^{-1})e^{ik_2} + e^{i(k_1+k_2)}} \right] \quad (5.98)$$

The ground state energy in a given sector $S^z = j$ can be simply obtained taking $I_j^0 = j = 1, \dots, n$.

5.7.2 Thermodynamic Limit and Conformal Behaviour

It is very interesting to study the thermodynamic limit of this spin-chain, since it gives information about its scaling behaviour and the field theory describing it [25].

From Bethe ansatz equations, the scaling limit of the ground state energy in the $j = 0$ sector is given by ($q = \exp \left[\frac{i\pi p'}{p} \right]$)

$$\lim_{N \rightarrow \infty} N \check{E}_0 = -\frac{1}{24} \left(1 - 6 \frac{(p - p')^2}{pp'} \right) \quad (5.99)$$

where \check{E} is a normalised version of the energy

$$\check{E} = \frac{E}{\pi \left(\frac{p'}{p} + 1 \right) \sin \frac{\pi}{\frac{p'}{p} + 1}} \quad (5.100)$$

The scaling behaviour of the ground state energy of a unitary open conformal system is ruled by [31]

$$\check{E}_0 = N\epsilon_0 + f_0 - \frac{\pi c}{24N} + O\left(\frac{1}{N}\right) \quad (5.101)$$

where ϵ_0 and f_0 are respectively the bulk energy per site and the surface energy. Comparing (5.99) and (5.101) we can obtain the central charge of the system

$$c = 1 - \frac{6(p - p')^2}{pp'} \quad (5.102)$$

which is the central charge of the $\mathcal{M}(p', p)$ Minimal Conformal Model [12]. Moreover from the scaling limit of Bethe ansatz equations, also the scaling dimensions of excited states can be obtained

$$\lim_{N \rightarrow \infty} N(\check{E}_j - \check{E}_0) = \frac{(p - 2p'j)^2 - (p - p')^2}{4pp'} \quad (5.103)$$

which corresponds to the conformal dimension $h_{1,1+2j}$ of the Kac table of the associated Minimal Model.

Since in non unitary minimal models ($p' \neq 1$) one or more negative conformal dimensions $h_{1,m}$ exists in the Kac table, we notice that E_0 is not the physical ground state, because the eigen-energy E_j (with j s.t. $h_{1,1+2j} < 0$) is less than E_0 . Furthermore, the equation (5.101) for the physical ground state reads [32]

$$\check{E}_0^{physical} = N\epsilon_0 + f_0 - \frac{\pi c_{eff}}{24N} + O\left(\frac{1}{N}\right) \quad (5.104)$$

in perfect agreement with (5.99) and (5.103).

These differences are due to the splitting of the physical ground state and of the conformal vacuum in non-unitary conformal field theory [12, 32].

Summarising, we found that the physical ground state of a non-unitary system does not belong to the $j = 0$ sector.

Brief Recall About Non-Unitary Conformal Field Theory

It is very important to focus on the difference between the physical ground state and the conformal vacuum ([32] and Appendices D and E).

The conformal vacuum $|0\rangle$ is defined as

$$L_n|0\rangle = 0 \quad \text{for all } n \geq -1 \quad (5.105)$$

The physical ground state is defined as the state which minimises the energy

$$H|g.s.\rangle = E_0|g.s.\rangle \quad (5.106)$$

where E_0 is the smallest eigenvalue of the Hamiltonian operator H .

In conformal field theories, the operator L_0 gives the conformal dimension of a state h

$$L_0|\phi\rangle = h|\phi\rangle \quad (5.107)$$

and it realises the Hamiltonian operator in a quantum system described by a conformal theory [12].

In unitary conformal models the conformal vacuum (and then the unity operator) has the smallest conformal dimension ($h = 0$); i.e. a primary field ϕ with negative conformal dimension does not exist, or, in the quantum state picture, there is not any state less energetic than the conformal vacuum. For this reason the conformal vacuum and the physical ground state coincide in unitary theories.

The equivalence between these two states is not valid anymore in non-unitary theories, thanks to the presence of states with negative conformal dimension. For this reason the physical ground state can be seen as an excitation of the conformal vacuum due to the primary field with the smallest conformal dimension $h < 0$.

While the central charge c in a non-unitary theory is still related to **conformal** properties of a system, such as the O.P.E. of the stress tensor, it does not influence directly **physical** properties, such as the Casimir energy, where its role it is played by the *effective* central charge.

5.8 Non-Hermitian Hamiltonians

As we said before if $q \notin \mathbb{R}$, the $U_q(\mathfrak{su}_2)$ -invariant Hamiltonian (5.28) is not Hermitian anymore, but it has real eigenvalues if $q \in S^1$ [22, 25]. The realness of the spectrum is not enough to build up a complete Hilbert space using eigenvectors.

5.8.1 \mathcal{PT} -symmetric Hamiltonians

Consider a non-Hermitian Hamiltonian H with real discrete spectrum//Denote with ϵ_n the eigenvalues of H and with $|\Phi_n\rangle$ and $|\Psi_n\rangle$ respectively its right and left eigenvectors

$$\begin{aligned} H|\Phi_n\rangle &= \epsilon_n|\Phi_n\rangle \\ \langle\Psi_n|H &= \epsilon_n\langle\Psi_n| \end{aligned} \quad (5.108)$$

In general they are not orthonormal

$$\langle\Phi_n|\Phi_m\rangle \neq \delta_{n,m} \quad (5.109)$$

but, according to [33], they form a bi-orthonormal basis

$$\begin{aligned} \langle\Psi_n|\Phi_m\rangle &= \delta_{n,m} \\ \sum_n |\Phi_n\rangle\langle\Psi_n| &= \mathbb{1} \end{aligned} \quad (5.110)$$

Suppose the existence of a self-adjoint parity operator² \mathcal{P} which maps H into its Hermitian conjugate H^\dagger

$$\mathcal{P}H\mathcal{P} = H^\dagger \quad \text{with} \quad \mathcal{P}^2 = \mathbb{1} \quad (5.111)$$

²In the $U_q(\mathfrak{su}_2)$ Hamiltonian this map is provided by the re-labelling of all sites

Thus this operator maps left eigenvectors in right ones and vice-versa:

$$\begin{aligned}\mathcal{P}|\Phi_n\rangle &= s_n|\Psi_n\rangle \\ \mathcal{P}|\Psi_n\rangle &= s_n|\Phi_n\rangle\end{aligned}\tag{5.112}$$

where $s_n = \pm 1$.

The set of all signatures $s = (s_1, \dots, s_n)$ defines the operator

$$\mathcal{C} = \sum_n s_n |\Phi_n\rangle \langle \Psi_n|\tag{5.113}$$

satisfying [33]

$$\begin{aligned}[\mathcal{C}, H] &= 0 \\ [\mathcal{C}, \mathcal{PT}] &= 0\end{aligned}\tag{5.114}$$

where the operator \mathcal{T} implements the complex conjugation.

We can now construct the *quasi-hermiticity* operator η as

$$\eta = \mathcal{PC}\tag{5.115}$$

with the property

$$H^\dagger \eta = \eta H\tag{5.116}$$

If the operator η is positive but not necessarily invertible, the Hamiltonian H is called *quasi-Hermitian*, while if η is invertible and not necessarily positive, H is called *pseudo-Hermitian*. If an Hamiltonian has both these properties we can define the operator $\sqrt{\eta}$ and its inverse which allows us to find a Hermitian counterpart of H

$$h = \sqrt{\eta} H \sqrt{\eta}^{-1} = h^\dagger\tag{5.117}$$

This Hermitian counterpart h of the non-Hermitian Hamiltonian H allows us to consider H as a ‘normal’ quantum Hamiltonian.

5.8.2 Case When q is a Root of Unity

As for the analysis of representations of Quantum Group when q is a root of unity, some complications arise [22] in the building up of a quasi-hermiticity operator.

If we restrict our analysis only to states belonging to type-II representations, the procedure is the same as the previous case; while if we include type-I states, we

5.8. Non-Hermitian Hamiltonians

can not construct a bi-orthonormal basis, since some eigenvectors related to the same eigenvalue are orthogonal

$$\langle \Psi_n | \Phi_n \rangle = 0 \tag{5.118}$$

The presence of such states makes the quasi-hermiticity operator η non-negative, while positivity is required in order to provide a hermitian counterpart h of the Hamiltonian H . As before, in order to define a hermitian version of the $U_q(\mathfrak{su}_2)$ -invariant Hamiltonian (5.28) at root of unity, we remove aforementioned states from the Hilbert space, reducing it. This procedure is called *Quantum Group Reduction at Root of Unity* ([22] and references therein).

In conclusion, in this chapter we have analysed the $U_q(\mathfrak{su}_2)$ -invariant Hamiltonian and we have shown that peculiarities of this system are evident in all its properties; All characteristics of Unitary and non-Unitary Minimal Conformal Models are reflected in various properties of this spin chain. In particular the necessity to remove some states from the Hilbert space of the system due to null states in the Conformal Theory is reflected in the requirement of removing some states from the eigenbasis of the Hamiltonian and from the representations of its symmetry group. Furthermore, difference between conformal vacuum and physical ground state in non-unitary Conformal Theories agree perfectly with results founded using Bethe Ansatz.

Chapter 6

Entanglement Entropy in RSOS Models

In this section we will use the Peschel-Kaulke-Legeza method ([7] and Chapter 2) for the evaluation of Entanglement Entropy in the RSOS model near its critical point. Since some unexpected result arise from these non-unitary models, we will make some considerations in order to interpret unusual behaviour of such systems. Of course the RSOS model describes a classical system and the entanglement is a genuine quantum phenomenon; for this reason it is vital to find a quantum one-dimensional system described by the RSOS model.

Note about the Evaluation of Rényi Entropy

As we said before, in following sections we will evaluate and analyse Rényi Entropy in RSOS models using the Corner Transfer Matrix technique (CTM). Notice that this method provides Rényi Entropy for an infinite bipartite 1 + 1-dimensional quantum system whose 2-dimensional statistical representation is given by the RSOS model. In [17] and [20] thermodynamic quantities are evaluated using temperature-like parameters k and p . In order to compare our results with Field Theory prediction, we will study the dependance of entropy on the correlation length ξ

$$\xi \sim p^{-2\nu} \tag{6.1}$$

Its scaling dimension ν can be obtained using CTM [17, 20, 34]

$$\nu = \frac{r}{4s} \tag{6.2}$$

Since the scaling behaviour of the correlation length ξ near a critical point is ruled by Conformal Field Theory (CFT), ν can also be obtained [32] from the scaling

dimension h of the most relevant field Φ of the theory

$$\nu = \frac{1}{2 - 2h} \tag{6.3}$$

which corresponds to (6.2) since in the Minimal Model $\mathcal{M}(r - s, s)$ the most relevant field is given by the primary field $\phi_{1,3}$ of the Kac table [12, 32] with conformal dimension

$$h_{1,3} = \frac{r - 2s}{r} \tag{6.4}$$

6.1 Evaluation of the Rényi Entropy in ABF models

In [9] Franchini and De Luca evaluated the α -Rényi Entropy for the r -th ABF RSOS [17] model in regime III, whose critical point is described by the unitary r -th minimal model $\mathcal{M}(r - 1, r)$ ([12] and Appendix E).

Rényi Entropy for this models is given by ([9] and Appendix A)

$$S_A^{(\alpha)} = \frac{\alpha + 1}{\alpha} \frac{c}{12} \log \xi + u_\alpha + a_\alpha \xi^{-\frac{h_{3,3}}{2\alpha}} + O\left(\xi^{-\frac{h_{3,3}}{\alpha}}\right) \tag{6.5}$$

where u_α and a_α are constants which do not depend on ξ (u_α is sometimes called *universal constant*).

The leading logarithmic term agrees exactly with the Cardy-Calabrese prediction ([11] and Chapt. 3). As noticed in [9] the scaling dimension appearing in power corrections is given by $h_{3,3}$ which is not the dimension of the the primary field $\phi_{1,3}$ opening the mass gap [35].

Notice that since this model is unitary, the physical ground state and the conformal vacuum can be identified (this identification is very important since the Peschel-Kaulke-Legeza's method evaluates Rényi entropy for the physical ground state, while the Cardy-Calabrese prediction refers to the conformal vacuum).

6.2 Evaluation of the Rényi Entropy in BF models

The main effort in this thesis was given in the evaluation of Rényi and Von-Neumann Entropy in BF RSOS models ([20] and Chapter 4), which are described by non-unitary minimal models; this non-unitarity provides some unexpected results which will be analysed and interpreted in following sections.

6.2. Evaluation of the Rényi Entropy in BF models

Following Appendix A, Rényi Entropy is given by

$$S_A^{(\alpha)} = \frac{\alpha + 1}{\alpha} \frac{c_{eff}}{12} \log \xi + U_\alpha + A_\alpha(\xi) \quad (6.6)$$

where c_{eff} is the *effective central charge*¹

$$c_{eff} = c - 24\Delta \quad (6.7)$$

and

$$\begin{aligned} U_\alpha &= -\frac{1}{2} \log [8r(r-s)] + \frac{1}{1-\alpha} \log \left[\frac{\mathfrak{f}_1(\alpha; r, s)}{\mathfrak{f}_1(1; r, s)} \right] \\ A_\alpha(\xi) &= \frac{1}{1-\alpha} \left[\frac{\mathfrak{f}_2(\alpha; r, s)}{\mathfrak{f}_1(\alpha; r, s)} \xi^{-\frac{3}{2\alpha r(r-s)}} - \alpha \frac{\mathfrak{f}_2(1; r, s)}{\mathfrak{f}_1(1; r, s)} \xi^{-\frac{3}{2r(r-s)}} + \right. \\ &\quad \left. - \frac{1}{2} \left[\frac{\mathfrak{f}_2(\alpha; r, s)}{\mathfrak{f}_1(\alpha; r, s)} \right]^2 \xi^{-\frac{3}{\alpha r(r-s)}} + \alpha \frac{1}{2} \left[\frac{\mathfrak{f}_2(1; r, s)}{\mathfrak{f}_1(1; r, s)} \right]^2 \xi^{-\frac{3}{r(r-s)}} + O\left(\xi^{-\frac{4}{\alpha r(r-s)}}\right) \right] \\ \mathfrak{f}_k(n; r, s) &= \sum_{a=1}^{r-1} \sin\left(k \frac{\pi d}{r-s}\right) \sin\left(k \frac{\pi a}{r}\right) \sin^n\left(\frac{\pi a s}{r}\right) \end{aligned} \quad (6.8)$$

From this expression two problems arise: the presence of the effective central charge c_{eff} instead of the central charge c and the anomalous behaviour of the universal term and of the corrections.

The presence of the effective central charge seems to contradict the Cardy-Calabrese ([11] and Chapt. 3) prediction.

The second problem is given by the vanishing of the \mathfrak{f}_1 function in $s \neq 1$ cases, which makes diverge both U_α and $A_\alpha(\xi)$ terms. Moreover if $\frac{\mathfrak{f}_1(\alpha; r, s)}{\mathfrak{f}_1(1; r, s)}$ does not tend to one when $\alpha \rightarrow 1^+$, Von-Neumann Entropy will diverge.

6.2.1 Interpretation of Results - Central Charge

These results can be justified focusing on the quantum state used by Cardy and Calabrese in the evaluation of Entanglement Entropy [11].

In their seminal work [11] they evaluate Entanglement Entropy for the conformal vacuum $|0\rangle$ which coincides with the ground state of the theory if and only if it is unitary. The physical ground state $|g.s.\rangle$, i.e. the one which minimises the energy,

¹ Δ denotes the lowest conformal dimension of the theory underlying the critical point ($\Delta = 0$ in unitary theories). For a brief review about the role of the effective central charge see Appendix D

differs from the conformal vacuum $|0\rangle$ ($L_n|0\rangle = 0 \forall n \geq -1$) if the theory is non-unitary. They are connected by an operator ϕ with conformal dimension $\Delta < 0$ which decreases the energy of the conformal vacuum

$$|gs\rangle = \phi(0)|0\rangle \tag{6.9}$$

$$\langle gs|L_0|gs\rangle = \langle 0|\phi^\dagger(t \rightarrow +\infty)L_0\phi(t \rightarrow -\infty)|0\rangle = \Delta\langle 0|0\rangle < \langle 0|L_0|0\rangle = 0 \tag{6.10}$$

In this way, the physical ground state can be seen as an excitation of the conformal vacuum and vice-versa. Notice that such an operator with negative conformal dimension exists only in non-unitary theories.

Thanks to this energy shift, the shift in the coefficient of the logarithm term in the Entanglement Entropy is supposed to be due to the different state whose Rényi Entropy is evaluated.

Moreover one expects that Rényi and Von-Neumann Entropy diverges at the critical point ($\xi \rightarrow \infty$) and decreases leaving it. Since the central charge can be negative for non-unitary theories, if the coefficient of the logarithm term of the entropy was the ‘usual’ central charge, Entropy would increase leaving the critical point, leading to a result whose physical interpretation would be difficult. Thanks to the positivity of the effective central charge, the entropy increases always when it reaches a critical point.

As we said in Chapter 5 studying the $U_q(\mathfrak{su}_2)$ -invariant Spin-Chain, the **effective** central charge rules **physical** properties of a non-unitary system belonging to its ground state; in the same way, we can suppose that Entanglement is ruled by the effective central charge.

From a Conformal Field Theory point of view, Rényi Entropy can also be evaluated for excited states. The Rényi Entropy related to a subsystem A with size ℓ of a critical periodic system with size L belonging to the excited state ϕ with conformal dimension h is given by

$$S_\phi^{(\alpha)} = S_{gs}^{(\alpha)} + \frac{1}{1-\alpha} \log F^{(\alpha)}\left(\frac{\ell}{L}\right) \tag{6.11}$$

where the function F is given by [36] for an integer value of α

$$F^{(n)}(x) = \frac{\langle \phi_1(0, -\infty)\phi_1^\dagger(0, \infty) \cdots \phi_n(0, -\infty)\phi_n^\dagger(0, \infty) \rangle_{\mathcal{M}_n}}{\langle \phi(0, -\infty)\phi^\dagger(0, \infty) \rangle_{\mathcal{M}_1}} \tag{6.12}$$

where \mathcal{M}_n is the n -Riemann surface with branch points at boundaries of the subsystem A and ϕ_k is the copy of the field ϕ belonging to the k -th sheet.

The evaluation of (6.11) and (6.12) require the evaluation of a $2n$ -point correlation function; this computation can be easily done for non-interacting theories, such as the free boson or the free fermion, but implies non trivial difficulties in the interacting case.

6.2.2 Interpretation of results - negativity of the entropy

As we said before, Rényi Entropy may be negative in some $s \neq 1$ cases. We can observe that this issue happens if we take the sum in (6.11) over all possible values of a , i.e. on all odd or even numbers from 1 to $r - 1$; indeed if we restrict our evaluation only to some values of a the problem of negativity disappear. We suppose that this negativity is due to the presence of negative normed states.

As we said before, if we restrict allowed values of a , the universal term U_α would become positive, avoiding interpretation problems about negativity of Entropy.

For example, keeping a fixed, Rényi Entropy is well defined and Von-Neumann Entropy reads

$$\begin{aligned}
 S_A &= \frac{c_{eff}}{6} \log \xi - \frac{1}{2} \log [8r(r-s)] + \log \left[\sin \frac{\pi a}{r} \sin \frac{\pi a s}{r} \sin \frac{\pi d}{r-s} \right] \\
 &+ \frac{\sin \frac{2\pi a}{r} \sin \frac{2\pi d}{r-s}}{\sin \frac{\pi a}{r} \sin \frac{\pi d}{r-s}} \xi^{-\frac{3}{2r(r-s)}} + \frac{\sin^2 \frac{2\pi a}{r} \sin^2 \frac{2\pi d}{r-s}}{2 \sin^2 \frac{\pi a}{r} \sin^2 \frac{\pi d}{r-s}} \xi^{-\frac{3}{r(r-s)}} \\
 &- \frac{3}{2r(r-s)} \frac{\sin \frac{2\pi a}{r} \sin \frac{2\pi d}{r-s}}{\sin \frac{\pi a}{r} \sin \frac{\pi d}{r-s}} \xi^{-\frac{3}{2r(r-s)}} \log \xi \\
 &+ \frac{3}{2r(r-s)} \frac{\sin^2 \frac{2\pi a}{r} \sin^2 \frac{2\pi d}{r-s}}{\sin^2 \frac{\pi a}{r} \sin^2 \frac{\pi d}{r-s}} \xi^{-\frac{3}{r(r-s)}} \log \xi + O\left(\xi^{-\frac{4}{r(r-s)}}\right)
 \end{aligned} \tag{6.13}$$

The first two lines of the above expression agree with the Cardy-Calabrese prediction (up to the presence of the effective central charge). In Von-Neumann Entropy of non-unitary models some unexpected corrections arise, given by extra power-logarithmic terms, which are sub-dominant for small values of ξ , i.e. near the critical point.

Notice that the removing some central heights a in the evaluation of Entanglement Entropy does not affect the leading logarithmic term, whose behaviour is ruled only by the effective central charge. The necessity to remove some central heights a from the statistical model can be viewed as a reminiscent of the quantum group reduction at root of unity ([22] and Chapter 5) extended to negative normed states. As we said in the previous chapter, in order to construct a ‘good’ Hilbert space for the $U_q(\mathfrak{su}_2)$ -invariant Spin-Chain, we remove some null states and we **restrict** the Hilbert space.

In the same way, we can restrict further the physical Hilbert space removing null states. From a quantum field theory point of view, this is reminiscent of what happens in $U(1)$ gauge theories: the auxiliary field B added to the lagrangian $\mathcal{L} = -\frac{1}{4}F_{\mu\nu}F^{\mu\nu}$ in order to fix the gauge parameter is negative normed and the

physical Hilbert space is obtained by removing all negative normed fields [37].

$$B^-(x)|phys.\rangle = 0 \tag{6.14}$$

Notice the resemblance between the expression (5.92) and terms in the f_1 summations: we suppose that elements which make negative the norm are the same which give problem in the well definition of Entropies in non-unitary models.

Moreover, the scaling dimensions δ of Rényi Entropy in the non-unitary case (6.6) is not given by the conformal dimension $h_{1,3}$ of the primary field $\phi_{1,3}$ opening the mass gap, neither by the conformal dimension $h_{3,3}$ as in the ABF case [9]: it is given by

$$\delta = h_{2,2} + 3\Delta = \frac{3}{4r(r-s)} > 0 \tag{6.15}$$

where Δ is the conformal dimension of the primary field with the lowest conformal dimension (see previous section).

As for the shift in the leading logarithmic term, we suppose that this difference is due to the difference between the conformal vacuum and the physical ground state for non-unitary theories.

6.3 Which Hamiltonian?

It is important to emphasise that we are not evaluating the Entanglement Entropy for the $U_q(\mathfrak{su}_2)$ -invariant XXZ Spin-Chain, but we are focusing on its off-critical thermal perturbation.

Notice that in Chapt. 4 we performed the Hamiltonian limit for the RSOS model at its critical point, and we found a connection between this model and the $U_q(\mathfrak{su}_2)$ -invariant XXZ model thanks to algebraic properties. The aforementioned Hamiltonian limit gives the Hamiltonian operator in the RSOS basis, i.e. in a basis built up by local heights which can run from 1 to $r-1$ with the constraint on neighbour sites. As noticed in Chapt. 4, we know that this Hamiltonian can be written in the $\text{spin-}\frac{1}{2}$, since a different representation of the Temperley-Lieb Algebra can be obtained using Pauli Matrices. Thanks to this equivalence, our analysis can be shifted to a better known model and the constraint on local heights is reflected in the boundary conditions of this Hamiltonian.

In the off-critical regime this equivalence can not be performed, since an Algebra underlying the off-critical RSOS transfer matrix is unknown. For this reason we search an off-critical Hamiltonian imposing some reasonable conditions. The first conditions requires that this Hamiltonian has to reach the the $U_q(\mathfrak{su}_2)$ -invariant

6.3. Which Hamiltonian?

one at its critical point.

Furthermore we impose that this Hamiltonian has to be **integrable**, since the RSOS model can be completely solved even at its off-critical regime [17, 20].

The integrability conditions restricts sharply the number of allowed spin $-\frac{1}{2}$ Hamiltonians, since T. Inami and H. Konno proposed [29] an explicit form for the most general spin- $\frac{1}{2}$ integrable Spin-Chain, which depends only on few parameters. As we said in the Chapter 5 the most general XYZ hamiltonian with **integrable** boundary conditions is given by [29]

$$\begin{aligned}
 H &= \sum_{n=1}^{N-1} \left[(1 + k \operatorname{sn}^2 \eta) \sigma_n^x \sigma_{n+1}^x + (1 - k \operatorname{sn}^2 \eta) \sigma_n^y \sigma_{n+1}^y + \operatorname{cn} \eta \operatorname{dn} \eta \sigma_n^z \sigma_{n+1}^z \right] \\
 &+ \operatorname{sn} \eta \left[\frac{\operatorname{cn} \xi_- \operatorname{dn} \xi_-}{\operatorname{sn} \xi_-} \sigma_1^z + \frac{\operatorname{cn} \xi_+ \operatorname{dn} \xi_+}{\operatorname{sn} \xi_+} \sigma_N^z \right] \\
 &+ \left[\frac{2\mu_- (\lambda_- + 1)}{\operatorname{sn} \xi_-} \sigma_1^+ + \frac{2\mu_- (\lambda_- - 1)}{\operatorname{sn} \xi_-} \sigma_1^- + \frac{2\mu_+ (\lambda_+ + 1)}{\operatorname{sn} \xi_+} \sigma_N^+ + \frac{2\mu_+ (\lambda_+ - 1)}{\operatorname{sn} \xi_+} \sigma_N^- \right]
 \end{aligned} \tag{6.16}$$

At the critical point ($k \rightarrow 0$) this Hamiltonian reads

$$\begin{aligned}
 H &= \sum_{n=1}^{N-1} \left[\sigma_n^x \sigma_{n+1}^x + \sigma_n^y \sigma_{n+1}^y + \cos \eta \sigma_n^z \sigma_{n+1}^z \right] \\
 &+ \sin \eta \left[\cot \xi_- \sigma_1^z + \cot \xi_+ \sigma_N^z \right] \\
 &+ \left[\frac{2\mu_- (\lambda_- + 1)}{\sin \xi_-} \sigma_1^+ + \frac{2\mu_- (\lambda_- - 1)}{\sin \xi_-} \sigma_1^- + \frac{2\mu_+ (\lambda_+ + 1)}{\sin \xi_+} \sigma_N^+ + \frac{2\mu_+ (\lambda_+ - 1)}{\sin \xi_+} \sigma_N^- \right]
 \end{aligned} \tag{6.17}$$

Since $\cot \xi_{\pm} \rightarrow \mp i$ when $\xi_{\pm} \rightarrow \pm i\infty$, this choice of the parameter ξ makes H to reach the $U_q(\mathfrak{su}_2)$ -invariant XXZ spin-chain at the critical point $k \rightarrow 0$.

Since for some values of the parameter k the limit $\xi \rightarrow \pm i\infty$ is not defined (e.g. for $k = 1$ $\operatorname{sn}(i\xi)$ becomes $-i \tan(\xi)$ whose limit $\xi \rightarrow \pm\infty$ is not defined) we set also $\mu_{\pm} = 0$ in order to define well all boundary terms.

Notice that fixing the parameter ξ_{\pm} to $\mp i\infty$ does not guarantee that this choice can be extended to the off-critical Hamiltonian. For this reason we can identify as the RSOS off-critical Hamiltonian as the Inami-Konno one with an arbitrary choice of the function $\xi_{\pm}(k)$, requiring that it tends to $\pm i\infty$ when the system reaches, for $k \rightarrow 0$, the critical point.

If we focus on Entanglement Entropy of this Spin-Chain, we suppose that the arbitrariness of the choice of ξ_{\pm} away from the critical point is not reflected on the logarithmic term, since it depends only on the critical point and on the universality class of the system, which depends on its critical properties.

In conclusion, using integrability arguments we identify this Hamiltonian with the one-dimensional quantum system whose two-dimensional statistical representation is given by the RSOS model, both critical and off-critical.

This identification is very important, since the Entanglement is a genuine quantum phenomenon and the knowledge of the RSOS model is only a statistical representation of a quantum one-dimensional model.

Conclusions and Outlook

After reviewing some important results about Entanglement and its evaluation in Integrable systems, we focused on a particular class of restricted integrable Spin-Chains whose statistical representation is given by BF-RSOS models.

One of the most important properties of these statistical models is that at their critical point they provide a lattice realisation of Minimal Conformal Models.

The first result of this thesis is the evaluation of Rényi and Von-Neumann Entropy for non-unitary gapped FB-RSOS models using the Corner Transfer Matrix (CTM) technique, noticing the arising of the **effective** central charge as a coefficient of the logarithmic term. The presence of the effective central charge instead of the ‘usual’ one is supposed to be due to the difference between **conformal vacuum** and **physical ground state**: while the Conformal Field Theory prediction is valid for the conformal vacuum, the CTM technique evaluates Rényi Entropy for the physical ground state. This difference arises only in non-unitary models, since in unitary ones conformal vacuum and physical ground state can be identified. From the analysis of Rényi and Von Neumann Entropy, we found that we have to **restrict** the physical Hilbert space by removing negative normed states in order to have a well defined Entropy.

The second result of this thesis is the proposal of a quantum one-dimensional Spin-Chain whose two-dimensional statistical representation is given by the RSOS model. The Hamiltonian limit of the RSOS provides a Hamiltonian operator in the RSOS basis whose physical interpretation is not clear; at the critical conformal point this Hamiltonian can be rewritten using Pauli Matrices thanks to algebraic properties of its elements. The critical Spin-Chain Hamiltonian is given by a XXZ one with boundary terms depending of the spatial anisotropy J_z of the bulk Hamiltonian and it has been studied deeply in literature. Unfortunately this ‘translation’ from the RSOS basis to a Spin-Chain one can not be performed away from the critical point, since the algebra underlying the Hamiltonian is unknown; for this reason we propose an off-critical **integrable** XYZ Hamiltonian with **integrable**

boundaries whose critical limit gives the critical Spin-Chain Hamiltonian. The integrability condition in the Spin-Chain is required since the RSOS model remains integrable even in its off-critical regime.

The proposed Hamiltonian depends on an extra parameter which can be fixed arbitrarily away the critical point, but we suppose that this arbitrariness does not affect the logarithmic behaviour of Entanglement Entropy, since it depends only on the universality class of the system, i.e. on its critical properties.

The removing of this arbitrariness would be a challenging problem related to a deeper comprehension of Quantum Algebras.

The Minimal Conformal structure of the critical point in RSOS models is reflected in the critical Spin-Chain, since it provides a Spin-Chain realisation of Minimal Conformal Models. The Hilbert space of this Spin-Chain has to be **reduced** in order to remove null states, i.e. states with zero norm; this procedure, called *quantum group reduction at root of unity* is a reminiscent of the removing of null states from a Verma modulus in order to build up the Hilbert space of Minimal Models.

The knowledge of an explicit form of the Spin-Chain related to RSOS models allow simulations of Entanglement Entropy for these models using the DMRG algorithm. The main problem about numerical studies is given by non-hermiticity of these Hamiltonians: even if they are acceptable from a physical point of view (Chapter 5), their non-hermiticity provides non trivial numerical problems, which we would like to solve in future.

Furthermore it is known that *Logarithmic Conformal Models* can be obtained as a limit of BF-RSOS models; for this reason we would like to extend our calculations of Entanglement to this class of models, studying possible unexpected terms due to the intrinsic logarithmic form of correlation functions in these models.

Appendix A

Entanglement Entropy in the BF-RSOS Model: regime III

In this appendix we will evaluate Rényi Entropy for ABF and BF RSOS models in the regime III. Since we are interested in the behaviour of Entropy, we will perform series expansion near the critical point $p, k \rightarrow 0$ or $\xi \rightarrow \infty$.

For any definition of variables used in this chapter, we will refer to Chapters 2 and 4. Definitions of elliptic functions can be found in [6]

Using Peschel-Kaulke-Legeza's method one can see that (Chapter 2 and [7, 9])

$$\rho_A = \frac{1}{Z_1} ABCD \tag{A.1}$$

$$:= \frac{\rho_c}{Z_1} \tag{A.2}$$

with

$$Z_1 = \text{Tr}[ABCD] \tag{A.3}$$

Thanks to these formulæ we can write the Rényi entropy as

$$S_\alpha = \frac{1}{1-\alpha} \log \text{Tr} \rho_A^\alpha \tag{A.4}$$

$$= \frac{1}{1-\alpha} \log \text{Tr} \left(\frac{\rho_c}{Z_1} \right)^\alpha \tag{A.5}$$

$$= \frac{1}{1-\alpha} \log \text{Tr} \rho_c^\alpha + \frac{\alpha}{\alpha-1} \log \text{Tr} \rho_c \tag{A.6}$$

$$:= \frac{1}{1-\alpha} \log Z_\alpha + \frac{\alpha}{\alpha-1} \log Z_1 \tag{A.7}$$

where

$$Z_\alpha := \text{Tr } \rho_c^\alpha \quad (\text{A.8})$$

In this regime

$$\eta = \frac{s}{r}K \quad (\text{A.9})$$

$$\mu = s \quad (\text{A.10})$$

The partition function for a system with m sites in the central row is given by

$$Z_1 = \sum_{l_1, \dots, l_m}^* E(x^{l_1}, y) x^{t\Phi(l)} \quad (\text{A.11})$$

where

$$x = \exp\left[-4\pi \frac{\eta}{K'}\right] \quad (\text{A.12})$$

$$= \exp\left[-4\pi \frac{sK}{rK'}\right] \quad (\text{A.13})$$

$$y = x^{\frac{r}{s}} \quad (\text{A.14})$$

$$E(z, x) = (z; x)_\infty (xz^{-1}; x)_\infty (x; x)_\infty \quad (\text{A.15})$$

$$= \sum_{n \in \mathbb{Z}} (-1)^n x^{\frac{n(n-1)}{2}} z^n \quad (\text{A.16})$$

$$p = \exp\left[-\pi \frac{K'}{K}\right] \quad (\text{A.17})$$

and $(a; b)_\infty$ is the q -Pochhammer symbol:

$$(a; b)_\infty = \prod_{n=0}^{\infty} (1 - ab^n) \quad (\text{A.18})$$

$$(q)_\infty = (q; q)_\infty = \prod_{n=1}^{\infty} (1 - q^n) \quad (\text{A.19})$$

and $\frac{K}{2}$ denotes the elliptic integral of the first kind with modulus k . K' is defined as K only with modulus equal to $k' = \sqrt{1 - k^2}$.

The symbol $*$ over sums indicates that the summation has to be performed only on even or odd values of l_1 . This choice depends on boundary conditions [20].

(A.11) can be written as

$$Z_1 = \sum_{a=1}^{r-1}^* E(x^{l_1}, y) D_m(a, b, c; x^2) \quad (\text{A.20})$$

where

$$D_m(a, b, c; x^2) := \sum_{l_2, \dots, l_m} x^{t\Phi(l)} \Big|_{l_1=a, l_{m+1}=b, l_{m+2}=c} \quad (\text{A.21})$$

The dependance of D_m on b and c is due to the fact that boundary conditions can influence the behaviour of the system, either in thermodynamic limit.

$$Z_\alpha = \text{Tr} \rho_c^\alpha \quad (\text{A.22})$$

$$= \text{Tr} \underbrace{\rho_c \rho_c \cdots \rho_c}_{\alpha \text{ times}} \quad (\text{A.23})$$

$$= \sum_{a=1}^{r-1} [E(x^a, y)]^\alpha D_m(a, b, c; x^{2\alpha}) \quad (\text{A.24})$$

In [20] one can find two explicit expressions for the thermodynamic limit $m \rightarrow \infty$ of D_m :

$$\lim_{m \rightarrow \infty} q^{-\frac{km}{2}} D_m(a, b, b+1; q) = (q)_\infty^{-1} q^{b\frac{b-1}{4} - b\frac{k-1}{2}} F(a, b-k; q^{\frac{1}{2}}) \quad (\text{A.25})$$

$$\lim_{m \rightarrow \infty} q^{\frac{km}{2}} D_m(a, b+1, b; q) = (q)_\infty^{-1} q^{b\frac{b+1}{4} - k\frac{b+1}{4}} F(a, b-k; q^{\frac{1}{2}}) \quad (\text{A.26})$$

with

$$k = \left\lfloor \frac{\mu(b+1)}{r} \right\rfloor \quad (\text{A.27})$$

in the first case and

$$k = \left\lfloor \frac{\mu b}{r} \right\rfloor \quad (\text{A.28})$$

in the second one

where $[a]$ is the integer part of a and

$$F(a, b-k; q^{\frac{1}{2}}) = q^{a\frac{a-1}{4}} \left\{ q^{-a\frac{b-k}{2}} E(-q^{r(b-k)+(r-a)(r-\mu)}, q^{2r(r-\mu)}) \right. \\ \left. - q^{a\frac{b-k}{2}} E(-q^{r(b-k)+(r+a)(r-\mu)}, q^{2r(r-\mu)}) \right\} \quad (\text{A.29})$$

Since we are interested in the thermodynamic limit of $\frac{Z_\alpha}{Z_1^\alpha}$, to perform the limit of this ratio is easier than performing the ratio of two limits.

$$\frac{Z_\alpha}{Z_1^\alpha} = \frac{\sum_{a=1}^{*r-1} [E(x^a, y)]^\alpha D_m(a, b, c; x^{2\alpha})}{\left[\sum_{a=1}^{*r-1} E(x^{l_1}, y) D_m(a, b, c; x^2) \right]^\alpha} \quad (\text{A.30})$$

Multiplying above and below the ratio by $x^{\mp km\alpha}$, one obtains

$$\frac{\sum_{a=1}^{*r-1} [E(x^a, y)]^\alpha x^{\mp km\alpha} D_m(a, b, c; x^{2\alpha})}{\left[\sum_{a=1}^{*r-1} E(x^a, y) x^{\mp km} D_m(a, b, c; x^2) \right]^\alpha} \quad (\text{A.31})$$

the limit $m \rightarrow \infty$ can be easily performed:

$$\frac{Z_\alpha}{Z_1^\alpha} = \frac{\sum_{a=1}^{*r-1} [E(x^a, y)]^\alpha (x^{2\alpha})_\infty^{-1} x^{\alpha(b\frac{b-1}{2} - b\frac{k-1}{2})} F(a, b-k; x^{2\alpha})}{\left[\sum_{a=1}^{*r-1} E(x^a, y) (x^2)_\infty^{-1} x^{b\frac{b-1}{2} - b\frac{k-1}{2}} F(a, b-k; x^2) \right]^\alpha} \quad (\text{A.32})$$

in this case we choose $c = b + 1$ and then $k = \left\lfloor \frac{\mu(b+1)}{r} \right\rfloor$

A.1 Computation of Z_α/Z_1^α in terms of Jacobi's θ functions

In this section we will compute the above ratio in terms of Jacobi's θ functions, trying to find an expression which can be compared with the one on [9] (in which $\eta = \frac{K}{r}$):

$$Z_\alpha = \sum_{a=1}^{r-1} \theta_1^\alpha \left(\frac{a\pi}{r}, \sqrt{p} \right) Z_\alpha^{(a)} \quad (\text{A.33})$$

where

$$Z_\alpha^{(a)} := \frac{\theta_3 \left(\frac{\pi d}{2(r-1)} - \frac{\pi a}{2r}, p^{\frac{1}{8\alpha(r-1)}} \right) - \theta_3 \left(\frac{\pi d}{2(r-1)} + \frac{\pi a}{2r}, p^{\frac{1}{8\alpha(r-1)}} \right)}{p^{\frac{r}{48\alpha}} \sqrt{2r(r-1)} \theta_4 \left(-i \frac{r \log p}{8\alpha}, p^{\frac{3r}{4\alpha}} \right)} \quad (\text{A.34})$$

with

$$d := \frac{b+c-1}{2} \quad (\text{A.35})$$

this model corresponds to a minimal conformal one with central charge

$$c_r = 1 - \frac{6}{r(r-1)} \quad (\text{A.36})$$

A.1. Computation of Z_α/Z_1^α in terms of Jacobi's θ functions

The value of the central charge can be also extracted by the leading term of the Rényi entropy

$$S_\alpha \approx -\frac{c_r}{24} \frac{1+\alpha}{\alpha} \log \tilde{q} \quad (\text{A.37})$$

$$\approx \frac{c_r}{12} \frac{1+\alpha}{\alpha} \log \xi \quad (\text{A.38})$$

in agreement with Cardy-Calabrese prediction ([11] and Chapter 3).

A.1.1 Computation of $E(x^a, y)$

Using the identity [9]

$$E(e^{2iz}, q^2) = iq^{-\frac{1}{4}} e^{iz} \theta_1(z, q) \quad (\text{A.39})$$

we can write

$$E(x^a, y) = i \exp \left[-\frac{\pi^2}{2 \log p} + \frac{2\pi^2 a s}{r \log p} \right] \theta_1 \left(\frac{s}{r} \frac{2\pi^2 a}{i \log p}, \exp \left[\frac{2\pi^2 a}{\log p} \right] \right) \quad (\text{A.40})$$

then we can use duality relations of Jacobi's functions:

$$q = e^{i\pi\tau} \quad \tilde{q} = e^{-i\frac{\pi}{\tau}} \quad (\text{A.41})$$

$$\theta_1(z, \tilde{q}) = -i\sqrt{i\tau} \exp \left[\frac{i\tau z^2}{\pi} \right] \theta_1(\tau z, q) \quad (\text{A.42})$$

$$\theta_2(z, \tilde{q}) = \sqrt{-i\tau} \exp \left[\frac{i\tau z^2}{\pi} \right] \theta_4(\tau z, q) \quad (\text{A.43})$$

$$\theta_3(z, \tilde{q}) = \sqrt{-i\tau} \exp \left[\frac{i\tau z^2}{\pi} \right] \theta_3(\tau z, q) \quad (\text{A.44})$$

$$\theta_4(z, \tilde{q}) = \sqrt{-i\tau} \exp \left[\frac{i\tau z^2}{\pi} \right] \theta_2(\tau z, q) \quad (\text{A.45})$$

$$E(x^a, y) = -\sqrt{\frac{\log p}{2\pi}} \theta_1 \left(\frac{\pi s}{r} a, \sqrt{p} \right) \exp \left[-\frac{\pi^2}{2 \log p} \right] \exp \left[\frac{2\pi^2 a s}{r \log p} \left(1 - \frac{sa}{r} \right) \right] \quad (\text{A.46})$$

A.1.2 Computation of $F(\dots)$

$$E \left(-q^{r(b-k)+(r-a)(r-\mu)}, q^{2r(r-\mu)} \right) = E \left(-q^{f(r)}, q^{2g(r)} \right) \quad (\text{A.47})$$

with

$$q = x^{2\alpha} \quad (\text{A.48})$$

$$f(r) = r(b-k) + (r-a)(r-\mu) \quad (\text{A.49})$$

$$g(r) = r(r-\mu) \quad (\text{A.50})$$

$$E\left(-q^{r(b-k)+(r-a)(r-\mu)}, q^{2r(r-\mu)}\right) = \exp\left[-\frac{2\pi^2\alpha s}{r \log p}(g-2f)\right] \theta_2\left(\frac{4\pi^2\alpha i s}{\log p} \frac{f}{r}, \exp\left[\frac{8\pi^2\alpha s}{\log p} \frac{g}{r}\right]\right)$$

using again duality relations we obtain

$$\begin{aligned} E\left(-q^{r(b-k)+(r-a)(r-\mu)}, q^{2r(r-\mu)}\right) &= \exp\left[-\frac{2\pi^2\alpha s}{\log p} \frac{g}{r} \left(g-2f+\frac{f^2}{g}\right)\right] \times \\ &\times \sqrt{-\frac{\log p}{8\pi\alpha g} \frac{r}{s}} \theta_4\left(\frac{f}{g} \frac{\pi}{2}, p^{\frac{r}{8s\alpha g}}\right) \end{aligned} \quad (\text{A.51})$$

$$E\left(-q^{r(b-k)+(r+a)(r-\mu)}, q^{2r(r-\mu)}\right) = E\left(-q^{f_1(r)}, q^{2g(r)}\right) \quad (\text{A.52})$$

with

$$f_1(r) = r(b-k) + (r+a)(r-\mu) \quad (\text{A.53})$$

$$\begin{aligned} E\left(-q^{r(b-k)+(r+a)(r-\mu)}, q^{2r(r-\mu)}\right) &= \exp\left[-\frac{2\pi^2\alpha s}{\log p} \frac{g}{r} \left(g-2f_1+\frac{f_1^2}{g}\right)\right] \times \\ &\times \sqrt{-\frac{\log p}{8\pi\alpha g} \frac{r}{s}} \theta_4\left(\frac{f_1}{g} \frac{\pi}{2}, p^{\frac{r}{8s\alpha g}}\right) \end{aligned} \quad (\text{A.54})$$

$$\begin{aligned} q^{-a\frac{b-k}{2}} &= x^{-a\alpha(b-k)} \\ &= \exp\left[-\frac{4\pi^2\alpha s}{\log p} \frac{a}{r}(b-k)\right] \end{aligned} \quad (\text{A.55})$$

$$\begin{aligned} q^{a\frac{a-1}{4}} &= x^{a\alpha\frac{a-1}{2}} \\ &= \exp\left[\frac{2\pi^2\alpha s}{\log p} \frac{a}{r}(a-1)\right] \end{aligned} \quad (\text{A.56})$$

A.1. Computation of Z_α/Z_1^α in terms of Jacobi's θ functions

Using (A.51),(A.54),(A.55),(A.56) we obtain

$$\begin{aligned} \frac{F}{q^{a\frac{a-1}{4}}} &= \sqrt{-\frac{\log p r}{8\pi\alpha g s}} \left\{ \exp \left[-\frac{2\pi^2\alpha s}{\log p r} \left(g - 2f + \frac{f^2}{g} + 2as(b-k) \right) \right] \theta_4 \left(\frac{f\pi}{g}, p^{\frac{r}{8s\alpha g}} \right) \right. \\ &\quad \left. - \exp \left[-\frac{2\pi^2\alpha s}{\log p r} \left(g - 2f_1 + \frac{f_1^2}{g} - 2as(b-k) \right) \right] \theta_4 \left(\frac{f\pi}{g}, p^{\frac{r}{8s\alpha g}} \right) \right\} \quad (\text{A.57}) \end{aligned}$$

As

$$g - 2f + \frac{f^2}{g} + 2as(b-k) = g - 2f_1 + \frac{f_1^2}{g} - 2as(b-k) \quad (\text{A.58})$$

$$= h \quad (\text{A.59})$$

we can write

$$\begin{aligned} \frac{F}{q^{a\frac{a-1}{4}}} &= \sqrt{-\frac{\log p r}{8\pi\alpha g s}} \exp \left[-\frac{2\pi^2\alpha s}{\log p r} h \right] \left\{ \theta_4 \left(\frac{\pi}{2} \left(\frac{r-a}{r} + \frac{b-k}{r-\mu} \right), p^{\frac{1}{8s\alpha(r-\mu)}} \right) \right. \\ &\quad \left. - \theta_4 \left(\frac{\pi}{2} \left(\frac{r+a}{r} + \frac{b-k}{r-\mu} \right), p^{\frac{1}{8s\alpha(r-\mu)}} \right) \right\} \quad (\text{A.60}) \end{aligned}$$

and

$$\begin{aligned} F &= \sqrt{-\frac{\log p r}{8\pi\alpha g s}} \exp \left[-\frac{2\pi^2\alpha s}{\log p r} (h - a(a-1)) \right] \times \quad (\text{A.61}) \\ &\quad \times \left\{ \theta_4 \left(\frac{\pi}{2} \left(\frac{r-a}{r} + \frac{b-k}{r-\mu} \right), p^{\frac{1}{8s\alpha(r-\mu)}} \right) - \theta_4 \left(\frac{\pi}{2} \left(\frac{r+a}{r} + \frac{b-k}{r-\mu} \right), p^{\frac{1}{8s\alpha(r-\mu)}} \right) \right\} \end{aligned}$$

Using the relation

$$\theta_4 \left(z + \frac{\pi}{2}, q \right) = \theta_3(z, q) \quad (\text{A.62})$$

we obtain

$$\begin{aligned} F &= \sqrt{-\frac{\log p r}{8\pi\alpha g s}} \exp \left[-\frac{2\pi^2\alpha s}{\log p r} (h - a(a-1)) \right] \times \quad (\text{A.63}) \\ &\quad \times \left\{ \theta_3 \left(\frac{\pi(b-k)}{2(r-\mu)} - \frac{\pi a}{2r}, p^{\frac{1}{8s\alpha(r-\mu)}} \right) - \theta_3 \left(\frac{\pi(b-k)}{2(r-\mu)} + \frac{\pi a}{2r}, p^{\frac{1}{8s\alpha(r-\mu)}} \right) \right\} \end{aligned}$$

A.1.3 Computation of $E^\alpha F(x^{2\alpha})$

$$\begin{aligned}
 [E(x^a, y)]^\alpha F(x^{2\alpha}) &= - \left(\frac{\log p}{2\pi} \right)^{\frac{\alpha}{2}} \exp \left[-\frac{\pi^2 \alpha}{2 \log p} \right] \exp \left[\frac{2\pi^2 \alpha s}{\log p r} \left(a - \frac{s}{r} a^2 - h \right) \right] \\
 &\times \sqrt{-\frac{\log p}{8\pi \alpha s (r - \mu)}} \theta_1^\alpha \left(\frac{\pi s}{r} a, \sqrt{p} \right) \\
 &\times \left[\theta_3 \left(\frac{\pi(b-k)}{2(r-\mu)} - \frac{\pi a}{2r}, p^{\frac{1}{8s\alpha(r-\mu)}} \right) - \theta_3 \left(\frac{\pi(b-k)}{2(r-\mu)} + \frac{\pi a}{2r}, p^{\frac{1}{8s\alpha(r-\mu)}} \right) \right]
 \end{aligned} \tag{A.64}$$

we can express

$$a - \frac{s}{r} a^2 + a(a-1) - h = \begin{cases} \frac{r(k-b)^2}{rs} & \mu = s \quad III \\ \frac{a^2 s(2s-r) + r^2(k-b)^2}{rs} & \mu = r-s \quad II \end{cases} \tag{A.65}$$

A.1.4 Computation of $(x^{2\alpha})_\infty$

The q-Pochhammer symbol can be parametrized as

$$(q)_\infty = \frac{1}{\sqrt{3}} q^{-\frac{1}{24}} \theta_2 \left(\frac{\pi}{6}, q^{\frac{1}{6}} \right) \tag{A.66}$$

thus

$$(x^{2\alpha})_\infty = \frac{1}{\sqrt{3}} x^{-\frac{\alpha}{12}} \theta_2 \left(\frac{\pi}{6}, x^{\frac{\alpha}{3}} \right) \tag{A.67}$$

$$= \frac{1}{\sqrt{3}} \exp \left[-\frac{\pi^2 \alpha s}{3 \log p r} \right] \theta_2 \left(\frac{\pi}{6}, \exp \left[\frac{4\pi^2 \alpha s}{3 \log p r} \right] \right) \tag{A.68}$$

after applying again duality relations, one obtains

$$= \sqrt{-\frac{3 \log p s}{4\pi \alpha r}} p^{\frac{r}{48s\alpha}} \theta_4 \left(-\frac{ir \log p}{s}, p^{\frac{3r}{4s\alpha}} \right) \tag{A.69}$$

A.1.5 Computation of Z_α

Following [9] we write

$$Z_\alpha = \sum_{a=1}^{r-1} \theta_1^\alpha \left(\frac{\pi a s}{r}, \sqrt{p} \right) Z_\alpha^{(a)} \tag{A.70}$$

A.1. Computation of Z_α/Z_1^α in terms of Jacobi's θ functions

where

$$Z_\alpha^{(a)} = \frac{\theta_3\left(\frac{\pi(b-k)}{2(r-\mu)} - \frac{\pi a}{2r}, p^{\frac{1}{8s\alpha(r-\mu)}}\right) - \theta_3\left(\frac{\pi(b-k)}{2(r-\mu)} + \frac{\pi a}{2r}, p^{\frac{1}{8s\alpha(r-\mu)}}\right)}{p^{\frac{r}{48s\alpha}} \theta_4\left(-\frac{ir \log p}{s} \frac{1}{8\alpha}, p^{\frac{3r}{4s\alpha}}\right)} \quad (\text{A.71})$$

$$\times \frac{\left(\frac{\log p}{2\pi}\right)^{\frac{\alpha}{2}} \sqrt{-\frac{\log p}{8\pi\alpha s(r-\mu)}}}{\sqrt{-\frac{3 \log p}{4\pi\alpha} \frac{s}{r}}} \frac{\sqrt{3}}{\exp\left[-\frac{\pi^2\alpha}{3 \log p} \frac{s}{r}\right]} \exp\left[\frac{2\pi^2\alpha}{\log p} \frac{s}{r} \left(a - \frac{s}{r} a^2 + a(a-1) - h\right)\right]$$

$$= \frac{\theta_3\left(\frac{\pi(b-k)}{2(r-\mu)} - \frac{\pi a}{2r}, p^{\frac{1}{8s\alpha(r-\mu)}}\right) - \theta_3\left(\frac{\pi(b-k)}{2(r-\mu)} + \frac{\pi a}{2r}, p^{\frac{1}{8s\alpha(r-\mu)}}\right)}{p^{\frac{r}{48s\alpha}} \theta_4\left(-\frac{ir \log p}{s} \frac{1}{8\alpha}, p^{\frac{3r}{4s\alpha}}\right) \sqrt{2r(r-\mu)}} \left(\frac{\log p}{2\pi}\right)^{\frac{\alpha}{2}} \quad (\text{A.72})$$

$$\times \exp\left[\frac{2\pi^2\alpha}{\log p} \frac{s}{r} \left(a - \frac{s}{r} a^2 - h + \frac{1}{6}\right)\right] \quad (\text{A.73})$$

The factor

$$\left(\frac{\log p}{2\pi}\right)^{\frac{\alpha}{2}} \exp\left[\frac{2\pi^2\alpha}{\log p} \frac{s}{r} u\right] = \left(\frac{\log p}{2\pi} \exp\left[\frac{2\pi^2}{\log p} \frac{s}{r} u\right]\right)^{\frac{\alpha}{2}} \quad (\text{A.74})$$

can be neglected since it does not affect the ratio Z_α/Z_1^α .

The factor u is the part of $a - \frac{s}{r} a^2 - h + \frac{1}{6}$ which does not depend on a . At last we obtain

$$Z_\alpha^{(a)} = \frac{\theta_3\left(\frac{\pi(b-k)}{2(r-\mu)} - \frac{\pi a}{2r}, p^{\frac{1}{8s\alpha(r-\mu)}}\right) - \theta_3\left(\frac{\pi(b-k)}{2(r-\mu)} + \frac{\pi a}{2r}, p^{\frac{1}{8s\alpha(r-\mu)}}\right)}{p^{\frac{r}{48s\alpha}} \theta_4\left(-\frac{ir \log p}{s} \frac{1}{8\alpha}, p^{\frac{3r}{4s\alpha}}\right) \sqrt{2r(r-\mu)}} \times \exp\left[\frac{2\pi^2\alpha}{\log p} \frac{s}{r} v\right] \quad (\text{A.75})$$

where

$$v = \begin{cases} 0 & \mu = r & \text{III} \\ a^2 \frac{2s-r}{r} & \mu = r-s & \text{II} \end{cases} \quad (\text{A.76})$$

which is the part of $a - \frac{s}{r} a^2 - h + \frac{1}{6}$ which depends on a .

Thus, in regime III we have

$$Z_\alpha^{(a)} = \frac{\theta_3\left(\frac{\pi(b-k)}{2(r-\mu)} - \frac{\pi a}{2r}, p^{\frac{1}{8s\alpha(r-\mu)}}\right) - \theta_3\left(\frac{\pi(b-k)}{2(r-\mu)} + \frac{\pi a}{2r}, p^{\frac{1}{8s\alpha(r-\mu)}}\right)}{p^{\frac{r}{48s\alpha}} \theta_4\left(-\frac{ir \log p}{s} \frac{1}{8\alpha}, p^{\frac{3r}{4s\alpha}}\right) \sqrt{2r(r-\mu)}} \quad (\text{A.77})$$

If following sections and in Chapter 4 and 6 we will denote $d = b - k$.

A.2 Entanglement Entropy

Setting

$$\tilde{q} = p^{\frac{r}{2s}} \quad (\text{A.78})$$

in [34] it has been shown that

$$\xi = -\frac{1}{\log K'(|\tilde{q}|^{\frac{1}{2}})} \quad (\text{A.79})$$

where $K'(q)$ is the complete elliptic integral of first kind of nome $\sqrt{1-q^2}$. It can be expressed also as:

$$K'(q) = \prod_{n=0}^{\infty} \left(\frac{1-q^{2n-1}}{1+q^{2n-1}} \right)^4 \quad (\text{A.80})$$

$$= \left(\frac{\theta_4(0, q)}{\theta_3(0, q)} \right)^2 \quad (\text{A.81})$$

from these formulæ one can find

$$\tilde{q} = \frac{1}{64}\xi^{-2} - \frac{1}{1536}\xi^{-4} + O(\xi^{-6}) \quad (\text{A.82})$$

The α -partition function then is given by

$$\begin{aligned} Z_\alpha &= \frac{1}{p^{\frac{r}{48s\alpha}} \theta_4 \left(-\frac{ir}{s} \frac{\log p}{8\alpha}, p^{\frac{3r}{48s\alpha}} \right) \sqrt{2r(r-\mu)}} \quad (\text{A.83}) \\ &\times \sum_{a=1}^{r-1} \theta_1^\alpha \left(\frac{\pi a s}{r}, \sqrt{p} \right) \left[\theta_3 \left(\frac{\pi(b-k)}{2(r-\mu)} - \frac{\pi a}{2r}, p^{\frac{1}{8s\alpha(r-\mu)}} \right) - \theta_3 \left(\frac{\pi(b-k)}{2(r-\mu)} + \frac{\pi a}{2r}, p^{\frac{1}{8s\alpha(r-\mu)}} \right) \right] \end{aligned}$$

taking the logarithm we obtain

$$\log Z_\alpha = -\frac{r}{48s\alpha} \log p - \log \sqrt{2r(r-\mu)} - \log \theta_4(\alpha) + \log \left(\sum_{a=1}^{r-a} \cdots (\alpha) \right) \quad (\text{A.84})$$

A.2.1 Computation of $\log \left(\sum_{a=1}^{r-a} \cdots (\alpha) \right)$

What we want to do in this section is to expand the summand using the product and sum expression for θ functions, thanks to the fact that $|p| < 1$.

$$\cdots (\alpha) = \theta_1^\alpha \left(\frac{a\pi s}{r}, \sqrt{p} \right) \left[\theta_3 \left(x - \frac{\pi a}{2r}, q \right) - \theta_3 \left(x + \frac{\pi a}{2r}, q \right) \right] \quad (\text{A.85})$$

A.2. Entanglement Entropy

with

$$q = p^{\frac{1}{8s\alpha(r-\mu)}} \quad (\text{A.86})$$

$$x = \frac{\pi(b-k)}{2(r-\mu)} \quad (\text{A.87})$$

Computation of θ_1^α

$$\theta_1\left(\frac{a\pi s}{r}, \sqrt{p}\right) = 2 \sum_{n=0}^{\infty} (-1)^n (\sqrt{p})^{(n+\frac{1}{2})^2} \sin\left((2n+1)\frac{a\pi s}{r}\right) \quad (\text{A.88})$$

$$\begin{aligned} &= 2 \left\{ p^{\frac{1}{8}} \sin\left(\frac{\pi a s}{r}\right) - p^{\frac{9}{8}} \sin\left(\frac{3\pi a s}{r}\right) + p^{\frac{25}{8}} \sin\left(\frac{5\pi a s}{r}\right) + O\left(p^{\frac{49}{8}}\right) \right\} \\ &= 2p^{\frac{1}{8}} \sin\left(\frac{\pi a s}{r}\right) \left\{ 1 - p \frac{\sin\left(\frac{3\pi a s}{r}\right)}{\sin\left(\frac{\pi a s}{r}\right)} + p^3 \frac{\sin\left(\frac{5\pi a s}{r}\right)}{\sin\left(\frac{\pi a s}{r}\right)} + O(p^6) \right\} \quad (\text{A.89}) \end{aligned}$$

for evaluate the α -power of the above expression we will use

$$(1+x)^n = 1 + nx + \frac{n(n-1)}{2}x^2 + \frac{n(n^2-3n+2)}{6}x^3 + O(x^4) \quad (\text{A.90})$$

obtaining

$$\theta_1^\alpha\left(\frac{a\pi s}{r}, \sqrt{p}\right) = 2^\alpha p^{\frac{\alpha}{8}} \sin^\alpha\left(\frac{\pi a s}{r}\right) \left\{ 1 - \alpha p \frac{\sin\left(\frac{3\pi a s}{r}\right)}{\sin\left(\frac{\pi a s}{r}\right)} + \alpha p^3 \frac{\sin\left(\frac{5\pi a s}{r}\right)}{\sin\left(\frac{\pi a s}{r}\right)} \right. \quad (\text{A.91})$$

$$\left. + \frac{\alpha(\alpha-1)}{2} p^2 \left(\frac{\sin\left(\frac{3\pi a s}{r}\right)}{\sin\left(\frac{\pi a s}{r}\right)}\right)^2 + \frac{\alpha(\alpha^2-3\alpha+2)}{6} p^3 \left(\frac{\sin\left(\frac{3\pi a s}{r}\right)}{\sin\left(\frac{\pi a s}{r}\right)}\right)^3 + O(p^4) \right\}$$

$$= 2^\alpha p^{\frac{\alpha}{8}} \sin^\alpha\left(\frac{\pi a s}{r}\right) \left\{ 1 - p\alpha \frac{\sin\left(\frac{3\pi a s}{r}\right)}{\sin\left(\frac{\pi a s}{r}\right)} + p^2 \frac{\alpha(\alpha-1)}{2} \left(\frac{\sin\left(\frac{3\pi a s}{r}\right)}{\sin\left(\frac{\pi a s}{r}\right)}\right)^2 \right. \quad (\text{A.92})$$

$$\left. + p^3 \alpha \left[\frac{\sin\left(\frac{5\pi a s}{r}\right)}{\sin\left(\frac{\pi a s}{r}\right)} + \frac{\alpha^2-3\alpha+2}{6} \left(\frac{\sin\left(\frac{3\pi a s}{r}\right)}{\sin\left(\frac{\pi a s}{r}\right)}\right)^3 \right] + O(p^4) \right\} \quad (\text{A.93})$$

Computation of $\theta_3(\alpha) - \theta_3(\alpha)$

Using

$$\theta_3(z, q) = 1 + 2 \sum_{n=1}^{\infty} q^{n^2} \cos(2nz) \quad (\text{A.94})$$

we obtain

$$\begin{aligned}
 \theta_3 \left(x - \frac{\pi a}{2r}, q \right) - \theta_3 \left(x + \frac{\pi a}{2r}, q \right) &= 2 \sum_{n=1}^{\infty} q^{n^2} \left[\cos \left(2n \left(x - \frac{\pi a}{2r} \right) \right) - \cos \left(2n \left(x + \frac{\pi a}{2r} \right) \right) \right] \\
 &= 4 \sum_{n=1}^{\infty} q^{n^2} \sin(2nx) \sin \left(\frac{n\pi a}{r} \right) \tag{A.95} \\
 &= 4 \left\{ q \sin(2x) \sin \left(\frac{\pi a}{r} \right) + q^4 \sin(4x) \sin \left(\frac{2\pi a}{r} \right) + q^9 \sin(6x) \sin \left(\frac{3\pi a}{r} \right) + O(q^{16}) \right\} \\
 &= 4q \sin(2x) \sin \left(\frac{\pi a}{r} \right) \left\{ 1 + q^3 \frac{\sin(4x) \sin \left(\frac{2\pi a}{r} \right)}{\sin(2x) \sin \left(\frac{\pi a}{r} \right)} + q^8 \frac{\sin(6x) \sin \left(\frac{3\pi a}{r} \right)}{\sin(2x) \sin \left(\frac{\pi a}{r} \right)} + O(q^{15}) \right\}
 \end{aligned}$$

Merging

Merging (A.91) and (A.95) we find an expression for $\dots(\alpha)$:

$$\dots(\alpha) = p^{\frac{\alpha}{8} + \frac{1}{8s\alpha(r-\mu)}} 2^{\alpha+2} \sin(2x) \sin \left(\frac{\pi a}{r} \right) \sin^{\alpha} \left(\frac{\pi a s}{r} \right) \tag{A.96}$$

$$\begin{aligned}
 &\times \left\{ 1 + p^{\frac{3}{8s\alpha(r-\mu)}} \frac{\sin(4x) \sin \left(\frac{2\pi a}{r} \right)}{\sin(2x) \sin \left(\frac{\pi a}{r} \right)} + p^{\frac{1}{s\alpha(r-\mu)}} \frac{\sin(6x) \sin \left(\frac{3\pi a}{r} \right)}{\sin(2x) \sin \left(\frac{\pi a}{r} \right)} + O \left(p^{\frac{15}{8s\alpha(r-\mu)}} \right) \right\} \\
 &\times \left\{ 1 - p\alpha \frac{\sin \left(\frac{3\pi a s}{r} \right)}{\sin \left(\frac{\pi a s}{r} \right)} + p^2 \frac{\alpha(\alpha-1)}{2} \left(\frac{\sin \left(\frac{3\pi a s}{r} \right)}{\sin \left(\frac{\pi a s}{r} \right)} \right)^2 \right\} \tag{A.97}
 \end{aligned}$$

$$+ p^3 \alpha \left[\frac{\sin \left(\frac{5\pi a s}{r} \right)}{\sin \left(\frac{\pi a s}{r} \right)} + \frac{\alpha^2 - 3\alpha + 2}{6} \left(\frac{\sin \left(\frac{3\pi a s}{r} \right)}{\sin \left(\frac{\pi a s}{r} \right)} \right)^3 \right] + O(p^4) \tag{A.98}$$

obtaining at last

$$\log \left(\sum_{a=1}^{r-a} \dots(\alpha) \right) = \left(\frac{\alpha}{8} + \frac{1}{8s\alpha(r-\mu)} \right) \log p + \log [2^{\alpha+2} \sin(2x)] \tag{A.99}$$

$$\begin{aligned}
 &+ \log \left[\sum_{a=1}^{r-1} \sin \left(\frac{\pi a}{r} \right) \sin^{\alpha} \left(\frac{\pi a s}{r} \right) \left\{ 1 + p^{\frac{3}{8s\alpha(r-\mu)}} \frac{\sin(4x) \sin \left(\frac{2\pi a}{r} \right)}{\sin(2x) \sin \left(\frac{\pi a}{r} \right)} \right. \right. \\
 &\left. \left. + p^{\frac{1}{s\alpha(r-\mu)}} \frac{\sin(6x) \sin \left(\frac{3\pi a}{r} \right)}{\sin(2x) \sin \left(\frac{\pi a}{r} \right)} + O \left(p^{\frac{15}{8s\alpha(r-\mu)}} \right) \right\} \right] \tag{A.100}
 \end{aligned}$$

Notice that we neglect p, p^2, \dots terms in the last expression, since they are dominated by $p^{\frac{15}{8s\alpha(r-\mu)}}$ for a wide set of value of r and s .

A.2. Entanglement Entropy

For the evaluation of the last term we can use

$$\log[A + Bx] = \log(A) + \frac{Bx}{A} - \frac{B^2 x^2}{2A^2} + \frac{B^3 x^3}{3A^3} + O(x^4) \quad (\text{A.101})$$

obtaining

$$\begin{aligned} \log\left(\sum_{a=1}^{r-a} \cdots (\alpha)\right) &= \left(\frac{\alpha}{8} + \frac{1}{8s\alpha(r-\mu)}\right) \log p + \log[2^{\alpha+2} \sin(2x)] \\ &+ \log\left[\sum_{a=1}^{r-1} \sin\left(\frac{\pi a}{r}\right) \sin^\alpha\left(\frac{\pi a s}{r}\right)\right] \\ &+ p^{\frac{3}{8s\alpha(r-\mu)}} \frac{\sin(4x)}{\sin(2x)} \frac{\sum_{a=1}^{r-1} \sin\left(\frac{2\pi a}{r}\right) \sin^\alpha\left(\frac{\pi a s}{r}\right)}{\sum_{a=1}^{r-1} \sin\left(\frac{\pi a}{r}\right) \sin^\alpha\left(\frac{\pi a s}{r}\right)} \\ &- \frac{1}{2} p^{\frac{3}{4s\alpha(r-\mu)}} \left(\frac{\sin(4x)}{\sin(2x)}\right)^2 \left(\frac{\sum_{a=1}^{r-1} \sin\left(\frac{2\pi a}{r}\right) \sin^\alpha\left(\frac{\pi a s}{r}\right)}{\sum_{a=1}^{r-1} \sin\left(\frac{\pi a}{r}\right) \sin^\alpha\left(\frac{\pi a s}{r}\right)}\right)^2 \\ &+ p^{\frac{1}{s\alpha(r-\mu)}} \left(\frac{\sin(6x)}{\sin(2x)}\right)^2 \left(\frac{\sum_{a=1}^{r-1} \sin\left(\frac{3\pi a}{r}\right) \sin^\alpha\left(\frac{\pi a s}{r}\right)}{\sum_{a=1}^{r-1} \sin\left(\frac{\pi a}{r}\right) \sin^\alpha\left(\frac{\pi a s}{r}\right)}\right)^2 \\ &+ O\left(p^{\frac{3}{2s\alpha(r-\mu)}}\right) \end{aligned} \quad (\text{A.102})$$

$$\begin{aligned} &= \left(\frac{\alpha}{8} + \frac{1}{8s\alpha(r-\mu)}\right) \log p + \log[2^{\alpha+2} \sin(2x)] \\ &+ \log[\mathfrak{S}_\alpha(1; r, s)] + p^{\frac{3}{8s\alpha(r-\mu)}} \frac{\sin(4x) \mathfrak{S}_\alpha(2; r, s)}{\sin(2x) \mathfrak{S}_\alpha(1; r, s)} \\ &- \frac{1}{2} p^{\frac{3}{4s\alpha(r-\mu)}} \left(\frac{\sin(4x)}{\sin(2x)}\right)^2 \left(\frac{\mathfrak{S}_\alpha(2; r, s)}{\mathfrak{S}_\alpha(1; r, s)}\right)^2 \\ &+ p^{\frac{1}{s\alpha(r-\mu)}} \frac{\sin(6x) \mathfrak{S}_\alpha(3; r, s)}{\sin(2x) \mathfrak{S}_\alpha(1; r, s)} + O\left(p^{\frac{3}{2s\alpha(r-\mu)}}\right) \end{aligned} \quad (\text{A.103})$$

where

$$\mathfrak{S}_\alpha(n; r, s) = \sum_{a=1}^{r-1} \sin\left(n \frac{\pi a}{r}\right) \sin^\alpha\left(\frac{\pi a s}{r}\right) \quad (\text{A.104})$$

A.2.2 Computation of $\log \theta_4(\alpha)$

In this case it is easier to use the product representation of θ_4

$$\theta_4(z, q) = (q^2)_\infty \prod_{n=1}^{\infty} [1 - 2q^{2n-1} \cos(2z) + q^{4n-2}] \quad (\text{A.105})$$

where

$$z = -i \frac{r \log p}{s \cdot 8\alpha} \quad (\text{A.106})$$

$$q = p^{\frac{3r}{4s\alpha}} \quad (\text{A.107})$$

Performing some expansions we obtain

$$\log \theta_4(\alpha) = -\frac{1}{256} \xi^{-\frac{3}{\alpha}} + \frac{\cos(2z)}{4168} \xi^{-\frac{5}{\alpha}} - \frac{\cos^2(2z)}{131072} \xi^{-\frac{6}{\alpha}} - \frac{35915713 \cos(2z)}{2134698885120} \xi^{-\frac{7}{\alpha}} + O\left(\xi^{-\frac{8}{\alpha}}\right)$$

A.2.3 Full Entropy

Finally we get

$$\begin{aligned} \log Z_\alpha &= -\frac{r}{48s\alpha} \log p - \log \sqrt{2r(r-\mu)} \\ &+ \left(\frac{\alpha}{8} + \frac{1}{8s\alpha(r-\mu)} \right) \log p + \log [2^{\alpha+2} \sin(2x)] \\ &+ \log [\mathfrak{f}_\alpha(1; r, s)] + p^{\frac{3}{8s\alpha(r-\mu)}} \frac{\sin(4x) \mathfrak{f}_\alpha(2; r, s)}{\sin(2x) \mathfrak{f}_\alpha(1; r, s)} \\ &- \frac{1}{2} p^{\frac{3}{4s\alpha(r-\mu)}} \left(\frac{\sin(4x)}{\sin(2x)} \right)^2 \left(\frac{\mathfrak{f}_\alpha(2; r, s)}{\mathfrak{f}_\alpha(1; r, s)} \right)^2 \\ &+ p^{\frac{1}{s\alpha(r-\mu)}} \frac{\sin(6x) \mathfrak{f}_\alpha(3; r, s)}{\sin(2x) \mathfrak{f}_\alpha(1; r, s)} + O\left(p^{\frac{3}{2s\alpha(r-\mu)}}\right) \\ &+ \frac{1}{256} \xi^{-\frac{3}{\alpha}} - \frac{\cos(2z)}{4168} \xi^{-\frac{5}{\alpha}} + \frac{\cos^2(2z)}{131072} \xi^{-\frac{6}{\alpha}} + \frac{35915713 \cos(2z)}{2134698885120} \xi^{-\frac{7}{\alpha}} + O\left(\xi^{-\frac{8}{\alpha}}\right) \end{aligned}$$

since

$$p = \tilde{q}^{\frac{2s}{r}} \quad (\text{A.108})$$

$$= \left[\frac{\xi^{-2}}{64} - \frac{\xi^{-4}}{1536} + \frac{113}{2949120} \xi^{-6} + O(\xi^{-8}) \right]^{\frac{2s}{r}} \quad (\text{A.109})$$

$$= \frac{\xi^{-\frac{4s}{r}}}{64^{\frac{2s}{r}}} \left[1 - \frac{s}{12r} \xi^{-2} + \frac{80s^2 + 73rs}{23040r^2} \xi^{-4} + O(\xi^{-6}) \right] \quad (\text{A.110})$$

A.2. Entanglement Entropy

then

$$\log p = -\frac{4s}{r} \log \xi - \frac{12s}{r} \log 2 - \frac{s}{12r} \xi^{-2} + \frac{73s}{23040r} \xi^{-4} + O(\xi^{-6}) \quad (\text{A.111})$$

and

$$\begin{aligned} p^{\frac{3n}{8s\alpha(r-s)}} &= \frac{1}{64^{\frac{3n}{4\alpha r(r-s)}}} \xi^{-\frac{3n}{2\alpha r(r-s)}} \\ &\times \left[1 - \frac{n}{32\alpha r(r-s)} \xi^{-2} + \frac{n[30n + 73\alpha r(r-s)]}{15 [64\alpha r(r-s)]^2} \xi^{-4} + O(\xi^{-6}) \right] \end{aligned} \quad (\text{A.112})$$

Thus

$$\begin{aligned} \log Z_\alpha &= -\left(\frac{r}{48s\alpha} - \frac{\alpha}{8} - \frac{1}{8s\alpha(r-s)} \right) \left(-\frac{4s}{r} \log \xi - \frac{12s}{r} \log 2 - \frac{s}{12r} \xi^{-2} + \frac{73s}{23040r} \xi^{-4} + O(\xi^{-6}) \right) \\ &+ \log \left[\frac{\mathfrak{s}_\alpha(1; r, s)}{\sqrt{2r(r-s)}} 2^{\alpha+2} \sin(2x) \right] \\ &+ \frac{\sin(4x) \mathfrak{s}_\alpha(2; r, s)}{\sin(2x) \mathfrak{s}_\alpha(1; r, s)} \frac{1}{64^{\frac{3}{4\alpha r(r-s)}}} \xi^{-\frac{3}{2\alpha r(r-s)}} \left[1 - \frac{1}{32\alpha r(r-s)} \xi^{-2} \right. \\ &+ \left. \frac{30 + 73\alpha r(r-s)}{15 [64\alpha r(r-s)]^2} \xi^{-4} + O(\xi^{-6}) \right] \\ &- \frac{1}{2} \left(\frac{\sin(4x)}{\sin(2x)} \right)^2 \left(\frac{\mathfrak{s}_\alpha(2; r, s)}{\mathfrak{s}_\alpha(1; r, s)} \right)^2 \frac{1}{64^{\frac{3}{2\alpha r(r-s)}}} \xi^{-\frac{3}{\alpha r(r-s)}} \left[1 - \frac{1}{16\alpha r(r-s)} \xi^{-2} \right. \\ &+ \left. \frac{2[60 + 73\alpha r(r-s)]}{15 [64\alpha r(r-s)]^2} \xi^{-4} + O(\xi^{-6}) \right] \\ &+ \frac{\sin(6x) \mathfrak{s}_\alpha(3; r, s)}{\sin(2x) \mathfrak{s}_\alpha(1; r, s)} \frac{1}{64^{\frac{4}{\alpha r(r-s)}}} \xi^{-\frac{4}{\alpha r(r-s)}} \left[1 - \frac{1}{12\alpha r(r-s)} \xi^{-2} \right. \\ &+ \left. \frac{8[80 + 73\alpha r(r-s)]}{45 [64\alpha r(r-s)]^2} \xi^{-4} + O(\xi^{-6}) \right] \\ &+ O\left(\xi^{-\frac{6}{\alpha r(r-s)}} \right) + O\left(\xi^{-\frac{3}{\alpha}} \right) \end{aligned}$$

if we want neglect $O\left(\xi^{-\frac{3}{\alpha}}\right)$ terms in presence of $O\left(\xi^{-\frac{6}{\alpha r(r-s)}}\right)$ terms, we require

$$\xi^{-\frac{3}{\alpha}} \ll \xi^{-\frac{6}{\alpha r(r-s)}} \quad (\text{A.113})$$

since $\xi \gg 1$, the above inequality is satisfied if

$$\begin{aligned} 3 &\geq \frac{6}{r(r-s)} \\ r - \frac{2}{r} &\geq s \end{aligned} \quad (\text{A.114})$$

As $s \leq r - 1$, the above inequality is satisfied for each s , because for $s = r - 1$ it is satisfied for each $r \geq 1$:

$$\frac{2}{r} \leq 1 \quad (\text{A.115})$$

This argument allows us to neglect most of ξ^{-x} terms; recollecting all dominant terms we obtain

$$\begin{aligned} \log Z_\alpha &= \log \xi \left[-\frac{s\alpha}{r4} + \frac{1}{12\alpha} \left(1 - \frac{6}{r(r-s)} \right) \right] \\ &+ \log \left[\frac{\mathfrak{f}_\alpha(1; r, s)}{\sqrt{2r(r-s)}} 2^{\alpha+2} \sin(2x) \right] + \log 2 \left[-\frac{s3\alpha}{r4} + \frac{1}{4\alpha} \left(1 - \frac{6}{r(r-s)} \right) \right] \\ &+ \left[\frac{\sin(4x) \mathfrak{f}_\alpha(2; r, s)}{\sin(2x) \mathfrak{f}_\alpha(1; r, s)} \frac{1}{64^{\frac{3}{4\alpha r(r-s)}}} \right] \xi^{-\frac{3}{2\alpha r(r-s)}} \\ &- \left[\frac{1}{2} \left(\frac{\sin(4x)}{\sin(2x)} \right)^2 \left(\frac{\mathfrak{f}_\alpha(2; r, s)}{\mathfrak{f}_\alpha(1; r, s)} \right)^2 \frac{1}{64^{\frac{3}{2\alpha r(r-s)}}} \right] \xi^{-\frac{3}{\alpha r(r-s)}} \\ &+ \frac{\sin(6x) \mathfrak{f}_\alpha(3; r, s)}{\sin(2x) \mathfrak{f}_\alpha(1; r, s)} \frac{1}{64^{\frac{4}{\alpha r(r-s)}}} \xi^{-\frac{4}{\alpha r(r-s)}} \\ &+ O\left(\xi^{-\frac{6}{\alpha r(r-s)}}\right) \end{aligned} \quad (\text{A.116})$$

Now, we are able to write down an expression for Rényi Entropy near the critical point

$$S_\alpha = \frac{c_{eff} \alpha + 1}{12} \log \xi + U_\alpha + A_\alpha(\xi) \quad (\text{A.117})$$

with

$$c_{eff} = 1 - \frac{6}{r(r-s)} \quad (\text{A.118})$$

$$= c_{r,s} - \Delta \quad (\text{A.119})$$

$$U_\alpha = -\frac{1}{2} \log [8r(r-s)] + \frac{1}{1-\alpha} \log \left[\frac{\mathfrak{f}_1(\alpha; r, s)}{\mathfrak{f}_1^\alpha(1; r, s)} \right]$$

$$\begin{aligned} A_\alpha(\xi) &= \frac{1}{1-\alpha} \left[\frac{\mathfrak{f}_2(\alpha; r, s)}{\mathfrak{f}_1(\alpha; r, s)} \xi^{-\frac{3}{2\alpha r(r-s)}} - \alpha \frac{\mathfrak{f}_2(1; r, s)}{\mathfrak{f}_1(1; r, s)} \xi^{-\frac{3}{2r(r-s)}} + \right. \\ &\left. - \frac{1}{2} \left[\frac{\mathfrak{f}_2(\alpha; r, s)}{\mathfrak{f}_1(\alpha; r, s)} \right]^2 \xi^{-\frac{3}{\alpha r(r-s)}} + \alpha \frac{1}{2} \left[\frac{\mathfrak{f}_2(1; r, s)}{\mathfrak{f}_1(1; r, s)} \right]^2 \xi^{-\frac{3}{r(r-s)}} + O\left(\xi^{-\frac{4}{\alpha r(r-s)}}\right) \right] \end{aligned}$$

$$\mathfrak{f}_k(n; r, s) = \sum_{a=1}^{r-1} \sin\left(k \frac{\pi d}{r-s}\right) \sin\left(k \frac{\pi a}{r}\right) \sin^n\left(\frac{\pi a s}{r}\right) \quad (\text{A.120})$$

where we have rescaled $\xi \rightarrow 8\xi$.

Appendix B

Co-algebras and Hopf algebras

In this appendix we will introduce the Co-algebras and Hopf Algebra, following notations and definitions of [27]. The definition of Hopf Co-Algebra is required for the definition of the action of generators of the Quantum Group $U_q(\mathfrak{su}_2)$ on an N -site system.

B.1 Co-algebras

Let $(\mathcal{A}, \mathbf{m}, \mathbf{i})$ be an algebra whose *multiplication* $\mathbf{m} : \mathcal{A} \otimes \mathcal{A} \rightarrow \mathcal{A}$ is associative:

$$\mathbf{m} \circ (\mathbf{m} \otimes \mathbb{1}) = \mathbf{m} \circ (\mathbb{1} \otimes \mathbf{m}) \quad (\text{B.1})$$

In order to define the multiplication between a scalar $\lambda \in \mathbb{K}$ and an element $a \in \mathcal{A}$ of the Algebra, we define the application \mathbf{i} as $\mathbf{i} : \lambda \mapsto \lambda \mathbb{1}$. Moreover we require the compatibility between \mathbf{i} and \mathbf{m} , i.e.

$$\mathbf{m}(a \otimes \mathbf{i}(\lambda)) = a\lambda = \lambda a = \mathbf{m}(\mathbf{i}(\lambda) \otimes a) \quad (\text{B.2})$$

We can define now a **co-associative co-product** $\Delta : \mathcal{A} \rightarrow \mathcal{A} \otimes \mathcal{A}$:

$$(\Delta \otimes \mathbb{1}) \circ \Delta = (\mathbb{1} \otimes \Delta) \circ \Delta \quad (\text{B.3})$$

using a diagrammatic representation we have:

$$\begin{array}{ccc} \mathcal{A} & \xrightarrow{\Delta} & \mathcal{A} \otimes \mathcal{A} \\ \Delta \downarrow & & \downarrow \Delta \otimes \mathbb{1} \\ \mathcal{A} \otimes \mathcal{A} & \xrightarrow{\mathbb{1} \otimes \Delta} & \mathcal{A} \otimes \mathcal{A} \otimes \mathcal{A} \end{array} \quad (\text{B.4})$$

we can also define a **co-unit** map $\epsilon : \mathcal{A} \rightarrow \mathbb{K}$

$$(\mathbb{1} \otimes \epsilon) \circ \Delta = (\epsilon \otimes \mathbb{1}) \circ \Delta = \mathbb{1} \quad (\text{B.5})$$

whose diagrams read:

$$\begin{array}{ccc} \mathcal{A} & \xrightarrow{\mathbb{1}} & \mathcal{A} \\ \downarrow \Delta & & \parallel \\ \mathcal{A} \otimes \mathcal{A} & \xrightarrow{\mathbb{1} \otimes \epsilon} & \mathcal{A} \otimes \mathbb{K} \end{array} \quad (\text{B.6})$$

$$\begin{array}{ccc} \mathcal{A} & \xrightarrow{\mathbb{1}} & \mathcal{A} \\ \downarrow \Delta & & \parallel \\ \mathcal{A} \otimes \mathcal{A} & \xrightarrow{\epsilon \otimes \mathbb{1}} & \mathbb{K} \otimes \mathcal{A} \end{array} \quad (\text{B.7})$$

which defines the structure $(\mathcal{A}, \Delta, \epsilon)$, which is called **co-algebra**.

B.2 Hopf co-algebras

Using definitions of algebra and co-algebra, we can build up a larger object which contains both structures.

A structure $(\mathcal{A}, \mathbf{m}, \mathbf{i}, \Delta, \epsilon)$ which is simultaneously an algebra and a co-algebra is called **bi-algebra** if the co-multiplication Δ and the co-unit ϵ of the co-algebra are consistent with the multiplication \mathbf{m} of the algebra, i.e. if they are homomorphisms:

$$\epsilon(ab) = \epsilon(a)\epsilon(b) \quad (\text{B.8})$$

$$\Delta(ab) = \Delta(a)\Delta(b) \quad \forall a, b \in \mathcal{A} \quad (\text{B.9})$$

Actually the unit \mathbf{i} and the co-unit ϵ must also be compatible

$$\mathbf{i}(\epsilon(a)) = \epsilon(a)\mathbb{1} \quad \forall a \in \mathcal{A} \quad (\text{B.10})$$

An **Hopf algebra** is a bi-algebra on which is defined the map $\gamma : \mathcal{A} \rightarrow \mathcal{A}$, called **antipode**, which is an anti-homomorphism

$$\gamma(ab) = \gamma(b)\gamma(a) \quad (\text{B.11})$$

and satisfies

$$m \circ (\gamma \otimes \mathbb{1}) \circ \Delta = m \circ (\mathbb{1} \otimes \gamma) \circ \Delta = \epsilon \mathbb{1} \quad (\text{B.12})$$

all elements of the bi-algebra are involved in these properties, which can be represented in the following diagram

$$\begin{array}{ccccc}
 \mathcal{A} & \xrightarrow{\Delta} & \mathcal{A} \otimes \mathcal{A} & \xrightarrow{1 \otimes \gamma} & \mathcal{A} \otimes \mathcal{A} \\
 \parallel & & & & \downarrow \mathfrak{m} \\
 \mathcal{A} & \xrightarrow{\epsilon} & \mathbb{K} & \xrightarrow{i} & \mathcal{A}
 \end{array} \tag{B.13}$$

Commutativity and co-commutativity

If the Hopf algebra \mathcal{A} is commutative for the multiplication \mathfrak{m} , we have

$$\mathfrak{m} \circ \sigma = \mathfrak{m} \tag{B.14}$$

where $\sigma : \mathcal{A} \otimes \mathcal{A} \rightarrow \mathcal{A} \otimes \mathcal{A}$ is the permutation map $\sigma(a \otimes b) = b \otimes a$.

The algebra is called co-commutative if

$$\sigma \circ \Delta = \Delta \tag{B.15}$$

B.2.1 Quasi-triangular Hopf algebras and quantum groups

Define $\Delta' = \sigma \circ \Delta$. It can be shown that it is also a co-product and defines a Hopf algebra with antipode $\gamma' = \gamma^{-1}$.

A Hopf algebra is called **quasi-triangular** if exists an **universal matrix** $\mathcal{R} \in \mathcal{A} \otimes \mathcal{A}$ such that

$$\Delta'(a) = \mathcal{R} \Delta(a) \mathcal{R}^{-1} \quad \forall a \in \mathcal{A} \tag{B.16}$$

$$(1 \otimes \Delta) \mathcal{R} = \mathcal{R}_{13} \mathcal{R}_{12} = \sum_{i,j} A_i A_j \otimes B_j \otimes B_i \tag{B.17}$$

$$(\Delta \otimes 1) \mathcal{R} = \mathcal{R}_{13} \mathcal{R}_{23} = \sum_{i,j} A_i \otimes A_j \otimes B_i B_j \tag{B.18}$$

$$(\gamma \otimes 1) \mathcal{R} = (1 \otimes \gamma^{-1}) \mathcal{R} = \mathcal{R}^{-1} \tag{B.19}$$

Parametrizing \mathcal{R} as $\sum_i A_i \otimes B_i$ we obtain

$$\mathcal{R}_{12} = \sum_i A_i \otimes B_i \otimes 1 = \mathcal{R} \otimes 1 \tag{B.20}$$

$$\mathcal{R}_{13} = \sum_i A_i \otimes 1 \otimes B_i \tag{B.21}$$

$$\mathcal{R}_{23} = \sum_i 1 \otimes A_i \otimes B_i = 1 \otimes \mathcal{R} \tag{B.22}$$

The quasi-triangularity means that Δ and Δ' are linearly related. If \mathcal{A} is co-commutative it is also trivially quasi-triangular with $\mathcal{R} = 1 \otimes 1$. A Hopf algebra such that

$$\mathcal{R} \sigma \mathcal{R} = 1 \otimes 1 \tag{B.23}$$

is called **triangular** algebra.

Appendix C

From 8-vertex Boltzmann weights to the quantum XYZ Hamiltonian

In this appendix we will perform the Hamiltonian limit of the 8-vertex model.

Let us consider a 2D classical IRF (Interaction Round Faces) model. Let $w(a, b, c, d)$ be the Boltzmann weight associated to the tile:

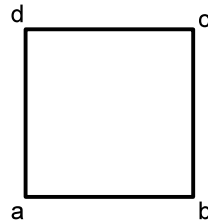


Figure C.1: Boltzmann weight $w(a, b, c, d)$ of the tile (a, b, c, d)

The Yang-Baxter Equation is given by [6]:

$$\begin{aligned} & \sum_c w(u|a, b, c, a'')w(u'|a'', c, b', a')w(u''|c, b, b'', b') \\ = & \sum_c w(u''|a'', a, c, a')w(u'|a, b, b'', c)w(u|c, b'', b', a') \end{aligned} \quad (\text{C.1})$$

and its solution is given by [6]

$$\begin{aligned}
 w(a, b, a, b) &= \rho \operatorname{snh} \lambda = A \\
 w(a, b, -a, -b) &= \rho k \operatorname{snh} \lambda \operatorname{snh} u \operatorname{snh} (\lambda - u) = B \\
 w(a, b, a, -b) &= \rho \operatorname{snh} (\lambda - u) = C \\
 w(a, b, -a, b) &= \rho \operatorname{snh} u = D
 \end{aligned} \tag{C.2}$$

The 8-vertex associated Boltzmann weight is given by

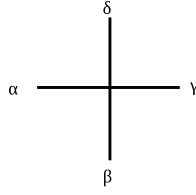


Figure C.2: Boltzmann weight $w(\alpha, \beta, \gamma, \delta)$ of the 8-vertex configuration $(\alpha, \beta, \gamma, \delta)$

$$\begin{aligned}
 w(\alpha, \beta, \gamma, \delta) &= \frac{1}{2} \delta(\alpha, \delta) \delta(\beta, \gamma) [(A + B) + (A - B) \alpha \beta] \\
 &+ \frac{1}{2} \delta(\alpha, -\delta) \delta(\beta, -\gamma) [(C + D) + (C - D) \alpha \beta]
 \end{aligned} \tag{C.3}$$

in matrix form

$$\mathbb{W} = \frac{A + B}{2} \mathbb{1} \otimes \mathbb{1} + \frac{C + D}{2} \sigma^x \otimes \sigma^x + \frac{D - C}{2} \sigma^y \otimes \sigma^y + \frac{A - B}{2} \sigma^z \otimes \sigma^z \tag{C.4}$$

Performing the Hamiltonian limit we obtain

$$\begin{aligned}
 H_{XYZ}^{(2)} &= \left. \frac{d}{du} \log \mathbb{W}(u) \right|_{u=0} = \left[\mathbb{W}^{-1}(u) \frac{d}{du} \mathbb{W}(u) \right]_{u=0} \\
 &= -i \frac{\operatorname{cn}(i\lambda, k) \operatorname{dn}(i\lambda, k)}{2 \operatorname{sn}(i\lambda, k)} \mathbb{1} \otimes \mathbb{1} \\
 &+ (-1) \frac{i(-1 + k \operatorname{sn}^2(i\lambda, k))}{2 \operatorname{sn}(i\lambda, k)} \sigma^x \otimes \sigma^x \\
 &+ \left[\frac{i}{2 \operatorname{sn}(i\lambda, k)} + \frac{ik}{2 \operatorname{sn}(i\lambda, k)} \right] \sigma^y \otimes \sigma^y \\
 &+ i \frac{\operatorname{cn}(i\lambda, k) \operatorname{dn}(i\lambda, k)}{2 \operatorname{sn}(i\lambda, k)} \sigma^z \otimes \sigma^z
 \end{aligned} \tag{C.5}$$

which is the 1D XYZ model.

Notice that in the limit $k \rightarrow 0$ it becomes the XXZ model:

$$H_{XXZ}^{(2)} = -\frac{1}{2} \coth \lambda \mathbb{1} \otimes \mathbb{1} + \frac{1}{2} \operatorname{csch} \lambda \sigma^x \otimes \sigma^x + \frac{1}{2} \operatorname{csch} \lambda \sigma^y \otimes \sigma^y + \frac{1}{2} \coth \lambda \sigma^z \otimes \sigma^z \quad (\text{C.6})$$

Appendix D

QFT Appendix

In this appendix we will recall some Quantum and Conformal Field Theory results. In particular we will briefly review the role of the effective central charge in non-unitary conformal theories and the Callan-Symanzik equation which is fundamental for the analysis of system near the critical point.

D.1 The Effective Central Charge

Consider a conformal theory defined on a cylinder of width L and infinite height and denote with $w = \tau + i\sigma$ its coordinates ($\sigma \in [0, L]$ and $\tau \in \mathbb{R}$).

Consider now the conformal transformation from the cylinder to the complex plane \mathbb{C} (with coordinate z)

$$z \mapsto w = \frac{L}{2\pi} \log z \tag{D.1}$$

Using the transformation law for the stress tensor under conformal transformation [12] we have

$$T_c(w) = \left(\frac{L}{2\pi}\right)^2 \left[T_{\mathbb{R}^2}(z) z^2 - \frac{c}{24} \right] \tag{D.2}$$

and the same for the anti-holomorphic part.

The hamiltonian of the system is given by [32]

$$H = \frac{1}{2\pi} \int_0^L d\sigma T_{\tau,\tau}(\sigma) = \frac{1}{2\pi} \int_0^L d\sigma (T(\sigma) + \bar{T}(\sigma)) \tag{D.3}$$

setting $\bar{w} = \tau - i\sigma$ we have

$$\sigma = \frac{1}{2i}(w - \bar{w}) = \frac{L}{4\pi i} \log \frac{z}{\bar{z}} \quad (\text{D.4})$$

$$d\sigma = \frac{L}{4\pi i} \left(\frac{dz}{z} - \frac{d\bar{z}}{\bar{z}} \right) \quad (\text{D.5})$$

obtaining

$$\begin{aligned} H &= \frac{1}{2\pi} \left(\frac{2\pi}{L} \right)^2 \left[\frac{L}{4\pi i} \oint T(z) z dz - \frac{L}{4\pi i} \oint \bar{T}(\bar{z}) d\bar{z} - L \frac{c}{12} \right] \\ &= \frac{2\pi}{L} (L_0 + \bar{L}_0) - \frac{\pi c}{6L} \end{aligned} \quad (\text{D.6})$$

The expectation value of the energy for a field with conformal dimension $(\Delta, \bar{\Delta})$ is then given by

$$\langle \Delta, \bar{\Delta} | \frac{2\pi}{L} (L_0 + \bar{L}_0) - \frac{\pi c}{6L} | \Delta, \bar{\Delta} \rangle = \frac{2\pi}{L} (\Delta + \bar{\Delta}) - \frac{\pi c}{6L} \quad (\text{D.7})$$

and its minimum is given by

$$E_0 = \frac{4\pi \Delta_{min}}{L} - \frac{\pi c}{6L} = -\frac{\pi c_{eff}}{6L} \quad (\text{D.8})$$

where

$$c_{eff} = c - 24\Delta_{min} \quad (\text{D.9})$$

is the *effective central charge*.

If we consider an open system with size L , the above expression change a bit, becoming

$$E_0 = -\frac{\pi c_{eff}}{24L} \quad (\text{D.10})$$

Notice that for unitary models $\Delta_{min} = 0$ and then $c_{eff} = c$. From a physical point of view, it implies that in unitary theories the conformal vacuum ($\Delta = 0$) corresponds to the ground state, but it is not true for non-unitary models, for which

$$|\text{g.s.}\rangle = \Phi(0)|0\rangle \quad (\text{D.11})$$

where $|0\rangle$ denotes the conformal vacuum ($\sim \mathbb{1} \leftrightarrow \Delta = 0$), and $|\text{g.s.}\rangle$ denotes the ground state, i.e. the state with the lowest energy and Φ is the primary field with conformal weight Δ_{min} .

D.2 Renormalisation group - Callan Symanzik equation

Consider the action functional $\mathcal{S}(g, a)$ which depends on some dimensionless coupling parameters $g = (g_1, g_2, \dots)$ and on a ultraviolet cut-off a that regularises divergencies in short distance correlators. Denote with G the space where coupling parameters belong. The main hypothesis of the renormalisation group is that exists a one-parameter semi-group of evolution on G :

$$R_t : G \rightarrow G \quad (\text{D.12})$$

such that the theory $\mathcal{S}(R_t g, e^t a)$ is equivalent to $\mathcal{S}(g, a)$. Equivalence of these two theories means that they give the same results in term of correlation function over a range scale $r \gg e^t a$.

Let us consider the correlation function of some local fields $A_i(x_i)$

$$\langle A_1(x_1) \dots A_n(x_n) \rangle = \int \mathcal{D}\varphi A_1(x_1) \dots A_n(x_n) e^{-\mathcal{S}[\varphi]} \quad (\text{D.13})$$

where the normalisation factor \mathcal{Z} is absorbed into the definition of \mathcal{S} . Consider the following transformation

$$x^\mu \rightarrow x'^\mu = x^\mu + \epsilon^\mu(x) \quad (\text{D.14})$$

Ward's identities give the variation of the action

$$\delta\mathcal{S} = \int d^2x T_{\mu\nu}(x) \partial^\mu \epsilon^\nu(x) \quad (\text{D.15})$$

whereas variations of fields are given by

$$A_i(x) \rightarrow A_i(x) + \delta A_i(x) \quad (\text{D.16})$$

We can now perform a variation of (D.13), obtaining

$$\sum_{i=1}^n \langle A_1(x_1) \dots \delta A_i(x_i) \dots A_n(x_n) \rangle = \int d^2x \langle T_{\mu\nu}(x) A_1(x_1) \dots A_n(x_n) \rangle \partial^\mu \epsilon^\nu(x) \quad (\text{D.17})$$

Focusing on global dilatation, fields are variated as follow

$$\delta A(x) = \epsilon \left(\frac{1}{2} x^\mu \partial_\mu + \hat{D} \right) A(x) \quad (\text{D.18})$$

where \hat{D} denotes the operator which implements internal transformation of fields under dilatation¹. The infinitesimal transformation of coordinates is given by²

$$\epsilon^\mu(x) = \epsilon x^\mu \quad (\text{D.19})$$

obtaining

$$\sum_{i=1}^n \left\langle \left(\frac{1}{2} x_\mu \partial^\mu + \hat{D} \right) A_1(x_1) \dots A_n(x_n) \right\rangle = \int d^2x \langle \Theta(x) A_1(x_1) \dots A_n(x_n) \rangle \quad (\text{D.20})$$

where $\Theta = T_\mu^\mu$.

Assuming that $\mathcal{S}(g, a)$ can be expressed as

$$\mathcal{S}(g, a) = \int d^2x \mathcal{L}_g \quad (\text{D.21})$$

Since \mathcal{L}_g is a Lagrangian

$$\varphi_i = \frac{\partial \mathcal{L}_g}{\partial g_i} \quad (\text{D.22})$$

are local fields of the theory.

Define operators \hat{B}_k as generators of transformations of fields A_i under variation of g_i :

$$\hat{B}_k A_i = \frac{\partial A_i}{\partial g_k} \quad (\text{D.23})$$

Deriving the correlation function we obtain

$$\frac{\partial}{\partial g_k} \langle A_1(x_1) \dots A_n(x_n) \rangle = \sum_{i=1}^n \langle A_1(x_1) \dots \hat{B}_k A_i(x_i) \dots A_n(x_n) \rangle - \int d^2x \langle \varphi_k(x) A_1(x_1) \dots A_n(x_n) \rangle \quad (\text{D.24})$$

the second term is due to the variation of the action.

Using (D.15) and (D.19) we have

$$\delta \mathcal{S} = \epsilon \int d^2x \Theta(x) \quad (\text{D.25})$$

¹For instance, in a Lorentz transformation the internal transformation is performed by the spin operator $S_{\mu\nu}$

² It comes from $x'^\mu = (1 + \epsilon)x^\mu = x^\mu + \epsilon^\mu(x)$.

D.2. Renormalisation group - Callan Symanzik equation

denoting $dt = \epsilon$ we have

$$\Theta = \frac{d\mathcal{L}}{dt} \quad (\text{D.26})$$

Expanding the above derivative in terms of coupling parameters we obtain

$$\Theta(x) = \frac{\partial \mathcal{L}}{\partial g_k} \frac{dg_k}{dt} = \beta^k(g) \varphi_k(x) \quad (\text{D.27})$$

We can thus parametrize the operator Θ in terms of the β -functions of the theory. Combining (D.24) and (D.27) we obtain the well-known Callan-Symanzik equation

$$\sum_{i=1}^n \left\langle A_1(x_1) \dots \left(\frac{1}{2} x_{i\mu} \partial_i^\mu + \hat{\gamma}(g) \right) A_i(x_i) \dots A_n(x_n) \right\rangle - \sum_k \beta^k(g) \frac{\partial}{\partial g_k} \langle A_1(x_1) \dots A_n(x_n) \rangle = 0 \quad (\text{D.28})$$

where

$$\hat{\gamma}(g) = \hat{D} + \beta^k(g) \hat{B}_k \quad (\text{D.29})$$

In the evaluation of Rényi Entropy for off-critical models, it is important to notice that the tensor Θ is trivially covariant under the action of the operator $\hat{\gamma}(m)$

$$\hat{\gamma}(m) \Theta(x) = 2\Theta(x) \quad (\text{D.30})$$

In off-critical models, the mass plays the role of the parameter g and it tends to zero when the model reaches the critical point.

Appendix E

Minimal Conformal Models

In this chapter we will introduce Minimal Conformal Models, which are the simplest conformal theories since they contain only a limited number of conformal families.

E.1 The Verma modulus

We will briefly review the algebra of the quantised angular momentum in order to make better understandable the idea of the Verma modulus.

E.1.1 The \mathfrak{su}_2 algebra

The \mathfrak{su}_2 algebra is given by three generators, J^\pm and J^z , which satisfy the commutator algebra

$$\begin{aligned} [J^+, J^-] &= 2J^z \\ [J^\pm, J^z] &= \pm J^\pm \end{aligned} \tag{E.1}$$

Let us denote with $|j, j\rangle$ the highest weight state in the j -sector, i.e.

$$\begin{aligned} J^z |j, j\rangle &= j |j, j\rangle \\ J^+ |j, j\rangle &= 0 \end{aligned} \tag{E.2}$$

The expectation value of the Casimir operator $\mathbf{J}^2 = \frac{1}{2}(J^+ J^- + J^- J^+) + J^{z2}$ for this state is given by $j(j+1)$. All other states in the sector defined by the Casimir operator can be obtained by successive applications of the operator J^- on the highest weight state.

The Hilbert space of this model is given by collecting together all possible highest weight states and their *descendant* states.

E.1.2 The Virasoro Algebra

For a given conformal theory with central charge c , the Virasoro Algebra \mathfrak{Vir}_c is given by

$$[L_n, L_m] = (n - m)L_{n+m} + \frac{c}{12}\delta_{n,-m}(n^3 - n) \quad (\text{E.3})$$

Recalling the \mathfrak{su}_2 structure, let us define a *highest weight state* $|h\rangle$ for the Virasoro algebra as the analog of the \mathfrak{su}_2 's one:

$$\begin{aligned} L_0|h\rangle &= h|h\rangle \\ L_n|h\rangle &= 0 \text{ for } n > 0 \end{aligned} \quad (\text{E.4})$$

The Hilbert space $V_c(h)$ generated by successive applications of L_{-n} ($n > 0$) on $|h\rangle$ is called *Verma modulus* or *conformal tower*. The operator L_0 measures the *dimension* of a state, while L_n plays the role of raising and lowering operators (respectively for $n < 0$ and $n > 0$). We can now define the *conformal vacuum* $|0\rangle$ as the highest weight state with zero conformal dimension:

$$L_n|0\rangle = 0 \text{ for } n \geq 0 \quad (\text{E.5})$$

If a state $|h\rangle$ does not belong to any other conformal tower except the itself one, this state is called *primary*. These primary states are strictly connected with primary fields of the conformal theory, since they are created applying a primary field ϕ with conformal dimension h to the conformal vacuum:

$$|h\rangle = \phi(0)|0\rangle \quad (\text{E.6})$$

The Hilbert space \mathcal{H} of the system is given by the direct sum of all Verma moduli with central charge c ;

$$\mathcal{H} = \bigoplus_h V_c(h) \quad (\text{E.7})$$

where the direct sum runs over all highest weight states of the theory.

E.1.3 The dimension of Verma moduli

Let us focus on the dimension of a given Verma modulus $V_c(h)$, since it gives the number of independent state belonging to it; in the field-theory picture, this dimension represents the number of independent conformal fields which can be builded up applying the functional version of L_n operators on a primary field ϕ

with conformal dimension h . Since the number of L_n operators applicable on a state $|h\rangle$ is not limited by above the dimension of a Verma modulus is infinite for an arbitrary values of c and h .

The application of L_{-n} operators on a state $|h\rangle$ increases by n the conformal dimensions of the state, since

$$\begin{aligned} L_0 L_{-n} |h\rangle &= (L_{-n} L_0 + [L_0, L_{-n}]) |h\rangle \\ &= h L_{-n} |h\rangle + n L_{-n} |h\rangle = (h + n) L_{-n} |h\rangle \end{aligned} \quad (\text{E.8})$$

The conformal dimension of a state $|h\rangle$ can be raised by n not only applying the operator L_{-n} but also applying a combination of m operators $L_{-k_1} \cdots L_{-k_m}$ such that $k_1 + \cdots + k_m = n$. In this way, for a given Verma modulus $V_c(h)$ the conformal dimension provides a natural level classifications: we can define the n -th level as the set of all states in the Verma modulus with conformal dimension $h + n$.

For instance, the first level contains only one state, given by

$$L_{-1} |h\rangle \quad (\text{E.9})$$

while second level states can be given by

$$L_{-2} |h\rangle \text{ or } L_{-1}^2 |h\rangle \quad (\text{E.10})$$

For this reason the number of independent states belonging to a level of the Verma modulus increases with the level and it is strictly connected with the *partition* \mathcal{P}_n of a number: the dimension on the n -th level is given by the number of combinations of natural number whose sum gives n .

E.2 Minimal models

For arbitrary values of c and h , conformal transformations spans the entire Verma module $V_c(h)$, since the action of conformal generators L_n create all states belonging to $V_c(h)$. If there is a state $|\chi\rangle$ belonging to the Verma module such that it is itself an highest weight state ($L_n |\chi\rangle = 0 \forall n > 0$) it is called *singular* or *null* vector and its norm is zero. The vanishing of the norm can be proofed as follows: if $|\chi\rangle$ belongs to $V_c(h)$ it can be written as sum of terms like

$$|\chi\rangle = L_{-k_1} \cdots L_{-k_n} |h\rangle \quad (\text{E.11})$$

and its norm is given by

$$\langle \chi | \chi \rangle = \langle \chi | L_{-k_1} \cdots L_{-k_n} |h\rangle = \langle h | L_{k_n} \cdots L_{k_1} | \chi \rangle^* = 0 \quad (\text{E.12})$$

In the operator-field picture, the field $\chi(z)$ is both primary and secondary, since it vanishes under the action of L_n , $n > 0$

$$L_n \chi(z) = 0 \tag{E.13}$$

but it is also secondary since it belongs to the descendant of the primary field $\phi(z)$ with conformal dimension h .

Thanks to the vanishing of (E.12) the state χ and all its descendants are orthogonal to the whole Verma module. Verma modules $V_c(h)$ are the basis for an irreducible representation of the Virasoro algebra \mathfrak{Vir}_c , but we have to pay attention in theories when null vector arises; Verma modules $V_c(h)$ have to be quotiented, identifying states which differ only by a null vector. Defining $M_c(h)$ as

$$M_c(h) = V_c(h)/\sim \tag{E.14}$$

they contain less states than ‘complete’ Verma moduli. Models which contains null vectors are called *minimal*, since their Hilbert space is **restricted**.

E.2.1 Existence of Minimal Models

The existence of null vectors and of Minimal models for a given value of the central charge c is not always guaranteed, but only for a restricted set of values. Thanks to a formula due to Kac¹, it has been demonstrated that only theories with central charge written as

$$c = 1 - 6 \frac{(p - p')^2}{pp'}, \text{ with } p, p' \in \mathbb{N}, p, p' \geq 3 \tag{E.15}$$

are minimal. In particular, we denote as $\mathcal{M}(p, p')$ the model with central charge given by (E.15). The Kac’s results also given the list of all highest weight states of the theory:

$$h_{r,s} = \frac{(pr - p's)^2 - (p - p')^2}{4pp'} \quad r = 1, \dots, p - 1 \quad s = 1, \dots, p' - 1 \tag{E.16}$$

Thanks to the above formula, the number of primary fields in a Minimal model is bounded, and for this reason the Operator Product Expansion (O.P.E.) in such a theory is limited to a finite number of conformal families.

¹See, for example [12]

E.3 Unitary and non-unitary minimal models

The Kac formulas gives a criterion to identify conformal theories with null vectors, but they can be unitary or not. A theory is called *unitary* if and only if non-negative-norm vectors belong to it. For example the norm of the state $|\psi\rangle = L_{-2}|0\rangle$ is non-negative if and only if $c > 0$ since

$$\langle\psi|\psi\rangle = \langle 0|L_2L_{-2}|0\rangle = \frac{c}{2} \quad (\text{E.17})$$

The above example is not exhaustive, since there exist non-unitary theories also with positive central charge. For minimal models, the related theories are unitary if and only if p and p' differ by one. For this reason we will denote with $\mathcal{M}(p)$ or \mathcal{M}_p the unitary minimal model $\mathcal{M}(p-1, p)$.

E.3.1 Non-unitary minimal models

In non-unitary minimal models the central charge can be negative, as in the archetypal Yang-Lee model $\mathcal{M}(2, 5)$ whose central charge is given by $-\frac{22}{5}$. Moreover, while in unitary theories the lowest conformal dimension is zero and it corresponds to the unity operator, in non-unitary models some negative conformal dimensions exist.

In non-unitary conformal models the central charge still rules **conformal** properties of a system, such as the O.P.E. of two stress tensors

$$T(z)T(w) \sim \frac{\frac{c}{2}}{(z-w)^4} + \frac{2T(w)}{(z-w)^2} + \frac{\partial_w T(w)}{z-w} \quad (\text{E.18})$$

but **physical** properties of the system are ruled by the *effective central charge* c_{eff}

$$c_{eff} = c - 24\Delta \quad (\text{E.19})$$

where Δ is the most negative conformal dimension of a primary field of the theory. Notice that in unitary models the lowest conformal dimension is zero and it is associated to the conformal vacuum $|0\rangle$ (or to the identity operator $\mathbb{1}$ in an operator picture), while in non-unitary theories there are primary fields with negative conformal dimensions which are associated to excited states of the conformal vacuum. The lowest conformal dimension Δ and the related primary field Φ defines the physical ground state $|gs\rangle$ as the state with the lowest energy

$$|gs\rangle = \Phi(0)|0\rangle \quad (\text{E.20})$$

Since the operator $L_0 + \bar{L}_0$ defines the Hamiltonian operator for a conformal model, the ground state energy is given by $\Delta < 0$ which is lower than the energy of the

conformal vacuum ($E = 0$).

As the central charge in a minimal model can take only discrete values set by a couple of relatively prime positive integers p and p' , also the effective central charge of a non-unitary minimal model has a definite expression [32]

$$c_{eff} = c - 24\Delta = 1 - \frac{6}{pp'} \quad (\text{E.21})$$

This expression is very important since it can be easily identified in expression involving physical properties of non-unitary minimal conformal models.

Bibliography

- [1] J. L. Cardy. Measuring Entanglement Using Quantum Quenches. *Phys. Rev. Lett.*, 106:150404, Apr 2011.
- [2] D. A. Abanin and E. Demler. Measuring Entanglement Entropy of a Generic Many-Body System with a Quantum Switch. *Phys. Rev. Lett.*, 109:020504, Jul 2012.
- [3] A. Rényi. On Measures Of Entropy And Information. *Proceedings of the 4th Berkeley Symposium on Mathematics, Statistics and Probability*, pages 547–561, 1960.
- [4] M. A. Nielsen and I. L. Chuang. Quantum computation and quantum information (cambridge series on information and the natural sciences). *Cambridge University Press*, 2004.
- [5] C. Degli Esposti Boschi. Introduzione alla Teoria dell’Informazione Quantistica - Lecture Notes. <http://www.bo.imm.cnr.it/users/degliesposti/TIQ.pdf>.
- [6] R. J. Baxter. Exactly Solved Models in Statistical Mechanics. *Dover Publications, London*, 2008.
- [7] L. Kaulke I. Peschel and M. Legeza. Density-matrix spectra for integrable models. *Annalen der Physik*, 8(2):153–164, 1999.
- [8] S. Evangelisti E. Ercolessi and F. Ravanini. Exact entanglement entropy of the XYZ model and its sine-Gordon limit . *Physics Letters A*, 374(21):2101 – 2105, 2010.
- [9] A. De Luca and F. Franchini. Approaching the restricted solid-on-solid critical points through entanglement: One model for many universalities. *Phys. Rev. B*, 87:045118, 2013.

- [10] O. A. Castro-Alvaredo J. L. Cardy and B. Doyon. Form Factors of Branch-Point Twist Fields in Quantum Integrable Models and Entanglement Entropy. *Journal of Statistical Physics*, 130:129–168, 2008.
- [11] P. Calabrese and J. L. Cardy. Entanglement entropy and quantum field theory. *Journal of Statistical Mechanics: Theory and Experiment*, 2004(06):P06002, 2004.
- [12] P. Mathieu P. Di Francesco and D. Senechal. Conformal field theory. *Springer*, 1997.
- [13] R. J. Baxter. Eight-vertex model in lattice statistics and one-dimensional anisotropic Heisenberg chain. I. Some fundamental eigenvectors. *Annals of Physics*, 76(1):1 – 24, 1973.
- [14] R. J. Baxter. Eight-vertex model in lattice statistics and one-dimensional anisotropic Heisenberg chain. II. Equivalence to a generalized ice-type lattice model. *Annals of Physics*, 76(1):25 – 47, 1973.
- [15] R. J. Baxter. Eight-vertex model in lattice statistics and one-dimensional anisotropic Heisenberg chain. III. Eigenvectors of the transfer matrix and hamiltonian. *Annals of Physics*, 76(1):48 – 71, 1973.
- [16] H. Saleur and M. Bauer. On some relations between local height probabilities and conformal invariance . *Nuclear Physics B*, 320(3):591 – 624, 1989.
- [17] R. J. Baxter G. E. Andrews and P. J. Forrester. Eight-vertex SOS Model and Generalized Rogers-Ramanujan-type Identities. *Journal of Statistical Physics*, 35:193–266, 1984.
- [18] D. A. Huse. Exact exponents for infinitely many new multicritical points. *Phys. Rev. B*, 30:3908–3915, 1984.
- [19] P. A. Pearce and Katherine A. Seaton. Off-Critical Logarithmic Minimal Models. *arxiv:1207.0259v3*, 2012.
- [20] P. J. Forrester and R. J. Baxter. Further Exact Solutions of the Eight-vertex SOS Model and Generalizations of the Rogers-Ramanujan Identities. *Journal of Statistical Physics*, 38:435–472, 1985.
- [21] A. W. W. Ludwig M. Troyer A. Kitaev Z. Wang A. Feiguin, S. Trebst and M. H. Freedman. Interacting Anyons in Topological Quantum Liquids: The Golden Chain. *Phys. Rev. Lett.*, 98:160409, 2007.

- [22] C. Korff and R. Weston. \mathcal{PT} symmetry on the lattice: the quantum group invariant XXZ spin chain. *Journal of Physics A: Mathematical and Theoretical*, 40(30):8845, 2007.
- [23] J. B. Zuber. Conformal field theories, Coulomb gas picture and integrable models. *Les Houches Summer School, Session XLIX, Les Houches, France, June 28-August 5 1988* (eds.: Brézin E., Zinn-Justin J.), pages 247–304, 1988.
- [24] F. C. Alcaraz, M. N. Barber, and M. T. Batchelor. Conformal invariance, the XXZ chain and the operator content of two-dimensional critical systems. *Annals of Physics*, 182(2):280 – 343, 1988.
- [25] V. Pasquier and H. Saleur. Common structures between finite systems and conformal field theories through quantum groups. *Nuclear Physics B*, 330(2-3):523 – 556, 1990.
- [26] G. Feverati A. Doikou, S. Evangelisti and N. Karaiskos. Introduction to Quantum Integrability. *International Journal of Modern Physics A*, 25(17):3307–3351, 2010.
- [27] M. Ruiz-Altaba C. Gómez and G. Sierra. Quantum Groups in Two-Dimensional Physics. *Cambridge University Press*, 1996.
- [28] E. K. Sklyanin. Boundary conditions for integrable quantum systems. *Journal of Physics A: Mathematical and General*, 21(10):2375, 1988.
- [29] T. Inami and H. Konno. Integrable XYZ spin chain with boundaries. *Journal of Physics A: Mathematical and General*, 27(24):L913, 1994.
- [30] M. Jimbo. A q-analogue of $U(\mathfrak{g}_{N+1})$, Hecke algebra, and the Yang-Baxter equation. *Letters in Mathematical Physics*, 11(3):247–252, 1986.
- [31] F. Göhmann A. Klümper F. H. Essler, H. Frahm and V. E. Korepin. The One-Dimensional Hubbard Model. *Cambridge University Press*, 2005.
- [32] G. Mussardo. Statistical Field Theory: An Introduction to Exactly Solved Models in Statistical Physics. *Oxford University Press, Oxford*, 2010.
- [33] O. A. Castro-Alvaredo and A. Fring. A spin chain model with non-Hermitian interaction: the Ising quantum spin chain in an imaginary field. *Journal of Physics A: Mathematical and Theoretical*, 42(46):465211, 2009.
- [34] D. L. O’Brien and P. A. Pearce. Surface free energies, interfacial tensions and correlation lengths of the ABF models. *Journal of Physics A: Mathematical and General*, 30(7):2353, 1997.

- [35] J. L. Cardy P. Calabrese and I. Peschel. Corrections to scaling for block entanglement in massive spin chains. *Journal of Statistical Mechanics: Theory and Experiment*, 2010(09):P09003, 2010.
- [36] F. Castilho Alcaraz M. Ibáñez Berganza and G. Sierra. Entanglement of excited states in critical spin chains. *Journal of Statistical Mechanics: Theory and Experiment*, 2012(01):P01016, 2012.
- [37] R. M. M. Soldati. Introduction to Quantum Field Theory - Lecture Notes. <http://robertosoldati.com/archivio/news/107/primonew.pdf>.

List of Figures

1.1	Dependance of Entropy S vs. p	19
2.1	Face (i, j, k, l)	23
2.2	Corner of a square lattice	24
2.3	Lattice composed by four corners	25
2.4	Graphical representation of U_i matrices	27
2.5	Graphical representation of the matrix $(S(a, a' b, b'))_{a'', b''}$	28
2.6	Graphical representation of the Yang-Baxter equation	29
2.7	Allowed vertex configurations that define the 8-vertex model	32
2.8	Ground State configuration in the Anti-ferroelectric regime	36
2.9	A lattice with two different anisotropy parameters	39
2.10	Magnetisation $\langle \sigma_1 \rangle$ vs. temperature parammeter k in the Ising case	46
2.11	A bipartite system divided into two subsystems A and B	48
2.12	The partition function \mathcal{Z} and its decompositions via CTM	50
3.1	The Riemann surface $\mathcal{M}_{3,1,b}$. Picture taken from [10]	53
3.2	Path integral representation of the density matrix ρ	58
3.3	Path integral representation of the partition function $\mathcal{Z}(\beta)$	58
3.4	Path integral representation of the reduced density matrix ρ_A : points belonging to the dotted lines (subsystem A) are not identified and integrated, while points in the continue line (subsystem B) are identified and integrated as in the evaluation of the partition function $\mathcal{Z}(\beta)$	58
4.1	Allowed Configurations of the RSOS Model	66
4.2	Dependance of the parameter p on the parameter k	67
4.3	Double row-to-row transfer matrix	77
5.1	Bratteli Diagram for \mathfrak{su}_2 and $U_q(\mathfrak{su}_2)$. Picture taken from [25]	94

LIST OF FIGURES

C.1 Boltzmann weight $w(a, b, c, d)$ of the tile (a, b, c, d)	133
C.2 Boltzmann weight $w(\alpha, \beta, \gamma, \delta)$ of the 8-vertex configuration $(\alpha, \beta, \gamma, \delta)$	134

Ringraziamenti

Mi pare a questo punto giusto ringraziare i miei relatori Francesco Ravanini ed Elisa Ercolessi, senza i quali non avrei certamente potuto completare questo lavoro di tesi. Vorrei ringraziare inoltre tutti coloro che con le loro considerazioni e riflessioni sull'argomento mi hanno aiutato a sviluppare questo lavoro e ad approfondire al meglio la materia, in particolare i Proff. Davide Fioravanti, Fabio Ortolani, Loris Ferrari, Cristian Degli Esposti Boschi, i Dott.ri Luca Taddia, Stefano Evangelisti, Alessandro Fabbri, Piero Naldesi. Un ringraziamento va anche ai miei compagni di studi Lorenzo Cevolani e Niccoló Vernazza, con cui ho condiviso idee e riflessioni di grande aiuto per il mio lavoro. Vorrei inoltre ringraziare gli altri ragazzi dello "stanzone" Caterina Specchia, Paolo Mattioli e Demetrio Vilardi, in compagnia dei quali lo studio é stato senz'altro maggiormente proficuo. Un ringraziamento anche a Gigi, per il suo insostituibile supporto anche da lontano. Mi piacerebbe poi rivolgere un ringraziamento a tutti i Professori che in questi cinque anni mi hanno insegnato ad apprezzare le splendide sfaccettature di vari rami della fisica.

Ci tengo inoltre a esprimere la mia gratitudine verso tutti coloro che mi hanno accompagnato e sostenuto nello scelta del corso di studi e nel percorso che ne é seguito; un pensiero particolare é quindi rivolto alla mia famiglia, che sempre mi é stata accanto in questi anni.

Vorrei infine ringraziare Costanza per il suo impareggiabile contributo nella correzione della tesi e il suo immancabile supporto.